Mapping Low-Energy Fission with RIBs

(nuclear fission in the 21st century from an experimentalist point of view ☺)

UNIVERSITY of York

Andrei Andreyev

University of York, UK

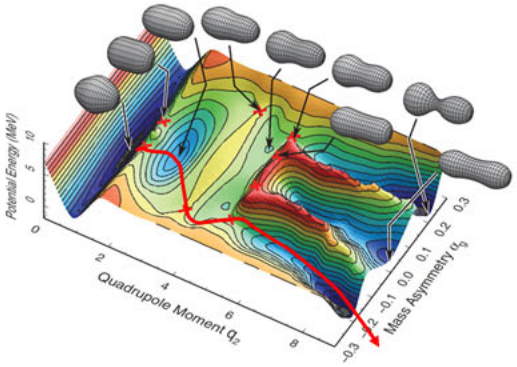

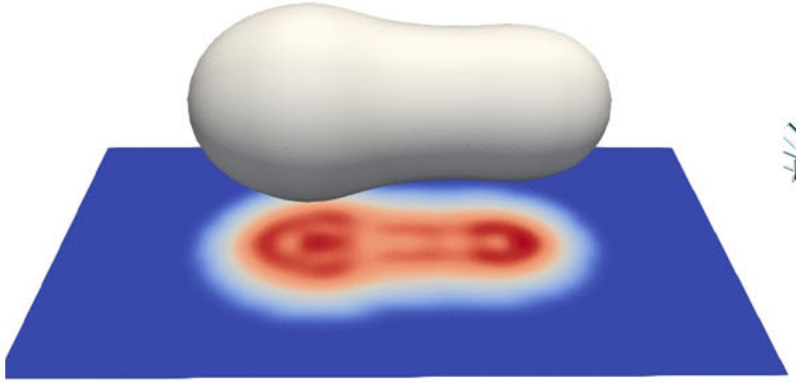

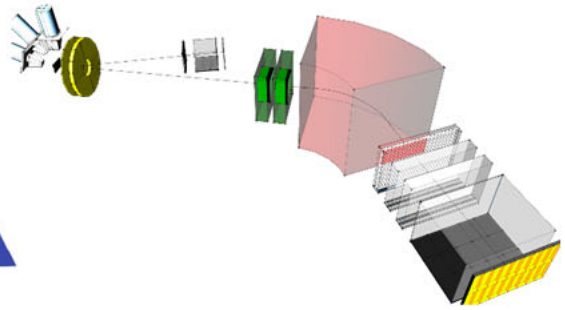

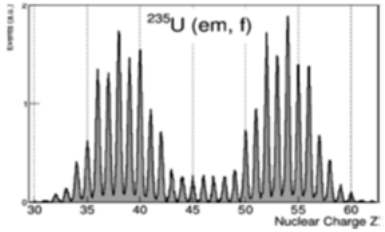

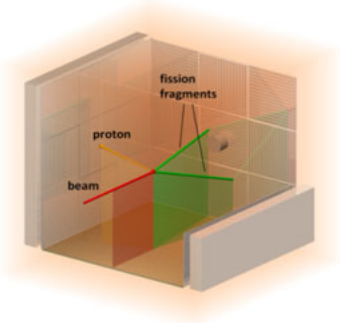

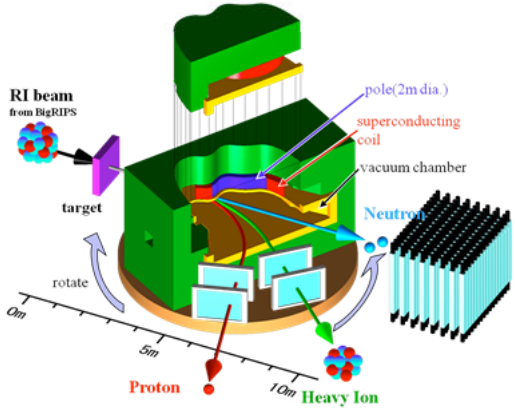

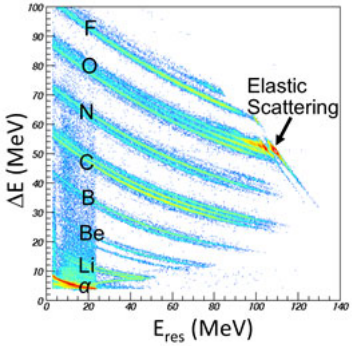

Chongqing, 11th May 2026

Mapping Low-Energy Fission with RIBs

(Nuclear Fission in the 21st Century from an experimentalist point of view ☺)

- Fission in the new" regions of the Nuclear Chart" –why?
- Brief (experimental) review on low-energy fission
- Electron- Capture Delayed Fission (ECDF) at ISOLDE (CERN) at 60 keV
- d,pf fission with post-accelerated RIBs at Coulomb energies
- Coulex fission at SOFIA@R3B@GSI with relativistic 1 AGeV energies
- ECDF of ^{180}Tl vs ECDF of ^{234}Bk (a challenge for theory)
- Conclusions
- Fission fragments angular momentum (J. Wilson, theory…)
- Spontaneous fission (SF) in heavy/SHE nuclei
- Fusion-fission/transfer reactions with heavy ions at Coulomb energies (Dubna, ANU, India..)
- n_ToF, n-induced fission experiments (ILL,n_ToF, LANSCE,J-PARC….)
- Future techniques: Photofission at ELI-NP with CBS-technique
- Future techniques: Fission in collision geometry with electrons (SCRIT@RIKEN)?

York city (UK), ~150.000 population

10 UK NP groups:
Birmingham, Brighton, Daresbury, Edinburgh, Glasgow, Liverpool, Manchester, Surrey, West of Scotland, York

University of York (est. 1963)

Academic staff	2,295
Students	**23,420**
Undergraduates	15,350
Postgraduates	8,070

York's Nuclear Physics group
10 "academics"
10+ postdocs
25+ PhD students

(some) UK-China similarities ☺

陕西地图VS英国地图

35 million

面积：20.6万平方公里
北部：黄土高原
著名建筑：钟楼、大雁塔
邻居：河南
资源：煤、石油、天然气
代表食品：肉夹馍
别称：大唐不夜城
艺人：郭达

69 million

面积：20.9万平方公里
北部：苏格兰高地
著名建筑：大笨钟、伦敦塔
邻居：荷兰
资源：煤、石油、天然气
代表食品：汉堡包
别称：日不落帝国
艺人：杰森斯坦森

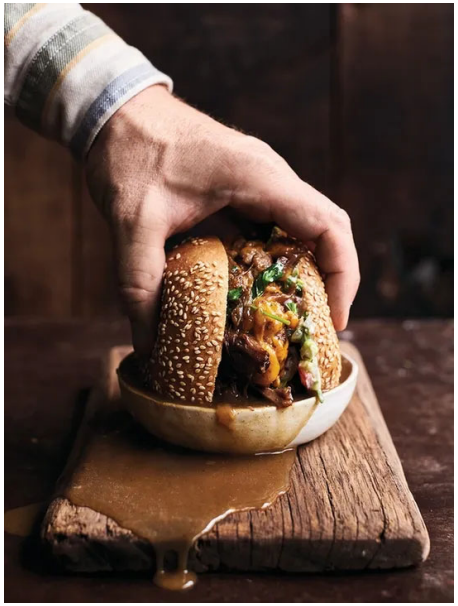

https://www.chinacheckup.com/blog/comparing-shaanxi-britain

What is Fission?

Time scale for fission from ‘compound nucleus’ to scission ~20 zs (~20×10^{-21}s)

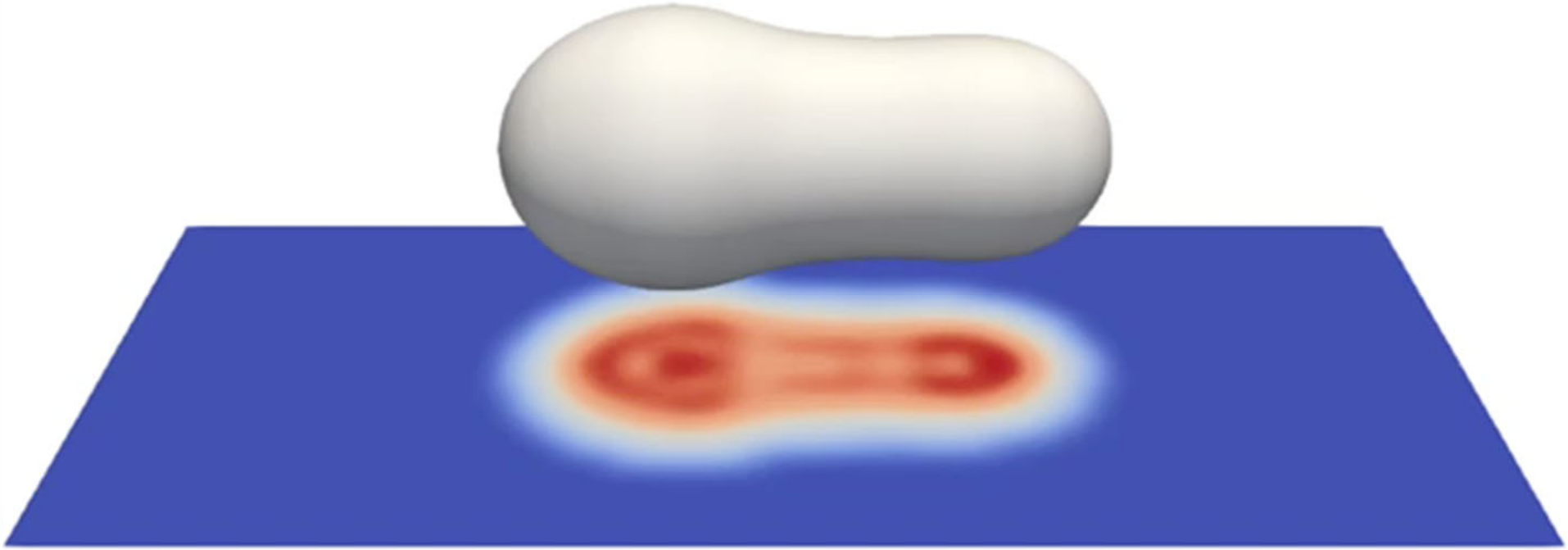

Time-dependent Hartree-Fock + BCS simulations for ^{240}Pu
G. Scamps, C.Seminel, *Nature* **564**, 382–385 (2018)

What are (typical) observables in fission?

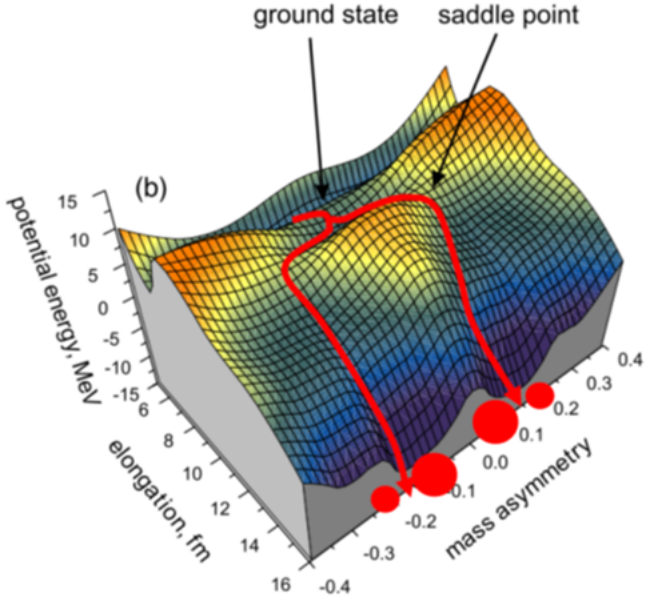

- **Half-lives** (e.g. for SF – from ms to billions of years)
- **Fission fragments mass and charge distributions** (symmetric, asymmetric, multimodal)
- **Kinetic energies of FFs**', & their sum – **Total Kinetic Energy(TKE)**
- **Prompt neutron and γ-ray multiplicities**, energies of γ's and n's
- **Angular momentum of fission fragments** (a derived value, hot topic nowadays)
- **Fission barrier height** (a derived value, can't be measured directly)

NB: Typical FFs energies in SF are ~1 AMeV, difficult to measure with sufficient precision (can be overcome **in inverse kinematics** – the modern approach)

Outlook: Why 'new regions of fission'?

- Theory models are (usually) 'tuned' along the β stability line

- However, many nuclear properties change far from stability line (e.g. disappearance of traditional magic numbers, appearance of new shell gaps, halos, skins…)

- **What happens to fission e.g. on the extremely neutron-deficient or neutron-rich sides? (e.g., r-process…)**

- Not simple to answer, as most of such nuclei are impossible to produce (e.g. very neutron-rich)

- Also to fission these nuclei **at low excitation energy** ($E^* \sim B_f$) is a very challenging task (we want to keep shell effects…)

- Need SF, beta-delayed fission, n-induced fission data

One of the reasons to study 'exotic' fission: r-process fission termination

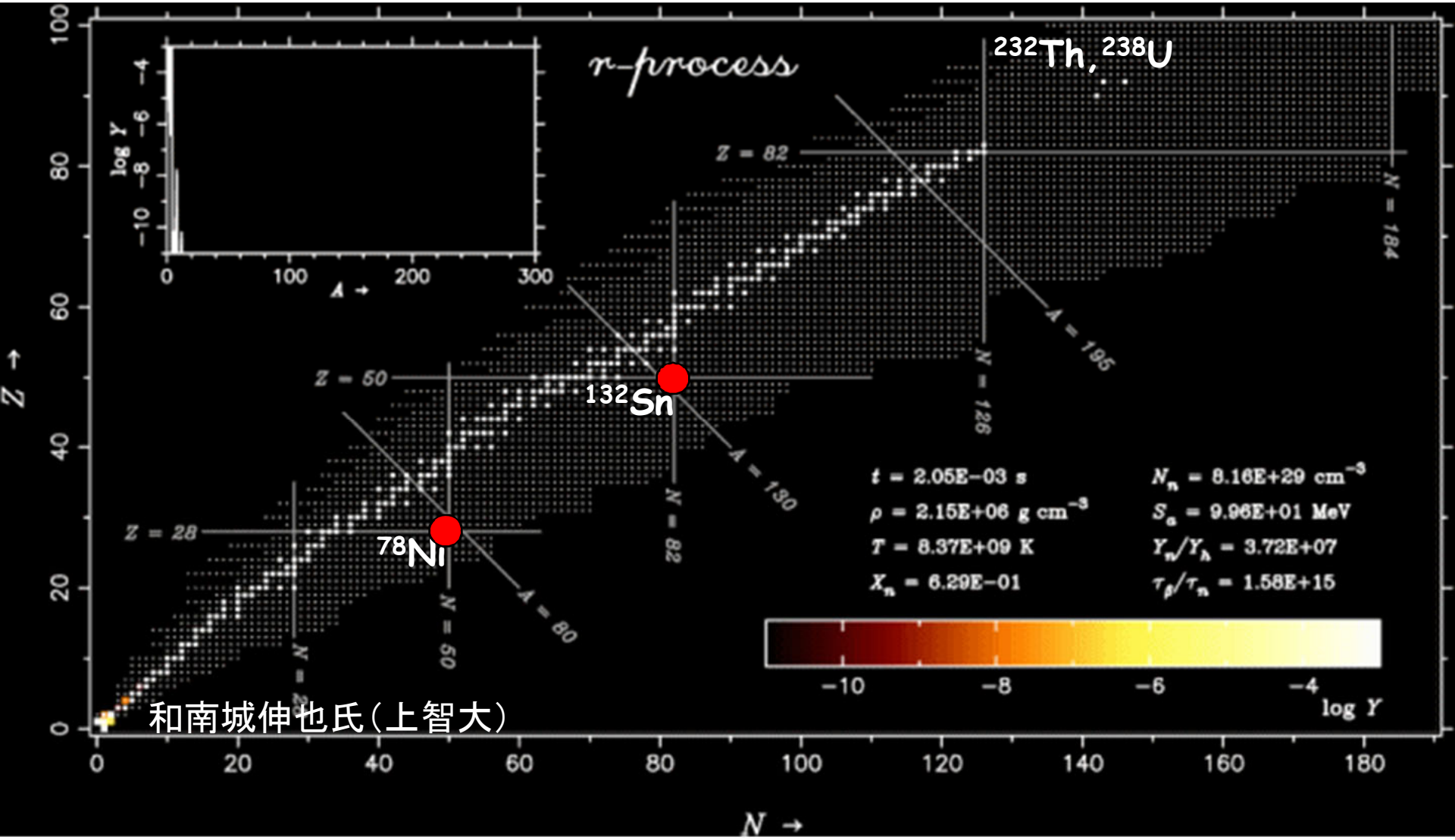

r-process termination by fission: need to know **fission barriers** and **FFs mass distributions for Z>82, N>180 nuclei! (hardly ever achievable in the lab?)**

Fission re-cycling in r-process: competition between spontaneous, neutron-induced and beta-delayed fission

Calculations of fission rates for r-process nucleosynthesis *

I.V. Panov [a,b,*], E. Kolbe [a], B. Pfeiffer [c], T. Rauscher [a], K.-L. Kratz [c], F.-K. Thielemann [a]

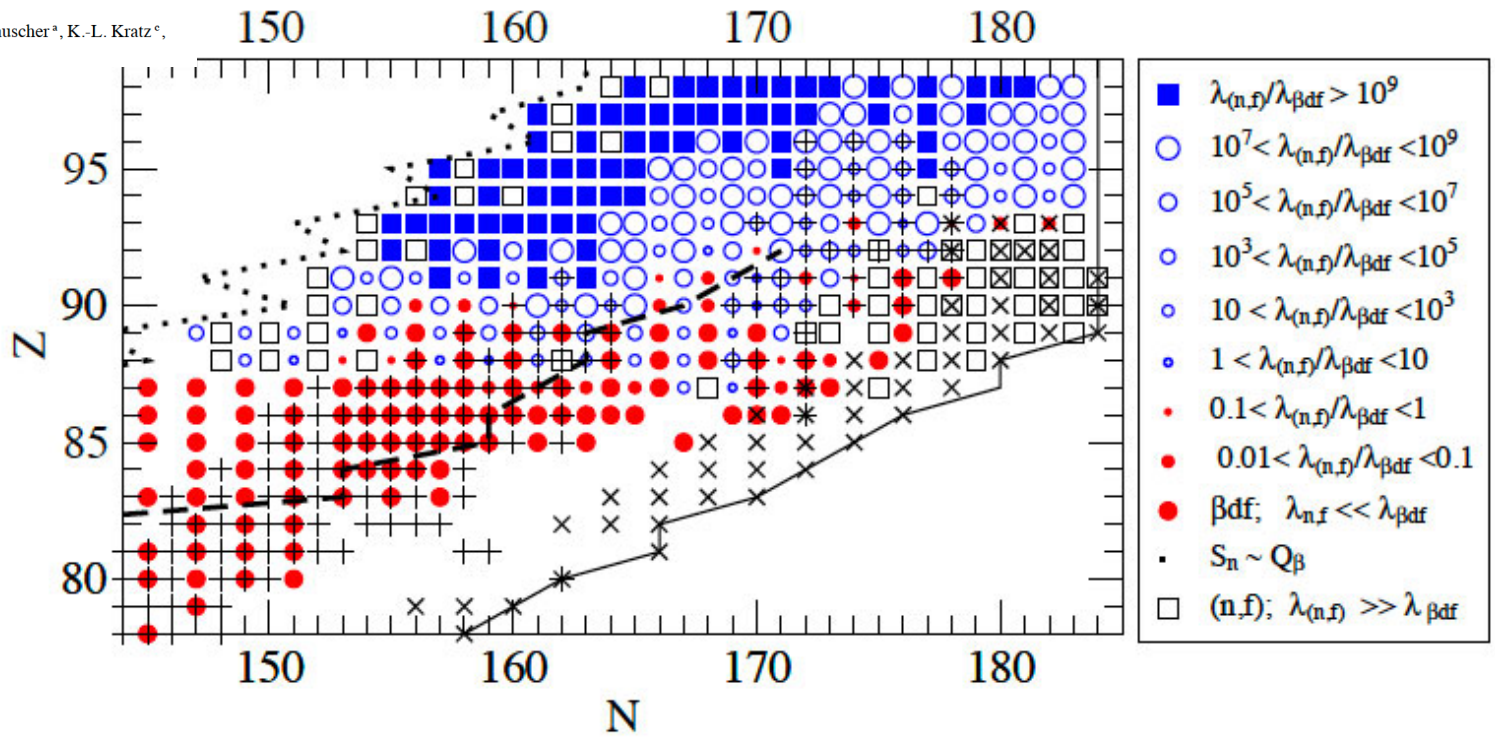

Fig. 7. The map of rates ratios $\lambda_{n,f}/\lambda_{\beta df}$ for $\rho Y_n = 1$ and $T_9 = 1$. The most abundant nuclei along the r-process path, for $n_n \approx 10^{26}$ (crosses), and $n_n \approx 10^{19}$ (pluses) are marked. The position of the neutron drip-line (full line), nuclei with neutron separation energy $S_n \approx 2MeV$ (dashed line) and nuclei with beta-decay energies $Q_\beta \sim S_n$ (dotted line) are denoted as well. These results were obtained for the mass model of Hilf et al. [22] and fission barriers by Howard and Moller [1].

Nuclear Physics A 747 (2005) 633–654

Example: Fission Barrier Calculations for r-process nuclei

Full symbols – experimental data
Lines – calculations (LDM,TF, ETFSI)

A. Mamdouh et al. NPA679 (2001), 337

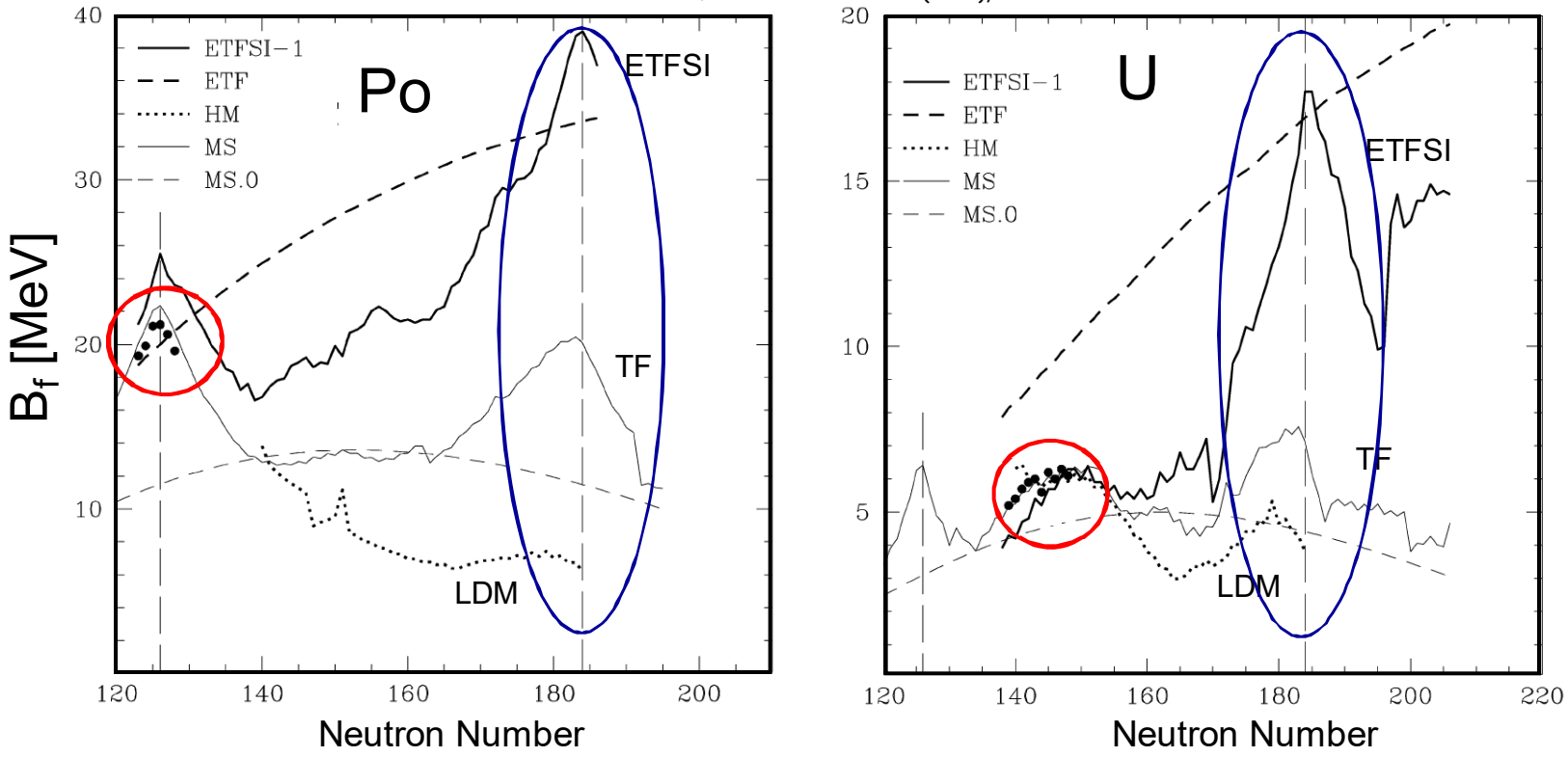

- Good agreement between $B_{f,cal}$ and $B_{f,exp}$ for nuclei close to stability
- Large disagreement far of stability (both on n-def. and n-rich sides)
- Need measured fission data far of stability to 'tune' fission models

Fission re-cycling in r-process: influence of the fission fragments mass distributions modelling

THE ASTROPHYSICAL JOURNAL, 808:30 (13pp), 2015 July 20

doi:10.1088/0004-637X/808/1/30

^{274}Pu

THE ROLE OF FISSION IN NEUTRON STAR MERGERS AND ITS IMPACT ON THE *r*-PROCESS PEAKS

M. EICHLER[1], A. ARCONES[2,3], A. KELIC[3], O. KOROBKIN[4], K. LANGANKE[2,3], T. MARKETIN[5], G. MARTINEZ-PINEDO[2,3], I. PANOV[1,6], T. RAUSCHER[1,7], S. ROSSWOG[4], C. WINTELER[8], N. T. ZINNER[9], AND F.-K. THIELEMANN[1]

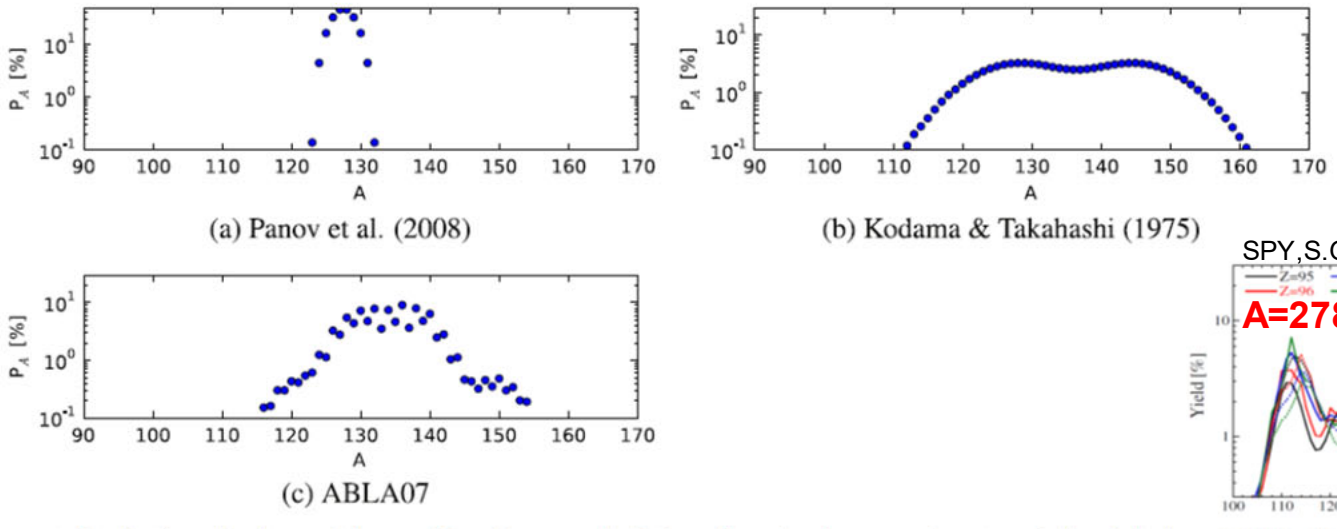

Figure 3. Fission fragment distributions for the models considered in our calculations, here for the case of neutron-induced fission of [illegible]Pu. For this reaction Panov et al. (2008) predict 19 ABLA07-released fission neutrons. Kodama & Takahashi (1975) do not predict any fission neutrons. For Panov et al. (2001) neutrons can be released if the fragments would lie beyond the neutron dripline. The distribution for Panov et al. (2001) consists only of two products with $A_1 = 130$ and $A_2 = 144$.

Recall: in r-process network calculations, we need fission data for e.g. ^{274}Pu, but so far the fission around ^{239}Pu was studied only

Fission and r-process: influence of the fission mass distributions modelling

IOP Publishing

Rep. Prog. Phys. **80** (2017) 084901 (16pp)

Report on Progress

Impact of new data for n nuclei on theoretical mo nucleosynthesis

Toshitaka Kajino[1,2,3] **and Grant J Mathews**[1,4]

[1] International Research Center for Big-Bang Cosmology and Element Genes and Nuclear Energy Engineering, Beihang University, Beijing 100191, People
[2] Division of Theoretical Astronomy, National Astronomical Observatory of J Mitaka, Tokyo, 181-8588, Japan
[3] Department of Astronomy, Graduate School of Science, The University of T Bunkyo-ku, Tokyo, 113-033, Japan
[4] Center for Astrophysics, Department of Physics, University of Notre Dame United States of America

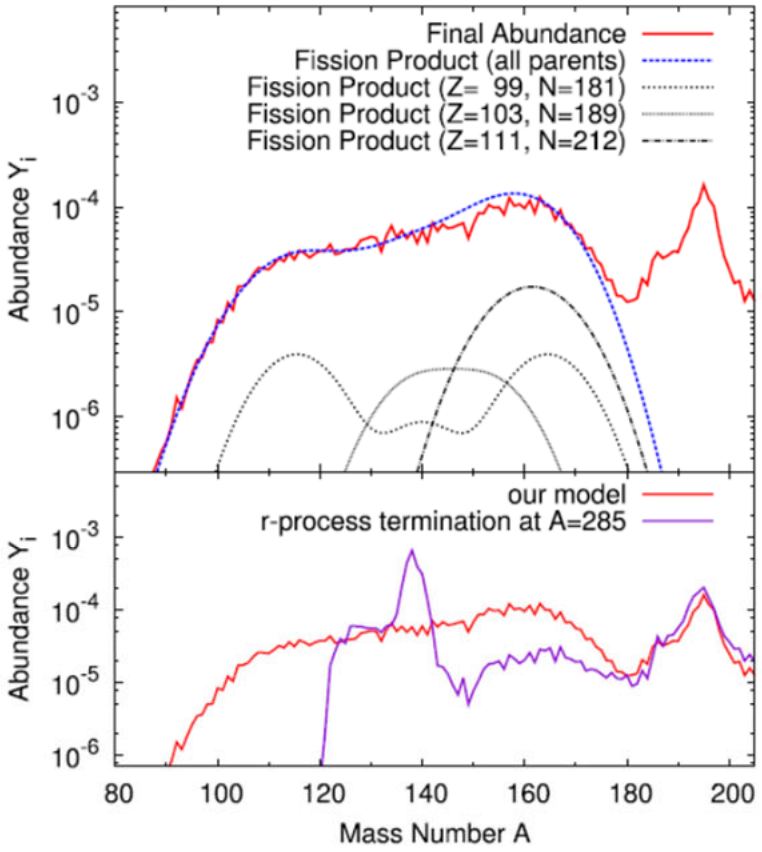

Figure 6. Illustration of the impact of fission yields and fission recycling on the final *r*-process abundances from Shibagaki *et al* (2016). Upper panel shows the relative contributions for 3 representative nuclei compared with the final abundance distribution. The lower panel shows the same final *r*-process yields compared with the distribution that would result if the termination of the *r*-process path were to occur at $A = 285$. Reproduced from Shibagaki *et al* (2016).

So, if we can't access neutron-rich, what can we do instead? Will neutron-deficient help?

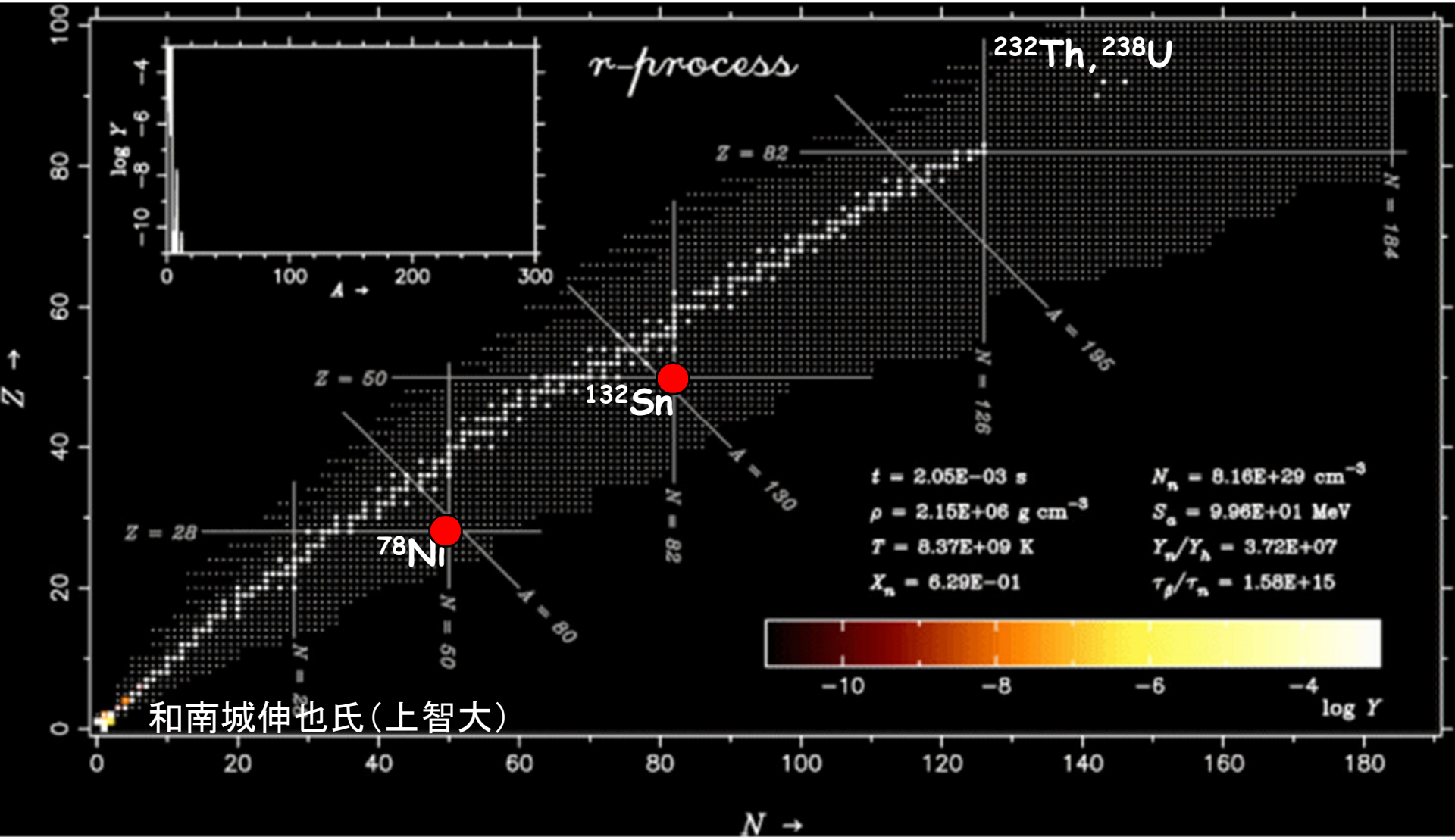

R-process termination by fission: need to know **fission barriers** and **FFs mass distributions for Z>82, N>180 nuclei! (hardly ever achievable in the lab?)**

Experimental information on low-energy fission
Nuclei with measured charge/mass split (RIPL-2 + GSI)

Heavy Actinides, N/Z~1.56: predominantly asymmetric; spontaneous fission, fission isomers, (bimodal)

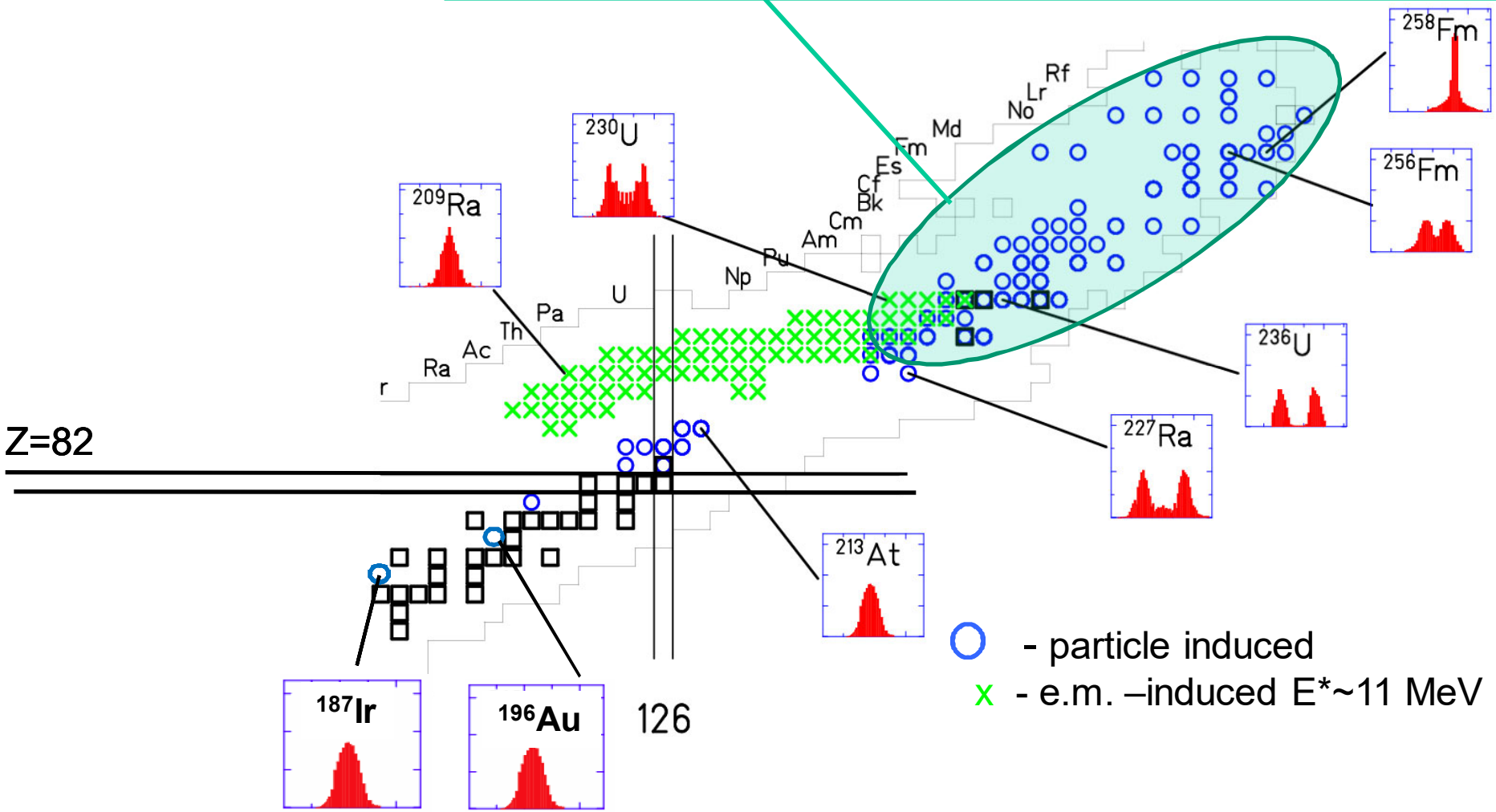

A.N. Andreyev, K. Nishio, K.-H. Schmidt, Reports on Progress in Physics, 1 (2018)

Experimental information on low-energy fission
Nuclei with measured charge/mass split (RIPL-2 + GSI)

Heavy Actinides, N/Z~1.56: predominantly asymmetric; spontaneous fission, fission isomers, (bimodal)

Region of our interest: fission of nuclei with A~180-200, N/Z~1.22-1.3: Hg,Pb,Po,Rn
JAEA,ISOLDE(CERN), ANU, Indian groups, R3B(GSI),Dubna

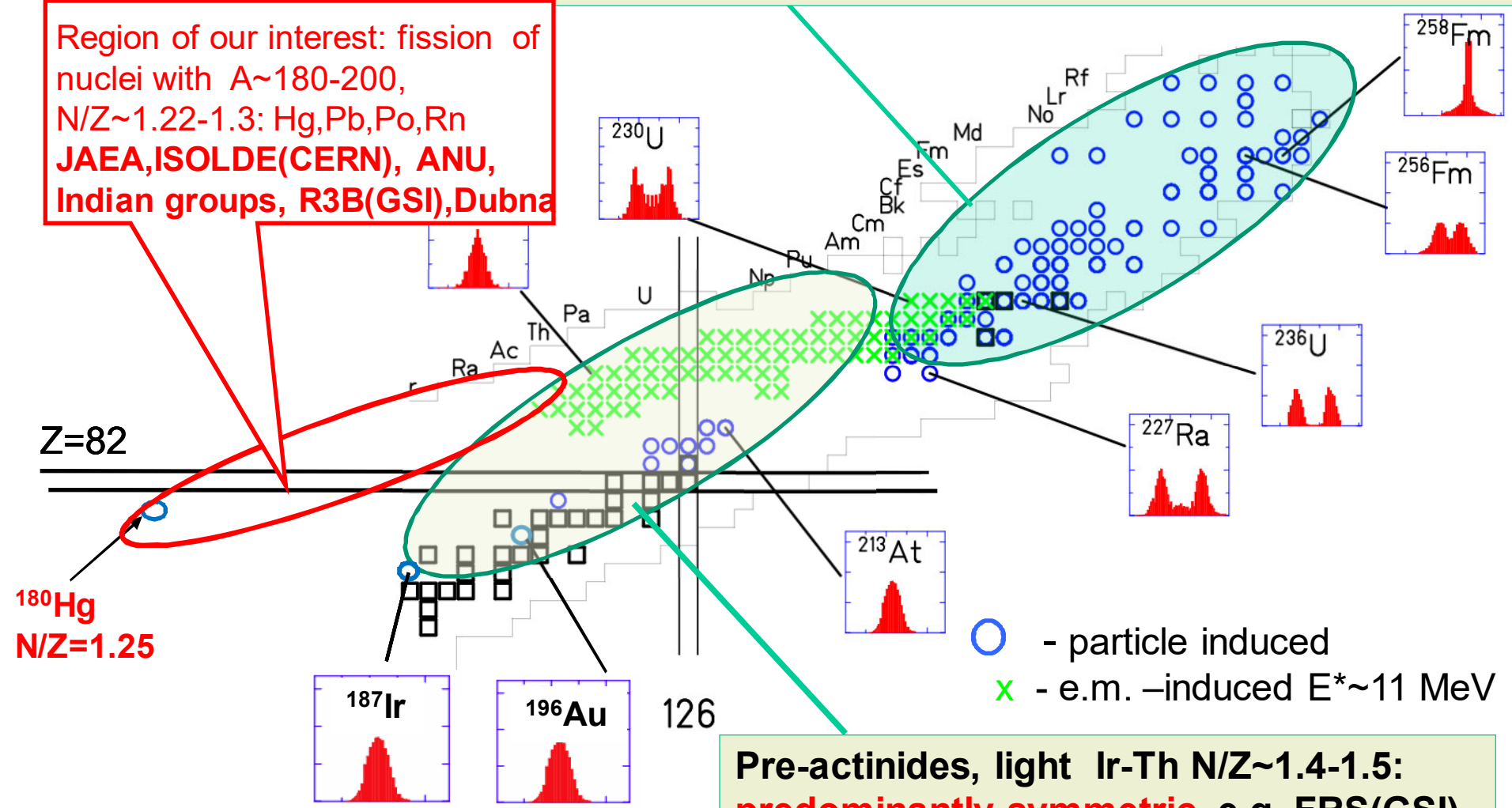

Pre-actinides, light Ir-Th N/Z~1.4-1.5: predominantly symmetric, e.g. FRS(GSI)

A.N. Andreyev, K. Nishio, K.-H. Schimidt, Reports on Progress in Physics, In

The ISOLDE facility at CERN

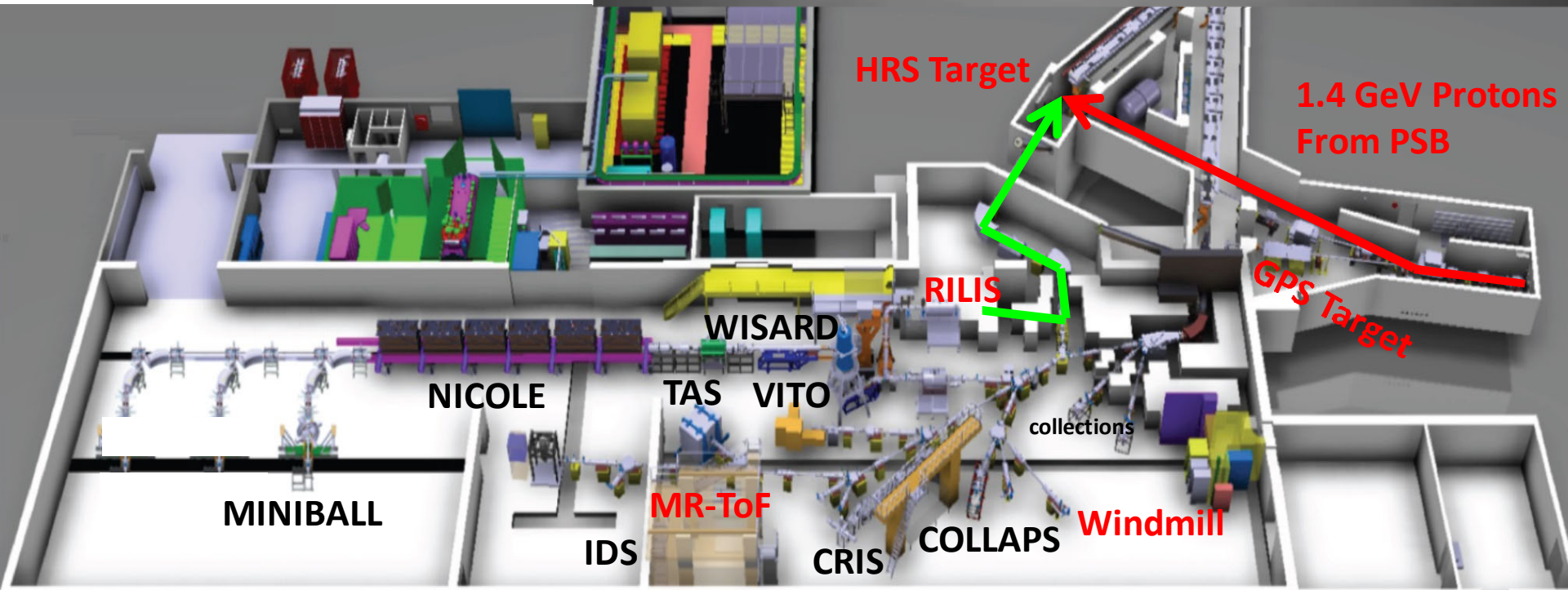

RIBs Production Reactions at ISOLDE (CERN) induced by p(1.4 GeV) with a thick Uranium Target

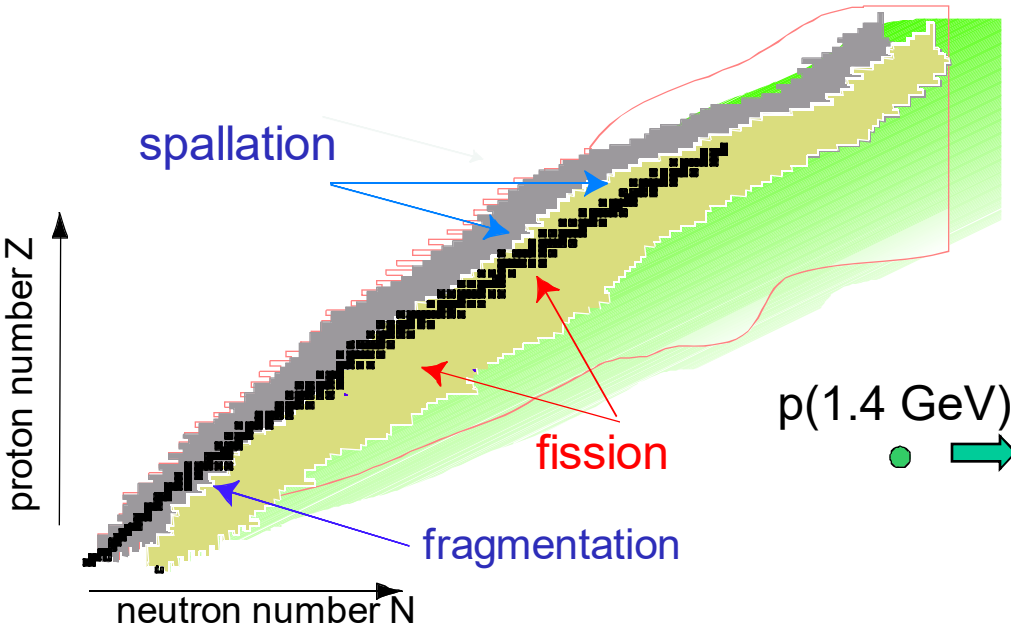

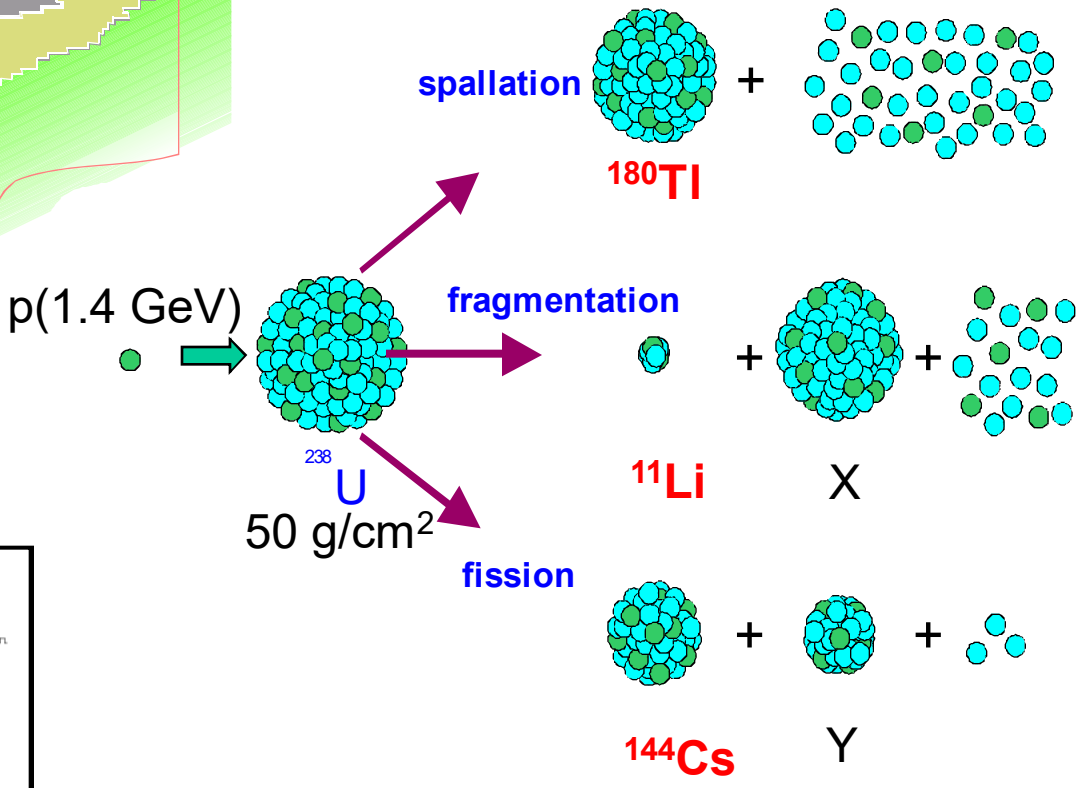

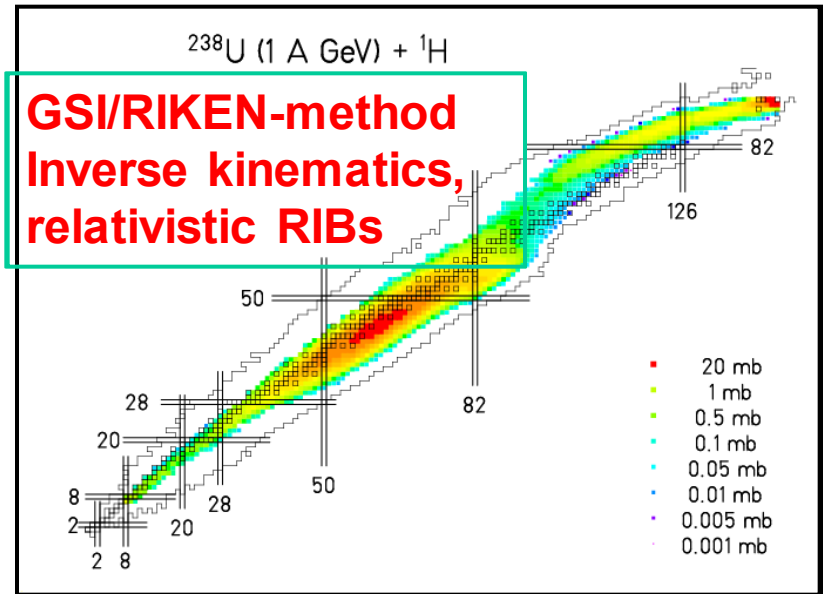

ISOLDE Facility (CERN, Geneva)
(example of a surface-ionization ion source)

ISOLDE Target Unit

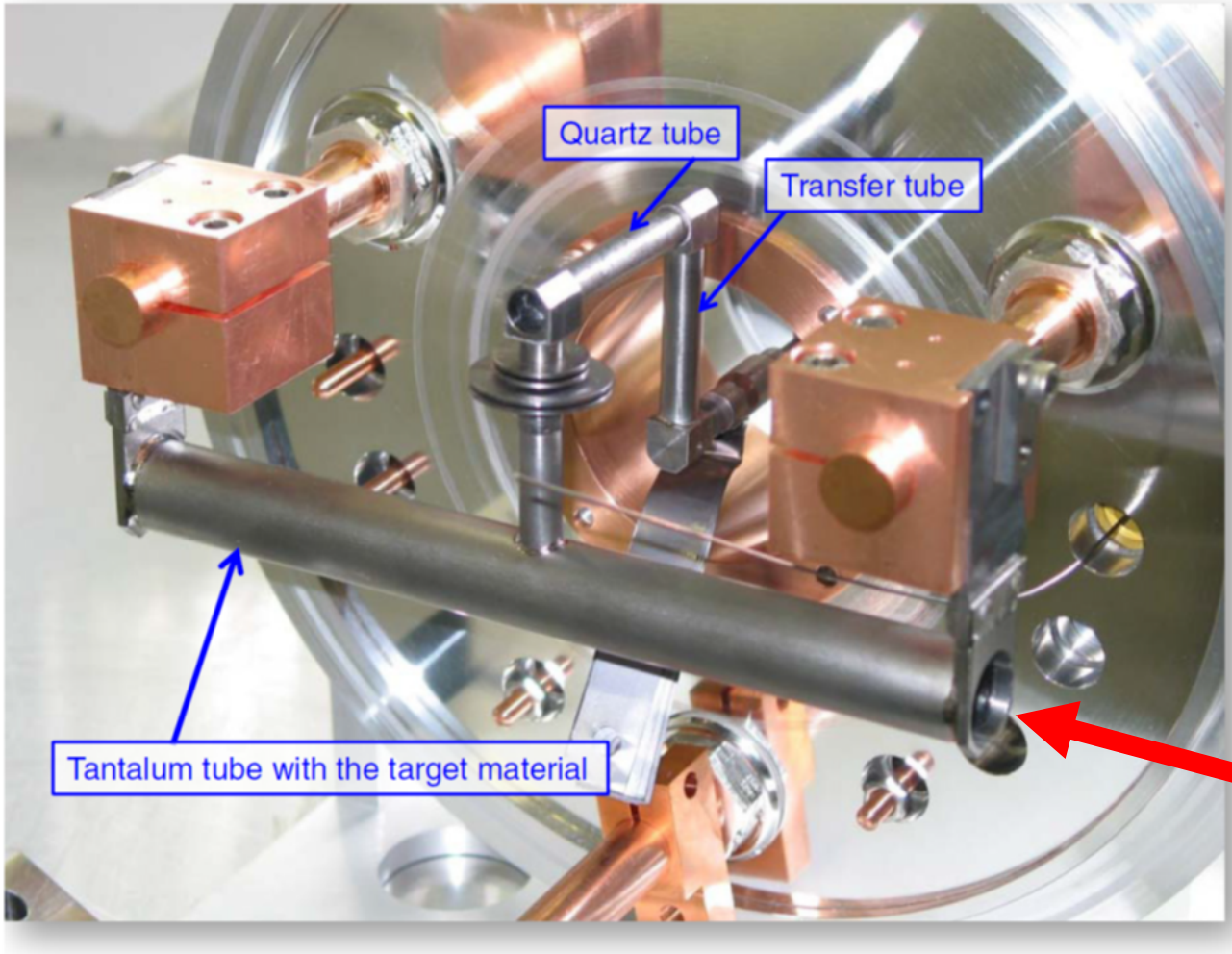

Figure 16. A photo of the ISOLDE target unit. The tantalum target container is ohmically heated. The radioactive atoms are transported to the ion source via the transfer tube. Part of the tube contains a quartz container that absorbs the rubidium atoms. This configuration was used to produce zinc beams using laser resonant ionization. Adapted from [48].

Getting clean laser-mass separated beams at ISOLDE

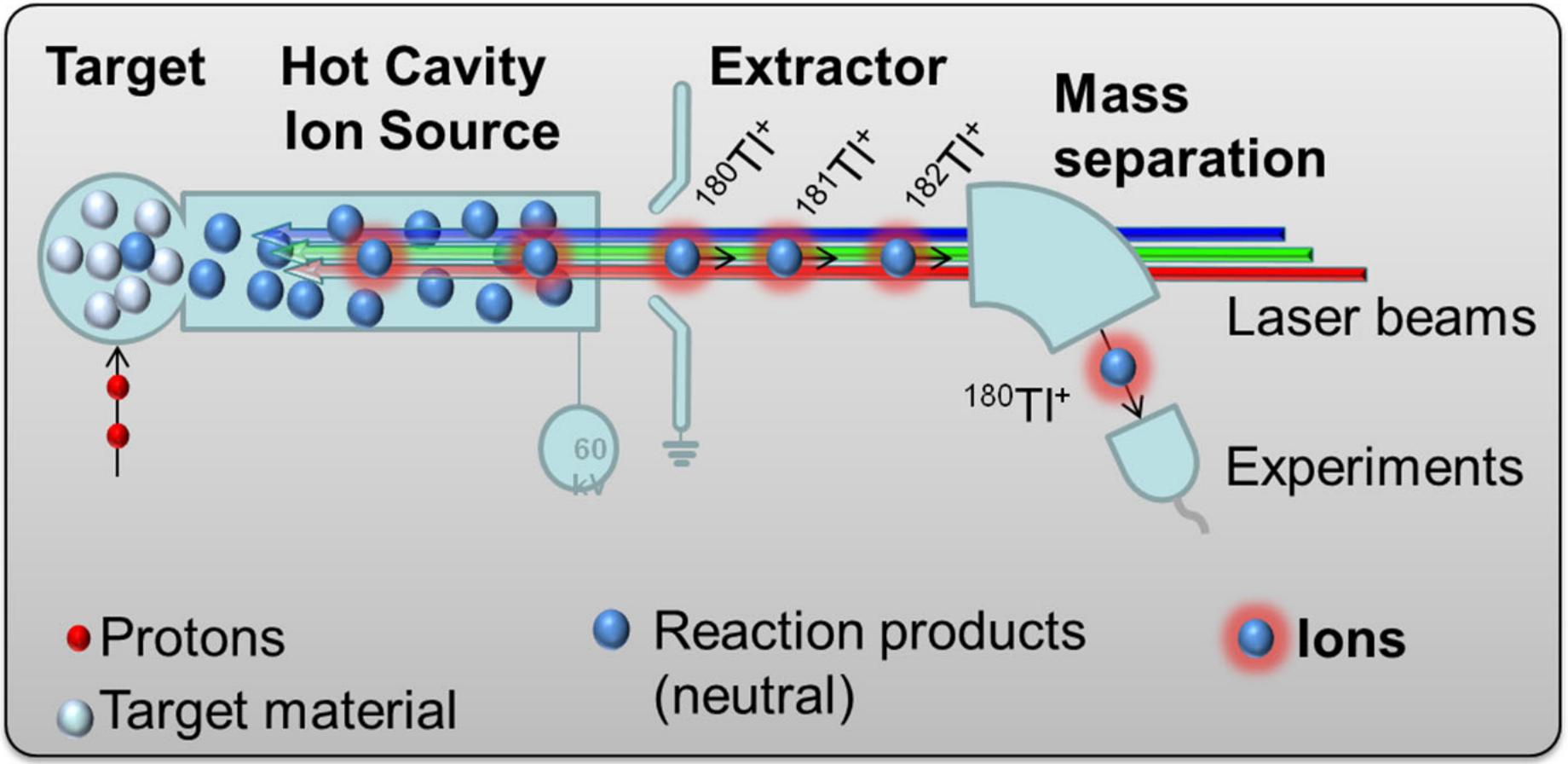

1st Study Case: ECDF of ^{180}Tl at ISOLDE-CERN

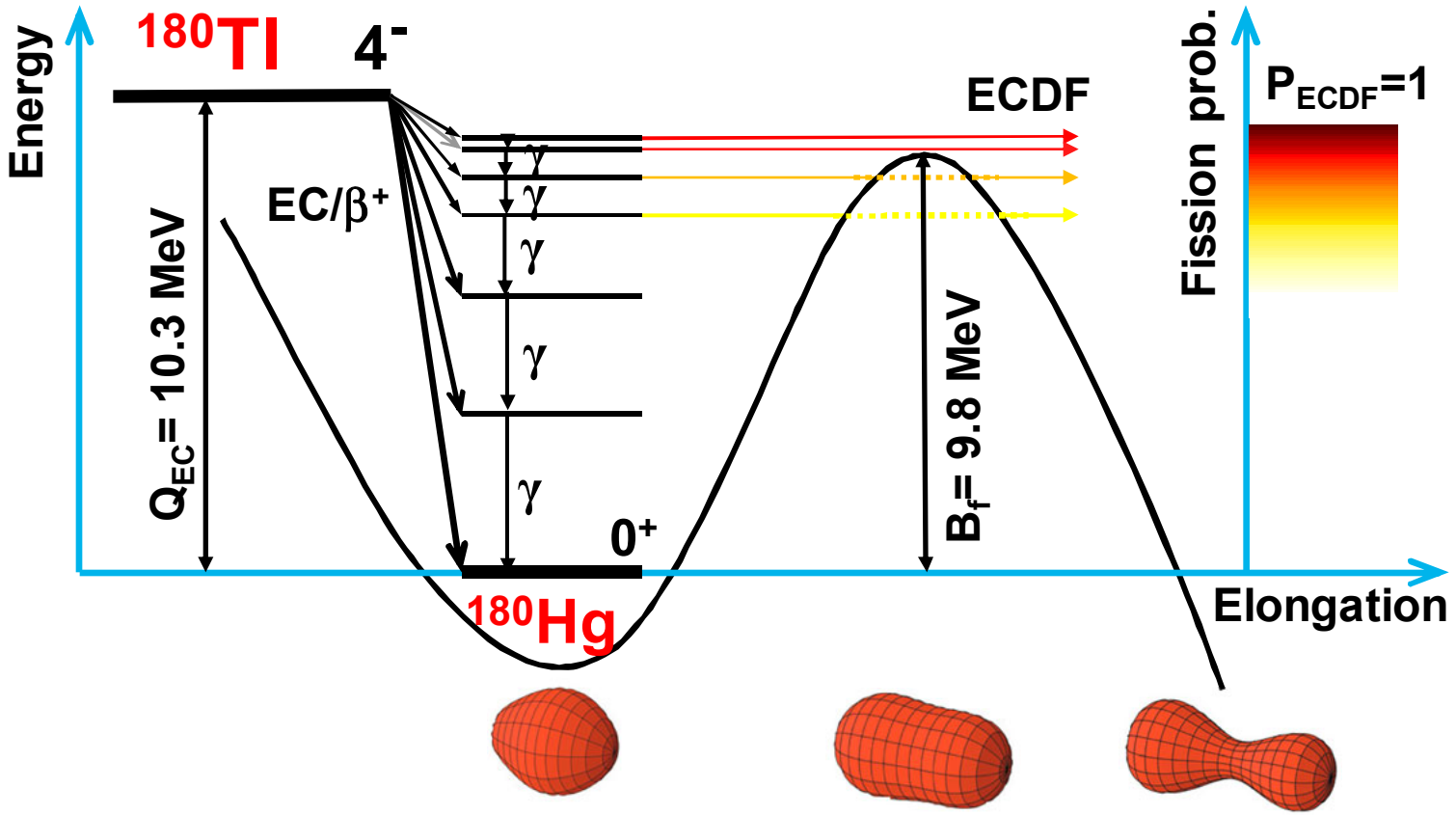

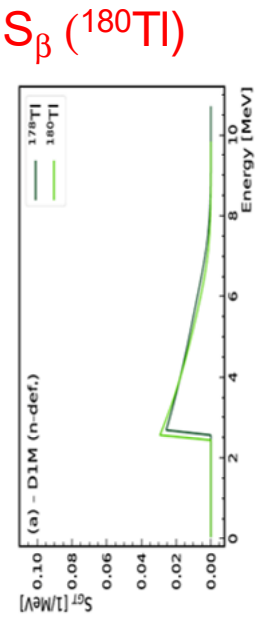

- Two step process: EC/β^+ decay of ^{180}Tl followed by fission of ^{180}Hg*
- Low-energy fission, E*<10.3 MeV, limited by Q_{EC}
- **Q_{EC}(^{180}Tl)-B_f(^{180}Hg)=0.5 MeV (FRDM/FRLDM values used)**
- **Mostly sub-barrier fission, as most of β–decay feeding to low E***

Mass distribution of fission fragments from βDF of ^{180}Tl (recall – it's daughter ^{180}Hg=2×^{90}Zr, who is actually fissionning!)

ASYMMETRIC energy split! Thus asymmetric mass split: M_H=100(4) and M_L= 80(4)

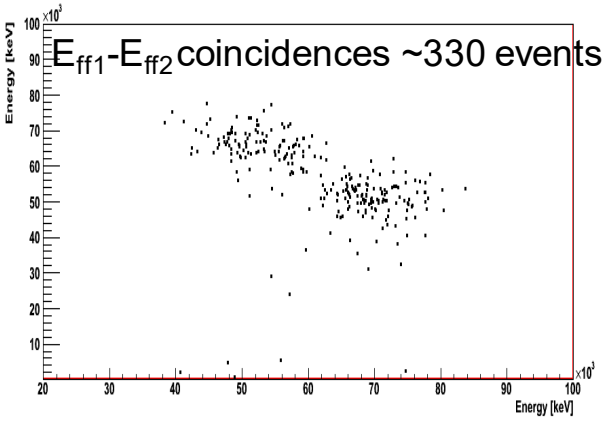

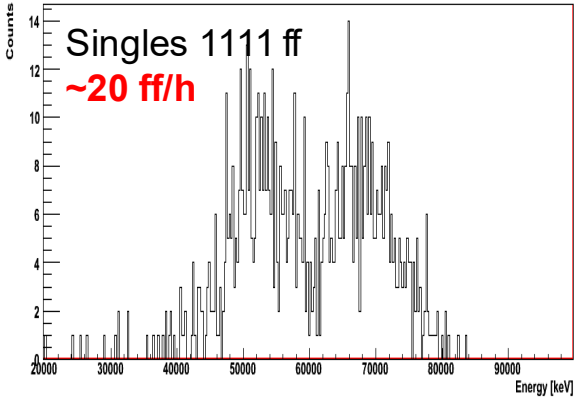

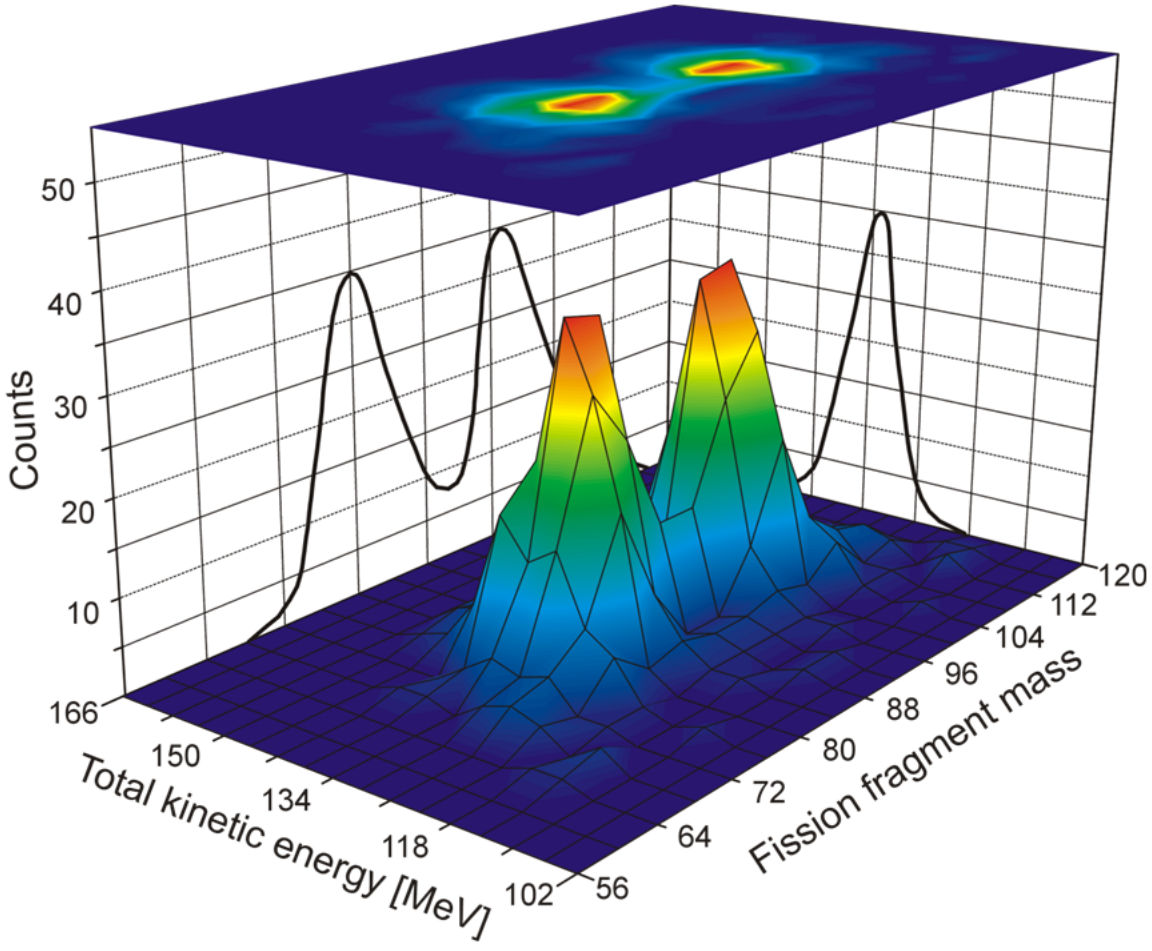

A problem: "low-energy" FF's - 1 AMeV only, A and Z identification difficult
The most probable fission fragments are ^{100}Ru (N=56,Z=44) and ^{80}Kr (N=44,Z=36)

Discovery of Asymmetric Fission in Proton-Rich Nuclei

PRL 105, 252502 (2010) PHYSICAL REVIEW LETTERS week ending 17 DECEMBER 2010

~~New Type of~~ Asymmetric Fission in Proton-Rich Nuclei via ECDF of ^{180}Tl

A. N. Andreyev,[1,2] J. Elseviers,[1] M. Huyse,[1] P. Van Duppen,[1] S. Antalic,[3] A. Barzakh,[4] N. Bree,[1] T. E. Cocolios,[1] V. F. Comas,[5] J. Diriken,[1] D. Fedorov,[4] V. Fedosseev,[6] S. Franchoo,[7] J. A. Heredia,[5] O. Ivanov,[1] U. Köster,[8] B. A. Marsh,[6] K. Nishio,[9] R. D. Page,[10] N. Patronis,[1,11] M. Seliverstov,[1,4] I. Tsekhanovich,[12,17] P. Van den Bergh,[1] J. Van De Walle,[6] M. Venhart,[1,3] S. Vermote,[13] M. Veselsky,[14] C. Wagemans,[13] T. Ichikawa,[15] A. Iwamoto,[9] P. Möller,[16] and A. J. Sierk[16]

[1]*Instituut voor Kern- en Stralingsfysica, K.U. Leuven, University of Leuven, B-3001 Leuven, Belgium*
[2]*School of Engineering, University of the West of Scotland, Paisley, PA1 2BE, United Kingdom, and the Scottish Universities Physics Alliance (SUPA)*

$P_{ECDF}(^{180}Tl)=3.6(7)\times10^{-5}$

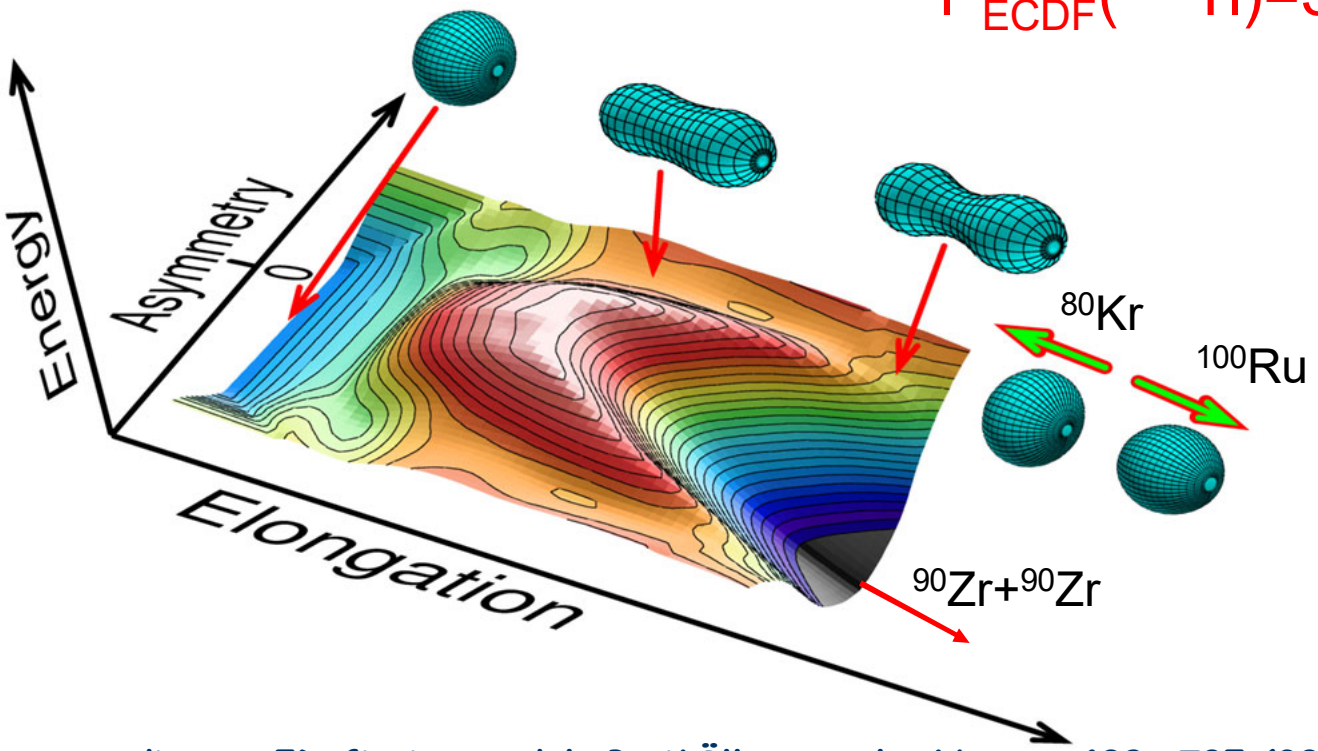

Calculations according to 5D fission model, P. MÖller et al., Nature 409, 785 (2001)

Two types of asymmetry: what's the difference?

PHYSICAL REVIEW C **86**, 024610 (2012)

Contrasting fission potential-energy structure of actinides and mercury isotopes

Takatoshi Ichikawa,[1] Akira Iwamoto,[2] Peter Möller,[3] and Arnold J. Sierk[3]

Conclusions: The mechanism of asymmetric fission must be very different in the lighter proton-rich mercury isotopes compared to the actinide region and is apparently unrelated to fragment shell structure. Isotopes lighter than ^{192}Hg have the saddle point shielded from a deep symmetric valley by a significant ridge. The ridge vanishes for the heavier Hg isotopes, for which we would expect a qualitatively different asymmetry of the fragments.

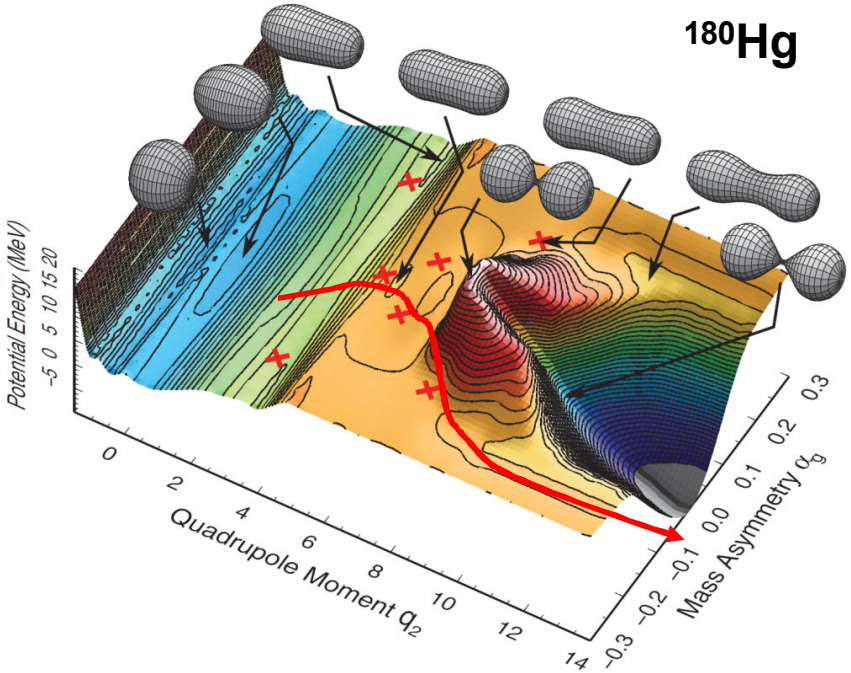

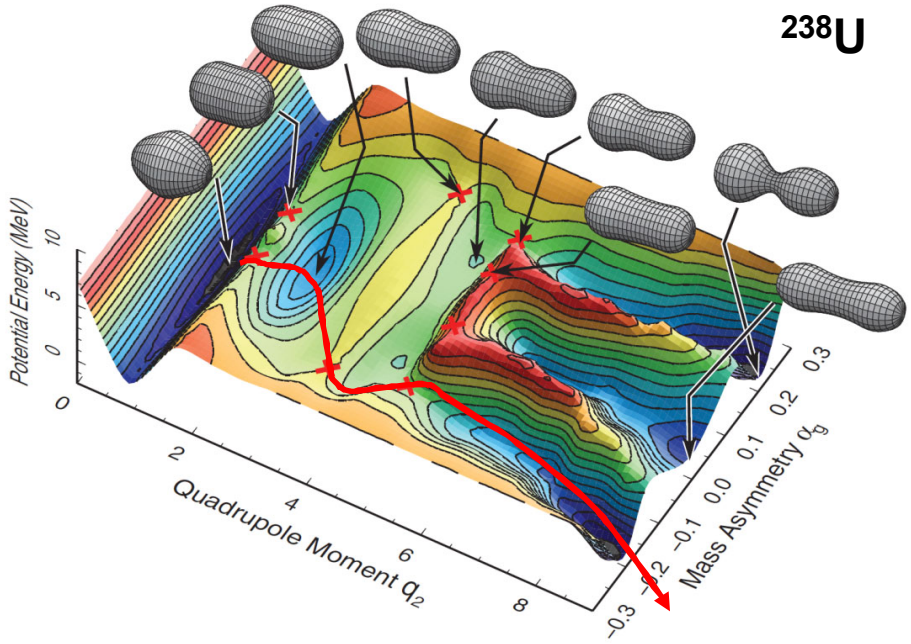

Asymmetry in the U-region is due to strong shell effects of fission fragments around ^{132}Sn
Asymmetry in the neutron-deficient Pb-region – due to shell effects of CN (but, octupoles?)

Brownian Metropolis Shape Motion

based on J. Randrup and P. Moller, PRL 106, 132503 (2011)

Phys. Rev. C 85, 024306 (2012)

Calculated fission yields of neutron-deficient mercury isotopes

Peter Möller[1],* Jørgen Randrup[2], and Arnold J. Sierk[1]
[1] *Theoretical Division, Los Alamos National Laboratory, Los Alamos, New Mexico 87545, USA*
[2] *Nuclear Science Division, Lawrence Berkeley National Laboratory, Berkeley, California 94720, USA*
(Dated: November 21, 2011)

The recent unexpected discovery of asymmetric fission of ^{180}Hg following the electron-capture decay of ^{180}Tl has led to intense interest in experimentally mapping the fission-yield properties over more extended regions of the nuclear chart and compound-system energies. We present here a first calculation of fission-fragment yields for neutron-deficient Hg isotopes, using the recently developed Brownian Metropolis shape motion treatment. The results for ^{180}Hg are in approximate agreement with the experimental data. For ^{174}Hg the symmetric yield increases strongly with decreasing energy, an unusual feature, which would be interesting to verify experimentally.
PACS numbers: 25.85.-w, 24.10.Lx,24.75.+i

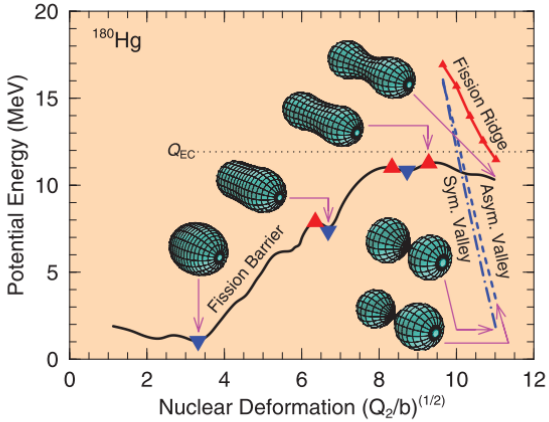

FIG. 4. (Color online) Minima, saddles, major valleys, and ridges in the 5D potential-energy surface of ^{180}Hg (see text). At the last plotted point on the fission barrier, $(Q_2/b)^{(1/2)} \approx 11$, the asymmetry of the shape is $A_H/A_L = 108/72$.

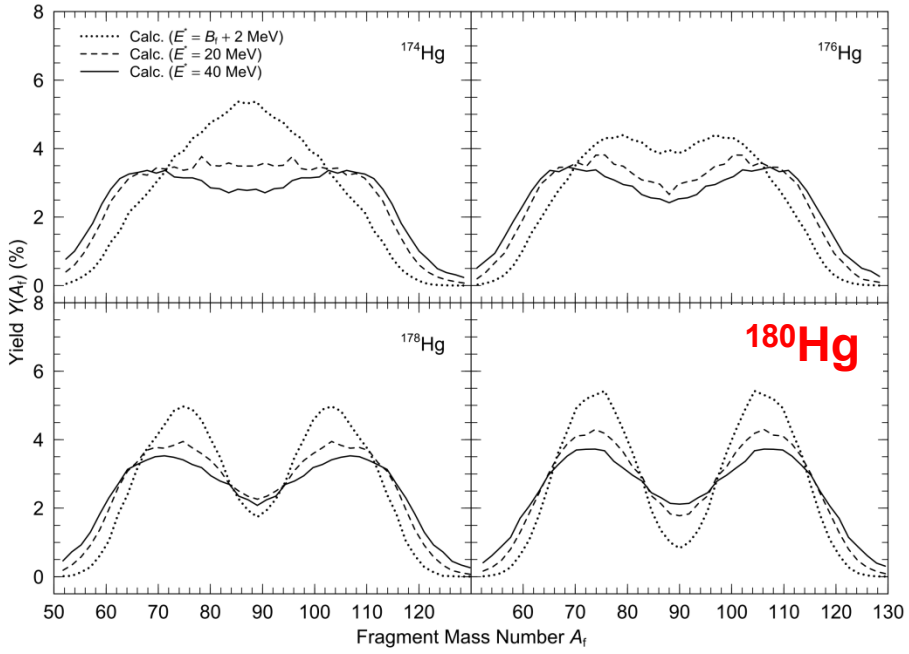

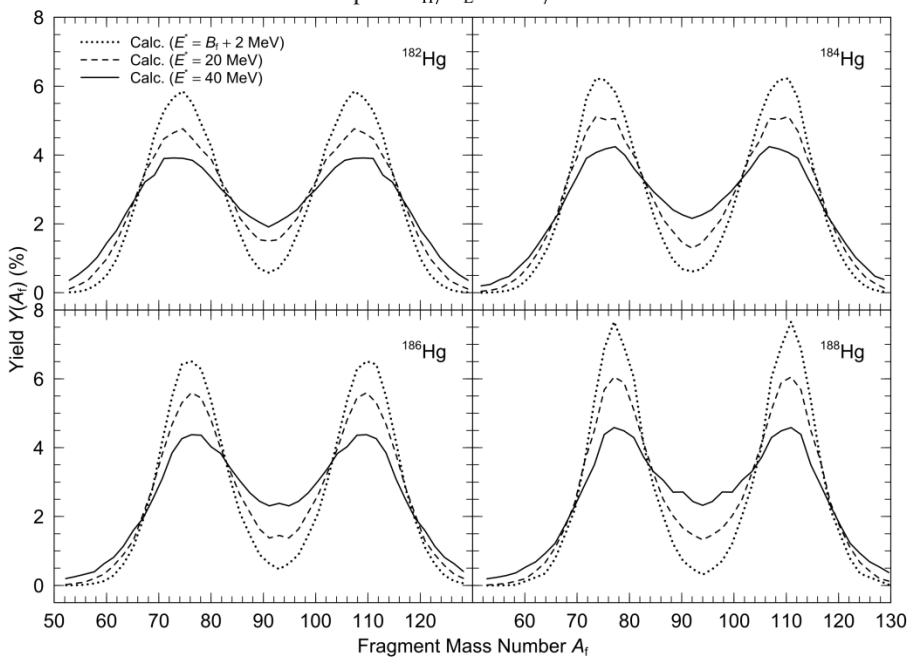

'Improved' Scission-Point Model

PHYSICAL REVIEW C **86**, 044315 (2012)

Mass distributions for induced fission of different Hg isotopes

A. V. Andreev, G. G. Adamian, and N. V. Antonenko
Joint Institute for Nuclear Research, 141980 Dubna, Russia
(Received 20 June 2012; revised manuscript received 6 September 2012; published 11 October 2012)

With the improved scission-point model mass distributions are calculated for induced fission of different Hg isotopes with even mass numbers $A = 180$, 184, 188, 192, 196, and 198. The calculated mass distribution and mean total kinetic energy of fission fragments are in good agreement with the existing experimental data. The asymmetric mass distribution of fission fragments of ^{180}Hg observed in the recent experiment is explained. The change in the shape of the mass distribution from asymmetric to more symmetric is revealed with increasing A of the fissioning ^{A}Hg nucleus, and reactions are proposed to verify this prediction experimentally.

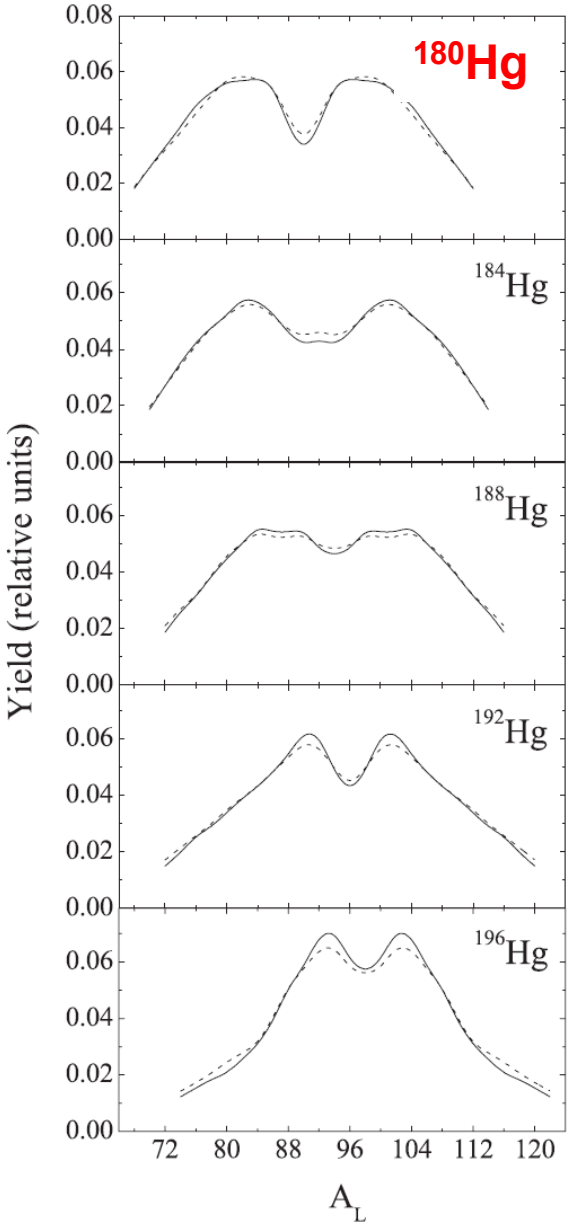

- Inter-fragment distance is not fixed and calculated.
- values of ~0.5-1 fm result (Wilkins – fixed at 1.4 fm)

- Mass symmetry/asymmetry doesn't change as a function of E* (up to E*~60 MeV) – good for future experiments

SPY self-consistent Scission-Point Model

PHYSICAL REVIEW C **86**, 064601 (2012)

Role of deformed shell effects on the mass asymmetry in nuclear fission of mercury isotopes

Stefano Panebianco, Jean-Luc Sida, Héloise Goutte, and Jean-François Lemaître
IRFU/Service de Physique Nucleaire, CEA Centre de Saclay, F-91191 Gif-sur-Yvette, France

Noël Dubray and Stéphane Hilaire
CEA, DAM, DIF, F-91297, Arpajon, France
(Received 9 October 2012; published 3 December 2012)

$$E_{\rm av}(Z_{1,2}, N_{1,2}, \beta_{1,2}, d) = E_{\rm tot} - E_{\rm HFB}(Z_1, N_1, \beta_1) - E_{\rm HFB}(Z_2, N_2, \beta_2) - E_{\rm nucl}(Z_{1,2}, N_{1,2}, \beta_{1,2}, d) - E_{\rm Coul}(Z_{1,2}, N_{1,2}, \beta_{1,2}, d).$$

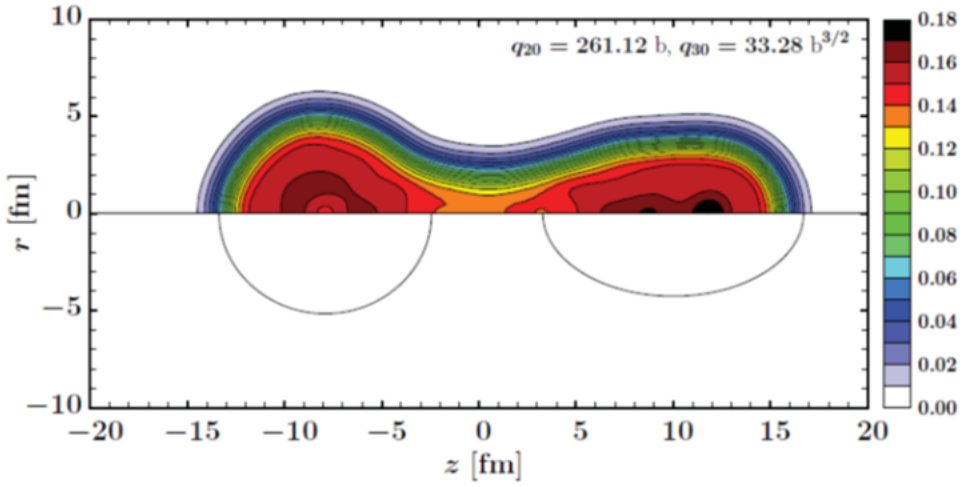

FIG. 4. (Color online) Total nuclear density for the most energetically favorable scission configuration in ^{180}Hg fission, extracted from a self-consistent HFB calculation. In the lower part of the figure, two

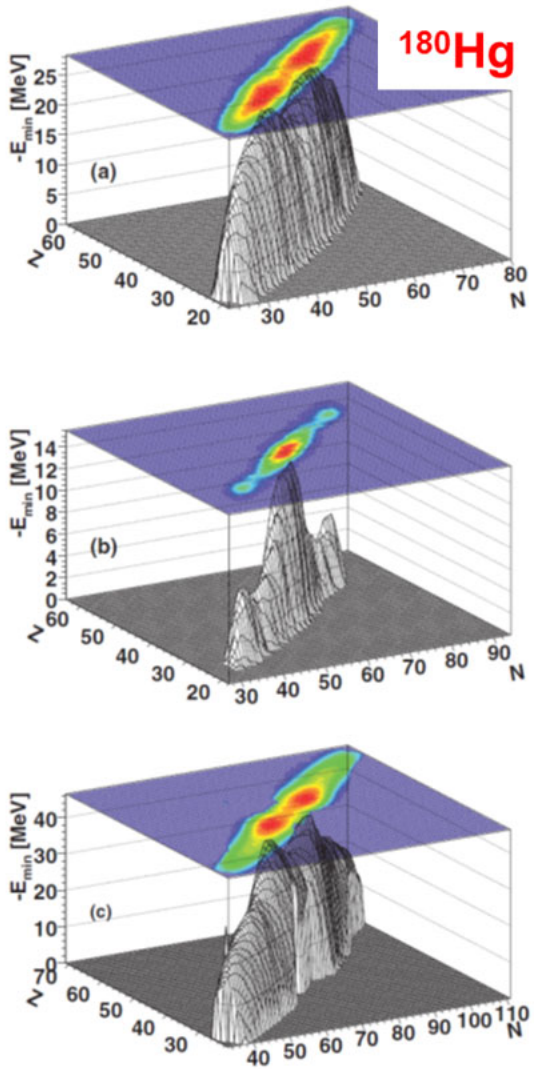

FIG. 2. (Color online) Minimum absolute available energy at scission calculated for all possible fragmentations in (a) ^{180}Hg and (b) ^{198}Hg fission at 10 MeV and in (c) the thermal n-induced fission of ^{235}U.

Mean-field HFB+Gogny D1S/SkM*

PHYSICAL REVIEW C **86**, 024601 (2012)

Fission modes of mercury isotopes

M. Warda,[1] A. Staszczak,[1,2,3] and W. Nazarewicz[2,3,4]

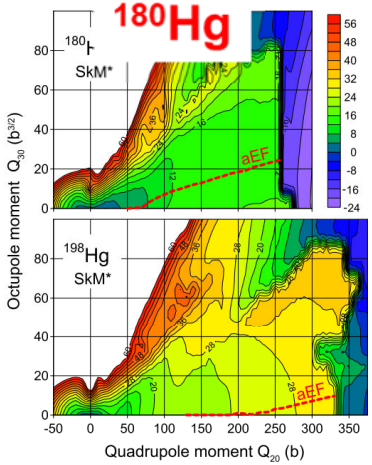

FIG. 2. (Color online) PES for ^{180}Hg (top) and ^{198}Hg (bottom) in the plane of collective coordinates $Q_{20} - Q_{30}$ in HFB-SkM*. The aEF fission pathway corresponding to asymmetric elongated fragments is marked. The difference between contour lines is 4 MeV. The effects due to triaxiality, known to impact inner fission barriers in the actinides, are negligible here.

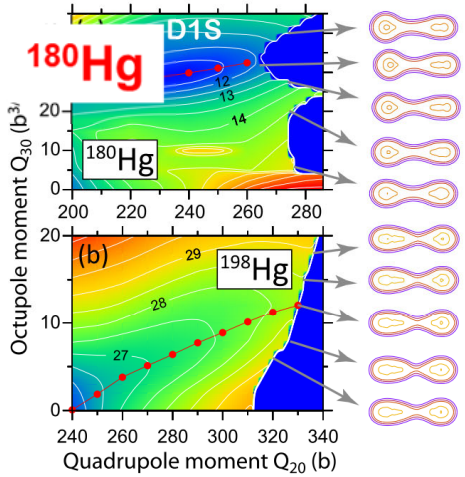

FIG. 3. (Color online) PES in HFB-D1S for ^{180}Hg (top) and ^{198}Hg (bottom) in the (Q_{20}, Q_{30}) plane in the pre-scission region of aEF valley. The symmetric limit corresponds to $Q_{30} = 0$. The aEF valley and density profiles for pre-scission configurations are indicated. The difference between contour lines is 0.5 MeV. Note different Q_{30}-scales in ^{180}Hg and ^{198}Hg plots.

PHYSICAL REVIEW C **90**, 021302(R) (2014)

Excitation-energy dependence of fission in the mercury region

J. D. McDonnell,[1,2] W. Nazarewicz,[2,3,4] J. A. Sheikh,[2,3,5] A. Staszczak,[2,6] and M. Warda[6]

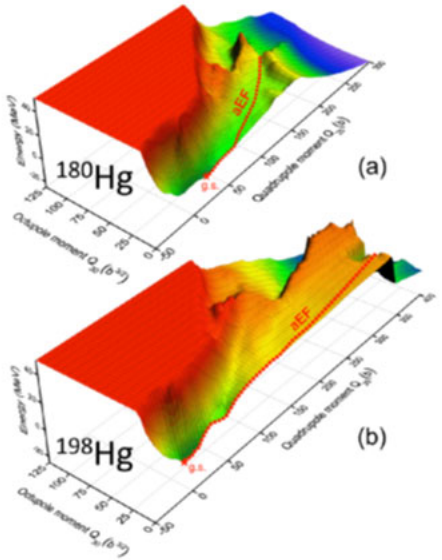

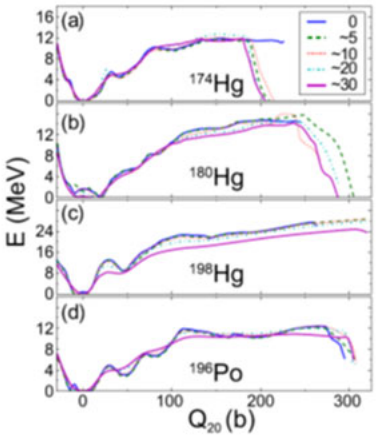

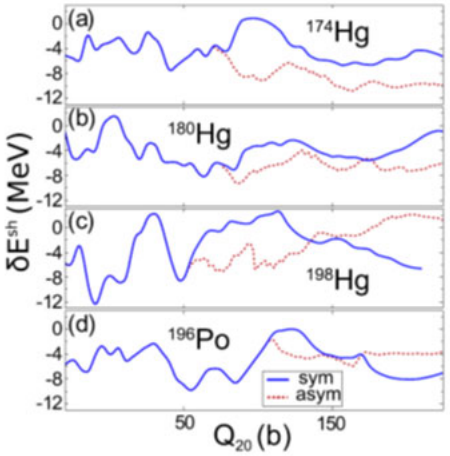

Octupole shapes of fission fragments as a culprit for mass-asymmetry?

PHYSICAL REVIEW C **100**, 041602(R) (2019)

Rapid Communications

Effect of shell structure on the fission of sub-lead nuclei

Guillaume Scamps*

Center for Computational Sciences, University of Tsukuba, Tsukuba 305-8571, Japan and Institut d'Astronomie et d'Astrophysique, UniversitéLibre de Bruxelles, Campus de la Plaine CP 226, BE-1050 Brussels, Belgium

Cédric Simenel†

Department of Theoretical Physics and Department of Nuclear Physics, Research School of Physics and Engineering, Australian National University, Canberra, Australian Capital Territory 2601, Australia

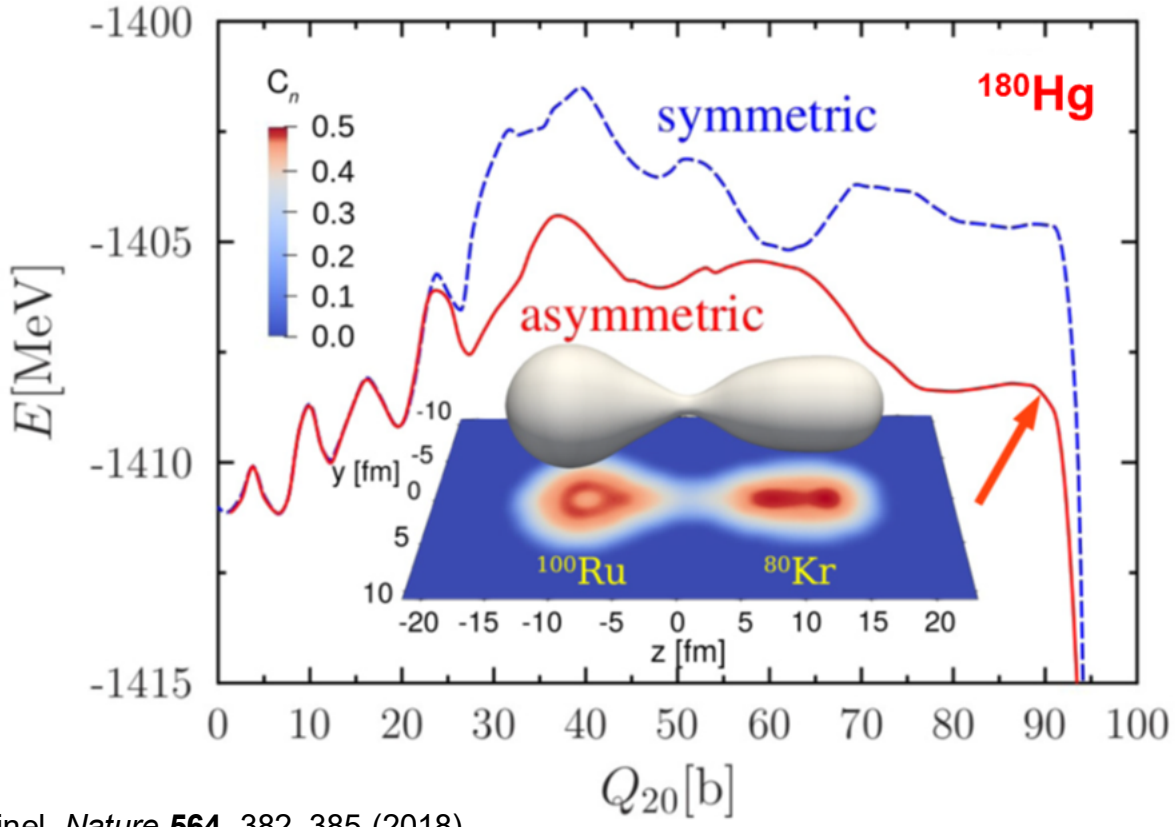

G. Scamps, C.Seminel, *Nature* **564**, 382–385 (2018)

ymmetry

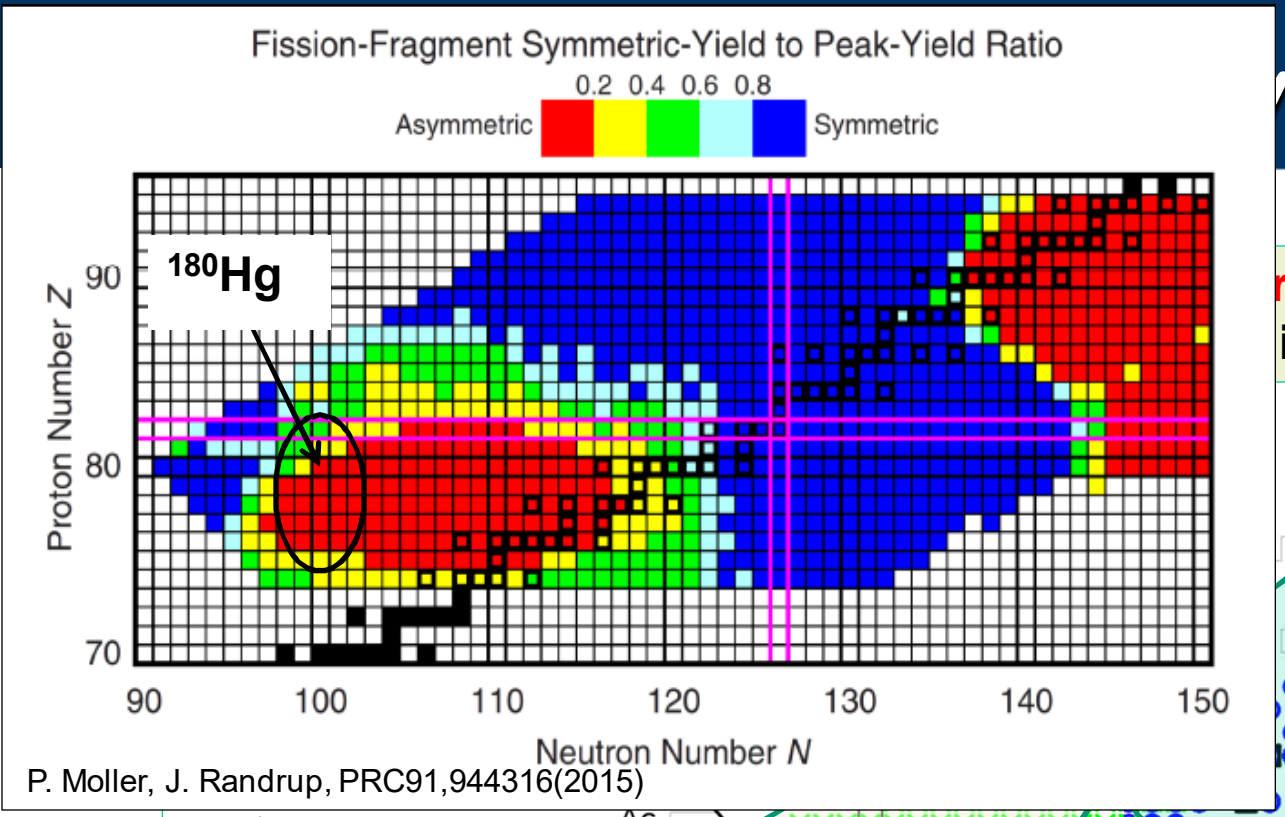

P. Moller, J. Randrup, PRC91,944316(2015)

redominantly asymmetric;
isomers

Pre-actinides, light Ir-Th N/Z~1.4-1.5: predominantly symmetric, e.g. FRS(GSI)

A.N. Andreyev, K. Nishio, K.-H. Schmidt, Reports on Progress in Fission, 1,

From Asymmetry to Symmetry
(what effect is responsible for asymmetry in the lead region?)

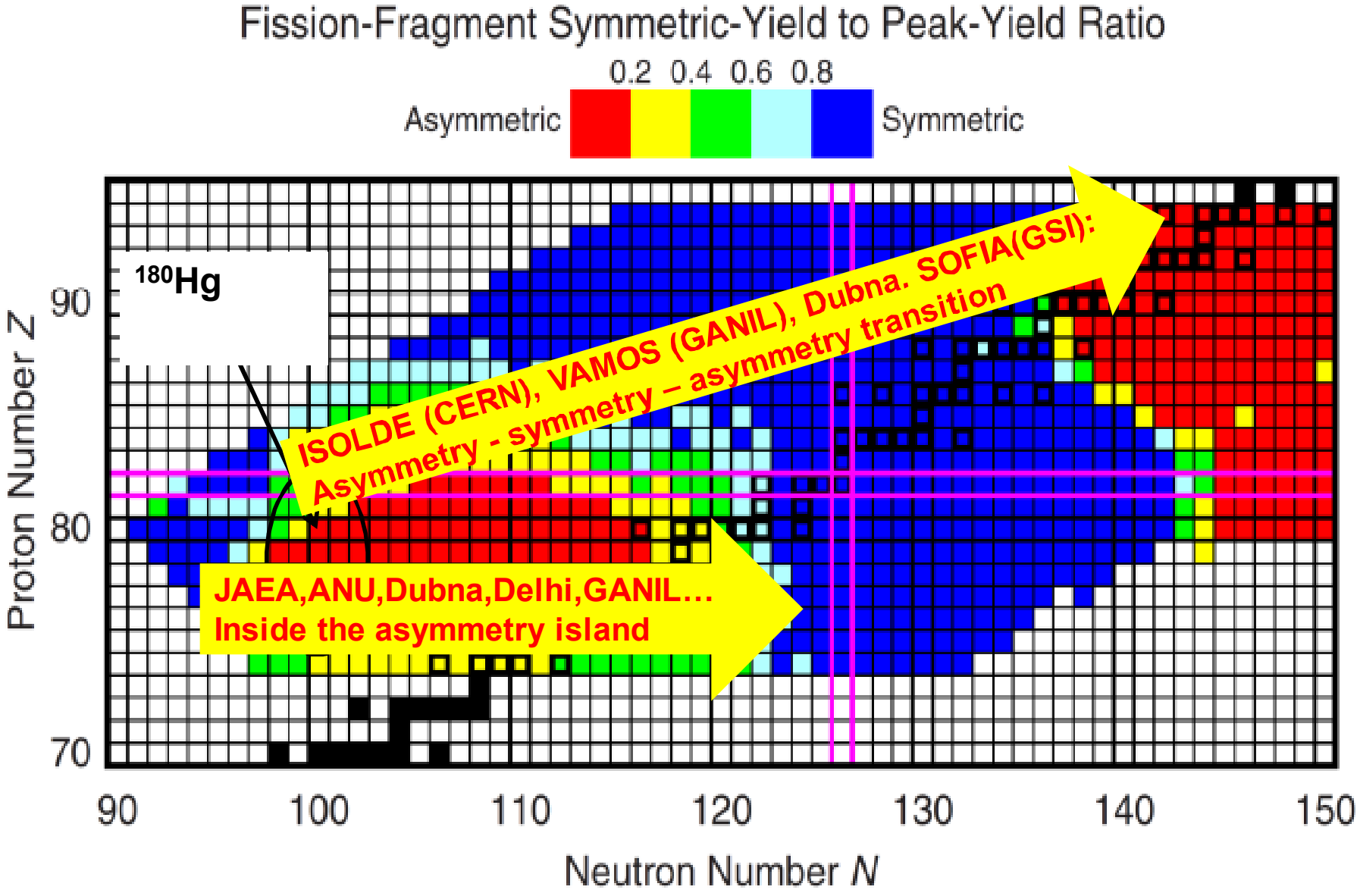

P. Moller, J. Randrup, PRC91,944316(2015)

Back to classics: 1970'ies - Fission in d,pf approach with stable/long-lived targets

Modern version - **inverse kinematics with post-accelerated RIBs at Coulomb energies impinging on a deuterated target (e.g. HIE-ISOLDE)**

1970'ies: Classical fission studies in d,pf approach: determination of fission modes and fission barriers

Fission probability as a function of E* : **direct nucleon transfer, e.g. (d,pf)** reactions with **stable/long-lived** targets.

d+^{239}Pu → ^{240}Pu*+p → 2FF+p

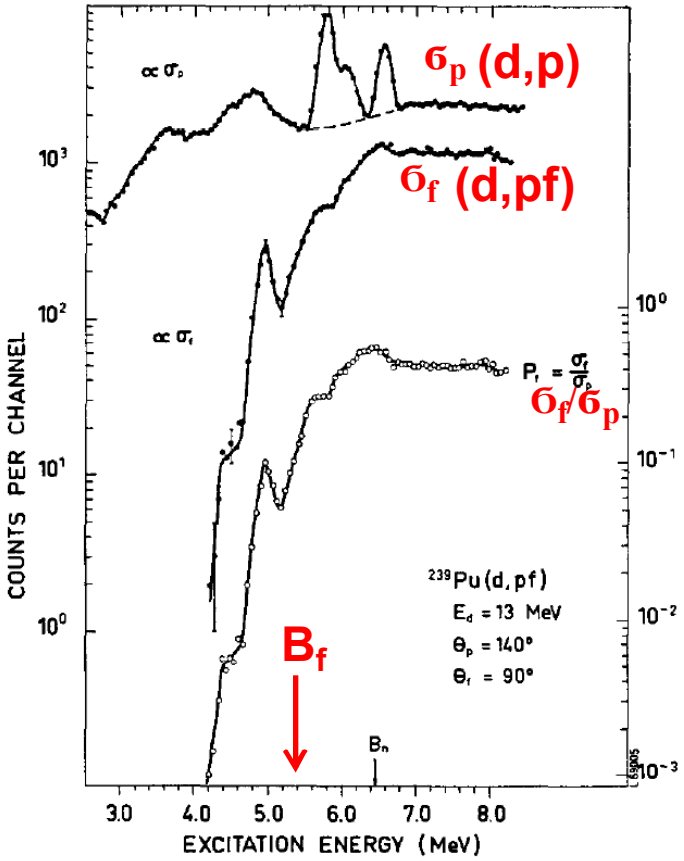

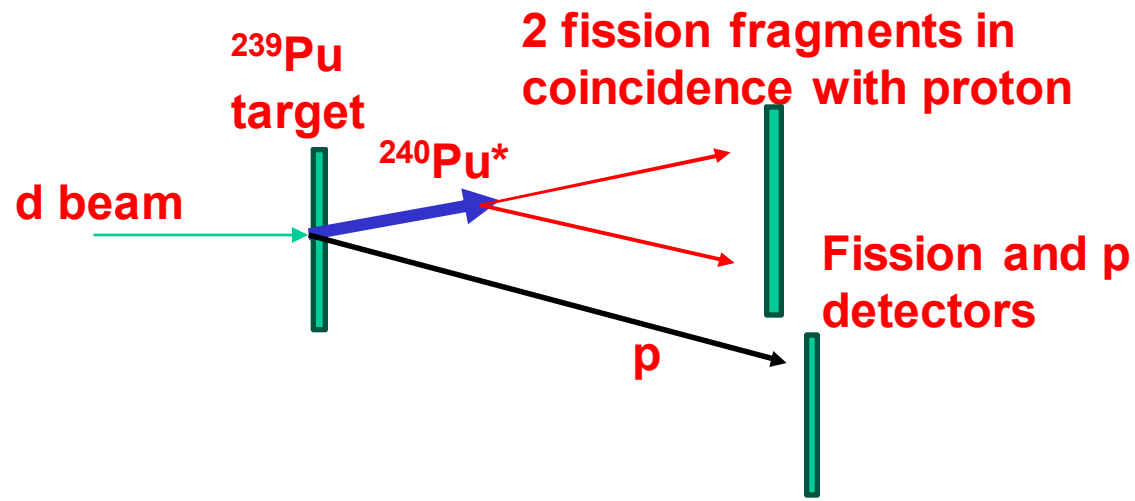

Allows to deduce e.g. the fission barrier height (with some assumptions)

$$P_{fis}(E^*) = \frac{P_0}{1+\exp\left(\frac{2\pi(B_f - E^*)}{\hbar\omega}\right)}$$

B.B. Back et al.; Nucl. Phys. **A165** (1971) 449
E. Konecny et al.; Phys. Lett. B **45** (1973) 329

Modern approach: the same reaction mechanism, but in inverse kinematics, with post-accelerated RIB's

Example-1: ^{209}Fr (51 s)+d → ^{210}Fr*+ p → 2FF+p

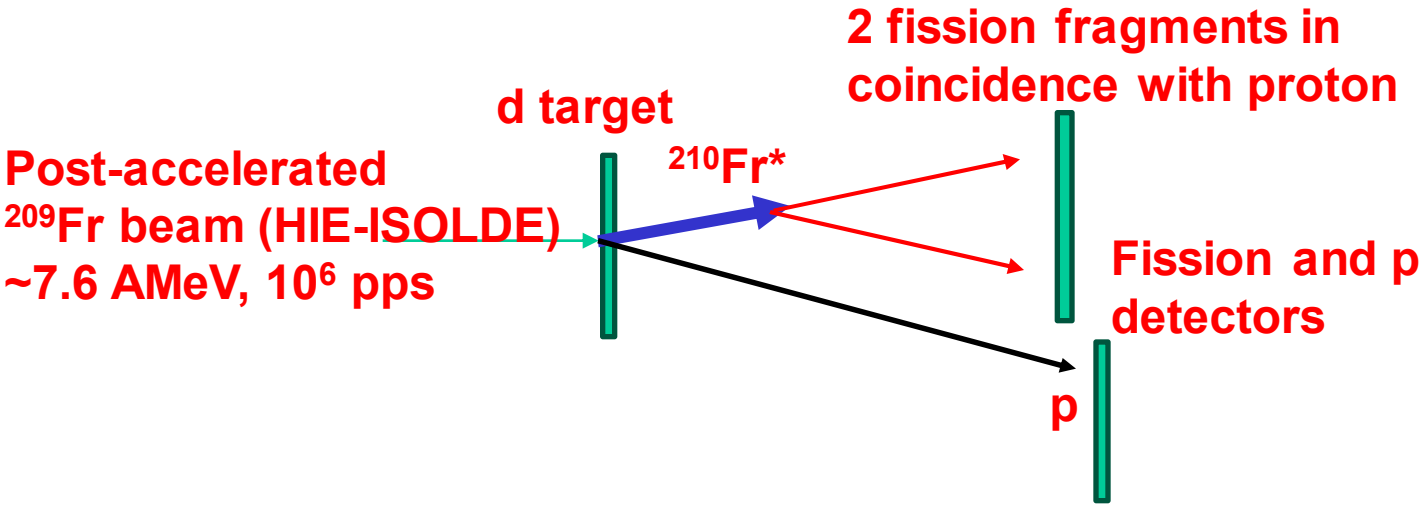

Main advantages in comparison to 'old' direct kinematics

1. Allows to study fission of **("any") RIB's**, even very short-lived
2. Higher fission fragment energies (easier identification of E, A, Z)
3. Kinematical focusing due to inverse reaction (easier identification)

Fission of ^{210}Fr with ACTAR@HIE-ISOLDE

ACTAR – time-projection chamber, filled with d gas

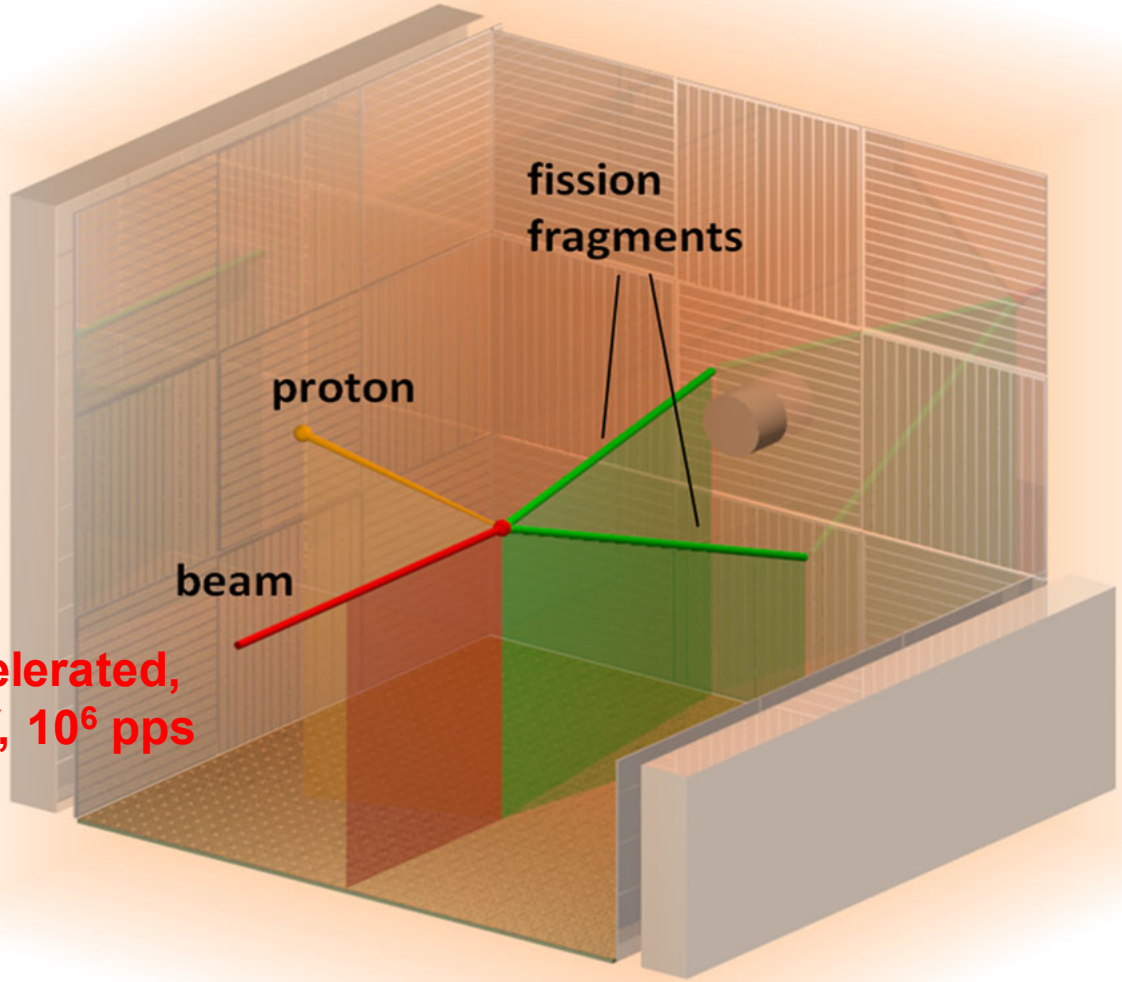

HIE-ISOLDE post-accelerated,
^{209}Fr beam, ~7.6 AMeV, 10^6 pps

Fission of ^{210}Fr with ACTAR@HIE-ISOLDE

PHYSICAL REVIEW C **109**, 014618 (2024)

Determination of fission barrier height of ^{210}Fr and ^{210}Ra via neutron measurement

M. Veselský,* P. Rubovič, V. Petousis,† H. Natal da Luz, P. Burian, P. Mánek, L. Meduna, and P. Smolyanskiy
Institute of Experimental and Applied Physics, Czech Technical University, Husova 240/5, 11000 Prague, Czechia

R. Raabe, A. Camaiani, J. Klimo, O. Poleshchuk, A. Youssef, A. Ceulemans, and M. Latif
KU Leuven, Instituut voor Kern- en Stralingsfysica, Celestijnenlaan 200d, 3001 Leuven, Belgium

M. Jandel
Department of Physics and Applied Physics, University of Massachusetts Lowell, Lowell, Massachusetts 01854, USA

M. Bírová, A. Herzán, A. Špaček, and M. Venhart
Institute of Physics, Slovak Academy of Sciences, Dúbravská cesta 9, 845 11 Bratislava, Slovakia

M. G. Pellegriti
INFN Catania, Via Santa Sofia 64, 95123 Catania, Italy

A. N. Andreyev and C. Page
School of Physics, Engineering and Technology, University of York, Heslington, York YO10 5DD, United Kingdom

G. A. Souliotis
Laboratory of Physical Chemistry, Department of Chemistry, National and Kapodistrian University of Athens, Zografou, 157 71 Athens, Greece

R. Lica
ISOLDE, CERN, Espl. des Particules 1, 1211 Meyrin, Switzerland and Horia Hulubei National Institute for Physics and Nuclear Engineering - IFIN-HH, R-077125, Bucharest, Romania

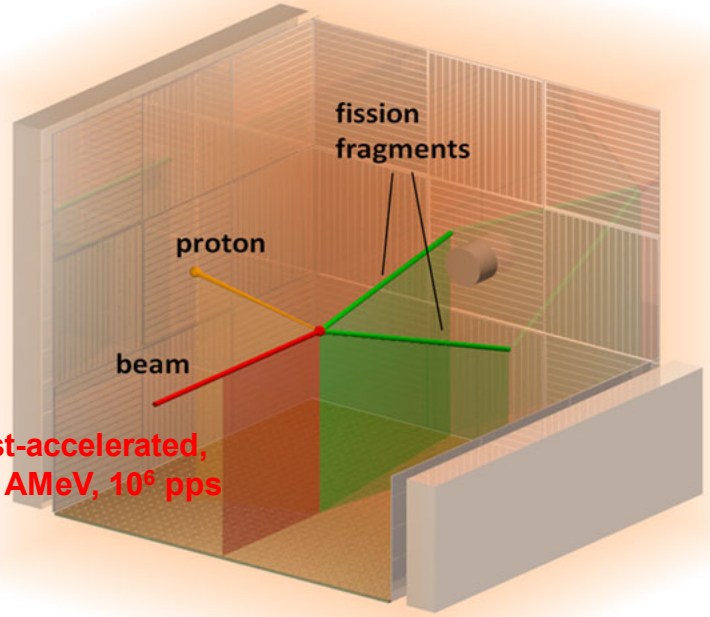

HIE-ISOLDE post-accelerated, ^{209}Fr beam, ~7.6 AMeV, 10^6 pps

Fission barrier heights of short-lived nuclei away from line of β stability are not known reliably. Low-energy fission of ^{210}Fr and ^{210}Ra, produced by (d, p) and (d, n) transfer reaction on the re-accelerated unstable beam ^{209}Fr was investigated at HIE-ISOLDE. Four Timepix3 pixel detectors were installed on the body of the ACTAR TPC demonstrator chamber. Polyethylene converters were used for the detection of fast neutrons. Since no significant background was observed, it was possible to measure the spatial distribution of emitted neutrons reflecting the fission excitation function. Subsequent simulations employing the results of the TALYS code and available data on fission fragment distributions allowed to estimate directly the value of the fission barrier height for the neutron-deficient nucleus ^{210}Fr. This first direct measurement confirmed the reduction of the fission barrier compared to available theoretical calculations by 15–30%.

Example-2: d,pf transfer-induced fission of post-accelerated RIBs in inverse kinematics with ISOLDE Solenoidal Spectrometer (ISS-ISOLDE)

Usual MRI magnet from a hospital (after some refurbishing)

HELIOS@ANL-ISS(ISOLDE) Collaboration
(a proof-of-principles experiment with stable ^{238}U)

PHYSICAL REVIEW LETTERS **130,** 202501 (2023)

Direct Determination of Fission-Barrier Heights Using Light-Ion Transfer in Inverse Kinematics

S. A. Bennett,[1] K. Garrett,[1] D. K. Sharp,[1,*] S. J. Freeman,[1,2] A. G. Smith,[1] T. J. Wright,[1] B. P. Kay,[3] T. L. Tang,[3,†] I. A. Tolstukhin,[3] Y. Ayyad,[4] J. Chen,[3] P. J. Davies,[5] A. Dolan,[6] L. P. Gaffney,[6] A. Heinz,[7] C. R. Hoffman,[3] C. Müller-Gatermann,[3] R. D. Page,[6] and G. L. Wilson[8,3]

[1]*Department of Physics and Astronomy, University of Manchester, Manchester M13 9PL, United Kingdom*
[2]*CERN, CH-1211 Geneva 23, Switzerland*
[3]*Physics Division, Argonne National Laboratory, Lemont, Illinois 60439, USA*
[4]*IGFAE, Universidade de Santiago de Compostela, E-15782 Santiago de Compostela, Spain*
[5]*School of Physics, Engineering and Technology, University of York, Heslington, York YO10 5DD, United Kingdom*
[6]*Oliver Lodge Laboratory, University of Liverpool, Liverpool L69 7ZE, United Kingdom*
[7]*Chalmers University of Technology, SE-41296 Göteborg, Sweden*
[8]*Louisiana State University, Baton Rouge, Louisiana 70803, USA*

variables. The fission-barrier height of ^{239}U has been determined via the ^{238}U(d, pf) reaction in inverse kinematics, the results of which are consistent with existing neutron-induced fission data indicating the validity of the technique.

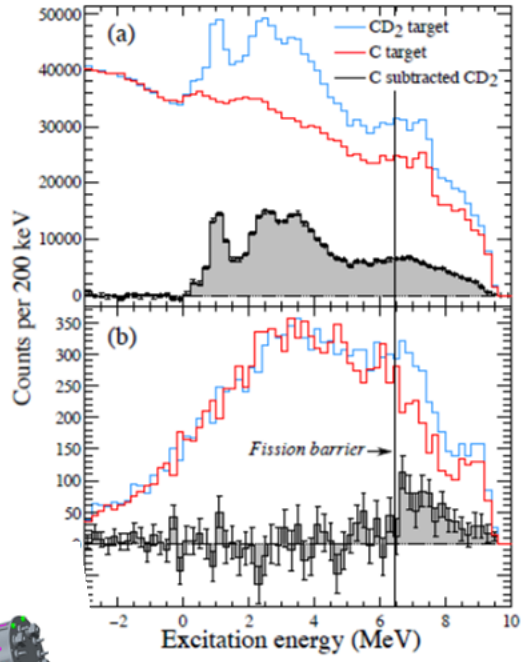

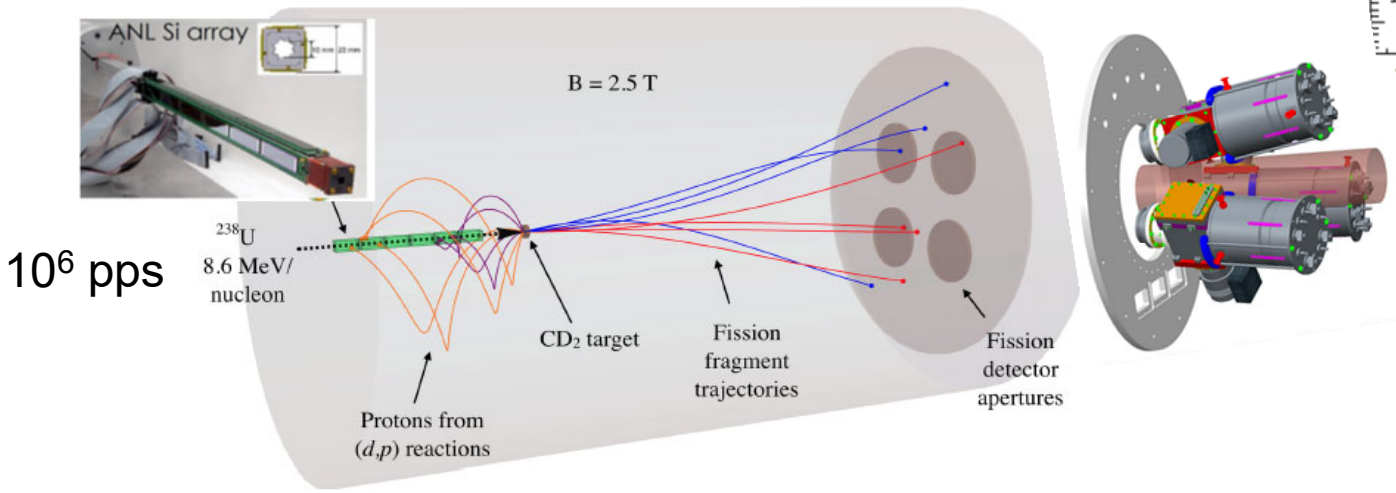

10^6 pps

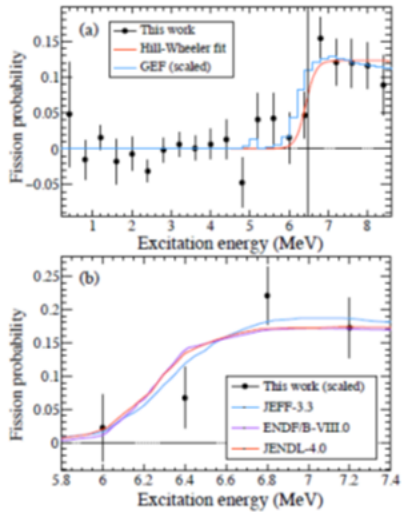

FIG. 1. To-scale schematic of the experimental setup with example particle trajectories for ^{238}U(d, pf) events. Example proton trajectories for reactions populating the ground state in ^{239}U (orange curves) and states at 7 MeV close to the fission barrier (purple curves) are shown for a range of c.m. proton angles. Example fission fragment trajectories are also shown for fragments with $A = 138$ (red curves) and $A = 100$ (blue curves), for a range of emission angles. The equally spaced circular detector apertures have radius 8 cm, and are centered 18 cm from the beam axis. The axial distance between the target and detector apertures is 70 cm.

What shells (protons? neutrons? both?) are responsible for asymmetric fission?

Dominance of proton shell effects in low-energy fission?

K. Mahata et al, PLB825, 136859 (2022) – including analysis of existing fusion-fission data in the lead region (relatively low A, Z resolution, typically a few units).

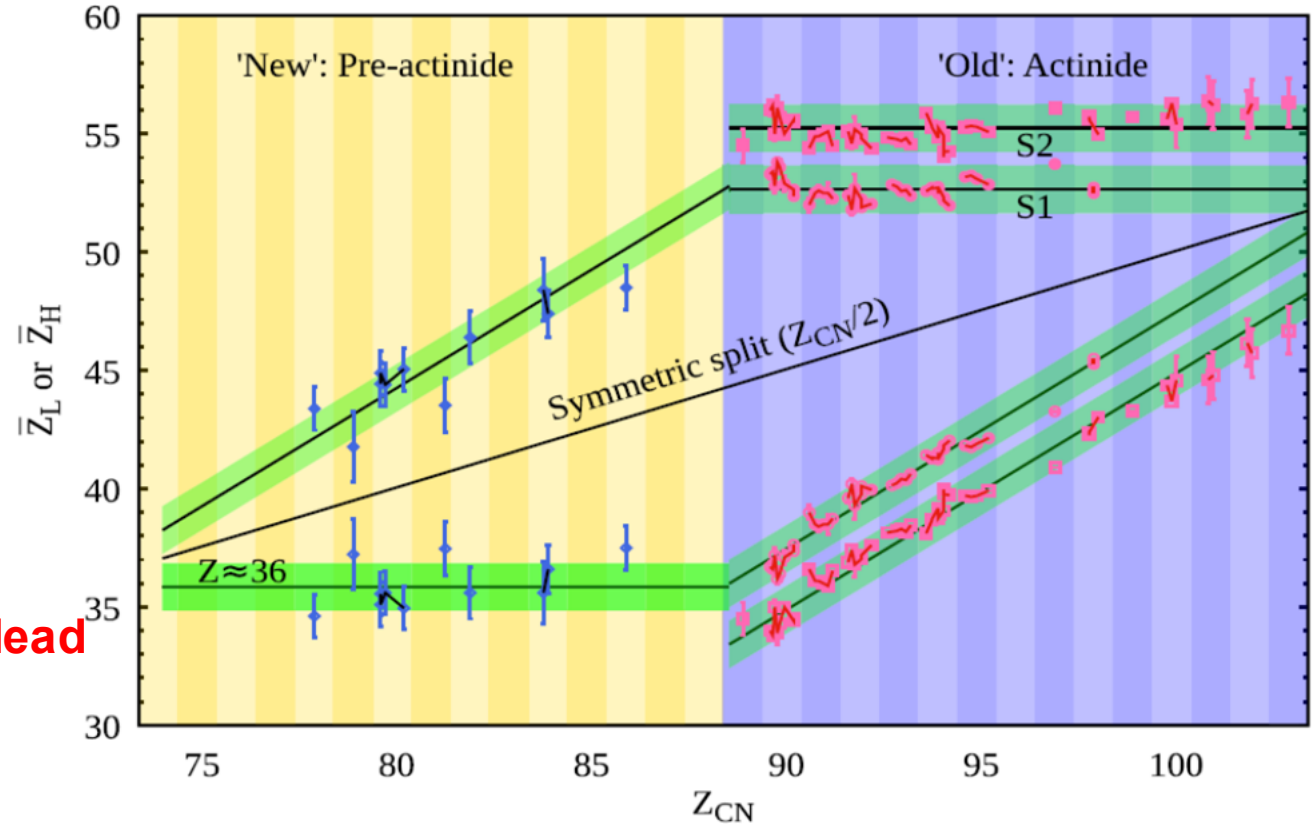

Z~52,54
Heavy actinides

Z~36
Sub-lead

Fig. 4. Evolution of the average $\bar{Z}_{L(H)}$ positions for the asymmetric fission channel as a function of Z_{CN} from above rare-earth to very-heavy and super-heavy elements. For clarity, isotopes of a same element are connected by a black segment and shifted according to the difference between their masses. The points are from

Low-Energy Fission of Relativistic RIBs in inverse kinematics at SOFIA@GSI (Coulex-induced and p,2pf reactions)

Two-step RIBs production at SOFIA@GSI

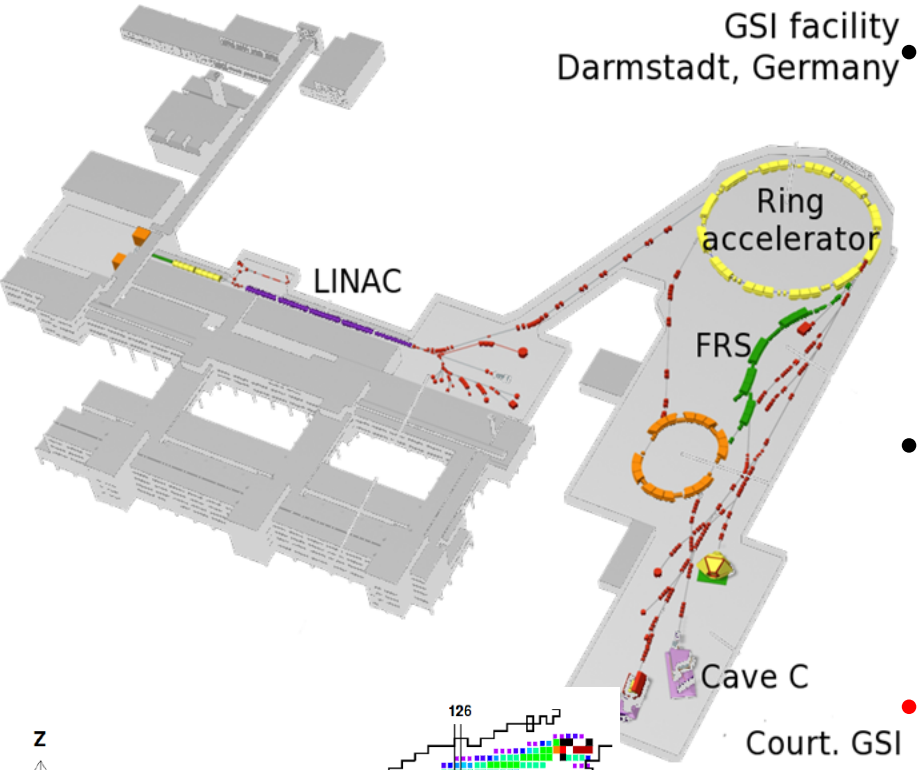

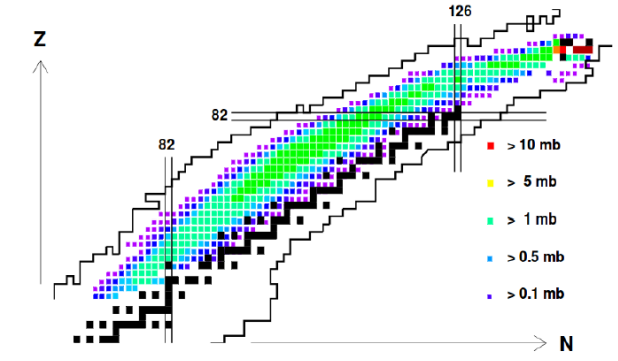

Figure 15. Measured formation cross sections of spallation residues, produced in the reaction ^{238}U (1 A GeV) + ^{2}H, are

- **Primary beam of ^{238}U, 1 A GeV**
- **Fragmentation reaction on a light target, e.g. Be** produces **secondary beam of fissile ions at ~700 AMeV (from Mercury up to Neptunium)**, sorted through FRS
- **Selected secondary ions from FRS** sent to Cave C for the fission experiment
- **Fission induced in-flight by Coulomb excitation on a heavy secondary Pb target (E*~12 MeV)**
- **Both fission fragments identified simultaneously, both in mass and in charge (FF's are at ~600 AMeV!)**

SOFIA Setup in Cave-C

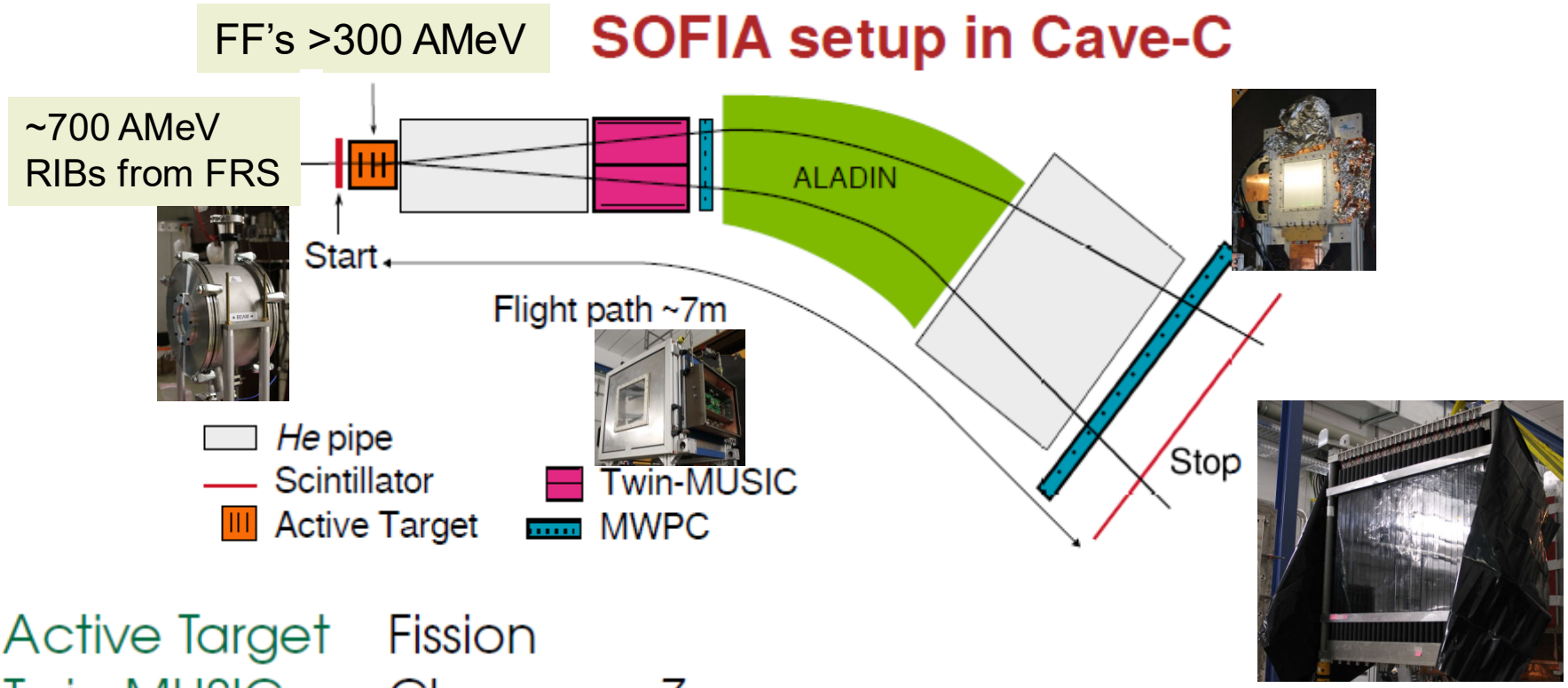

Active Target	Fission	
Twin-MUSIC	Charges	Z
MWPCs	Positions	ρ
ToF	Velocity	$\gamma\ v$
ALADIN	Dipole	B

$$(B\rho, Z, \gamma v) \rightarrow A$$

Two-step production at SOFIA@GSI

Some of the main advantages:

- **fission fragments are at much higher energies (~200-600 AMeV), thus much easier to identify their A and Z**
- **Emission of neutrons (neutron multiplicity) is easier to study (due to their kinematic focusing)**

BUT: Needs a much more complex production method and detection system (e.g. R3B, SAMURAI)

Some examples … (note fantastic A and Z resolution, hardly achievable by other techniques)

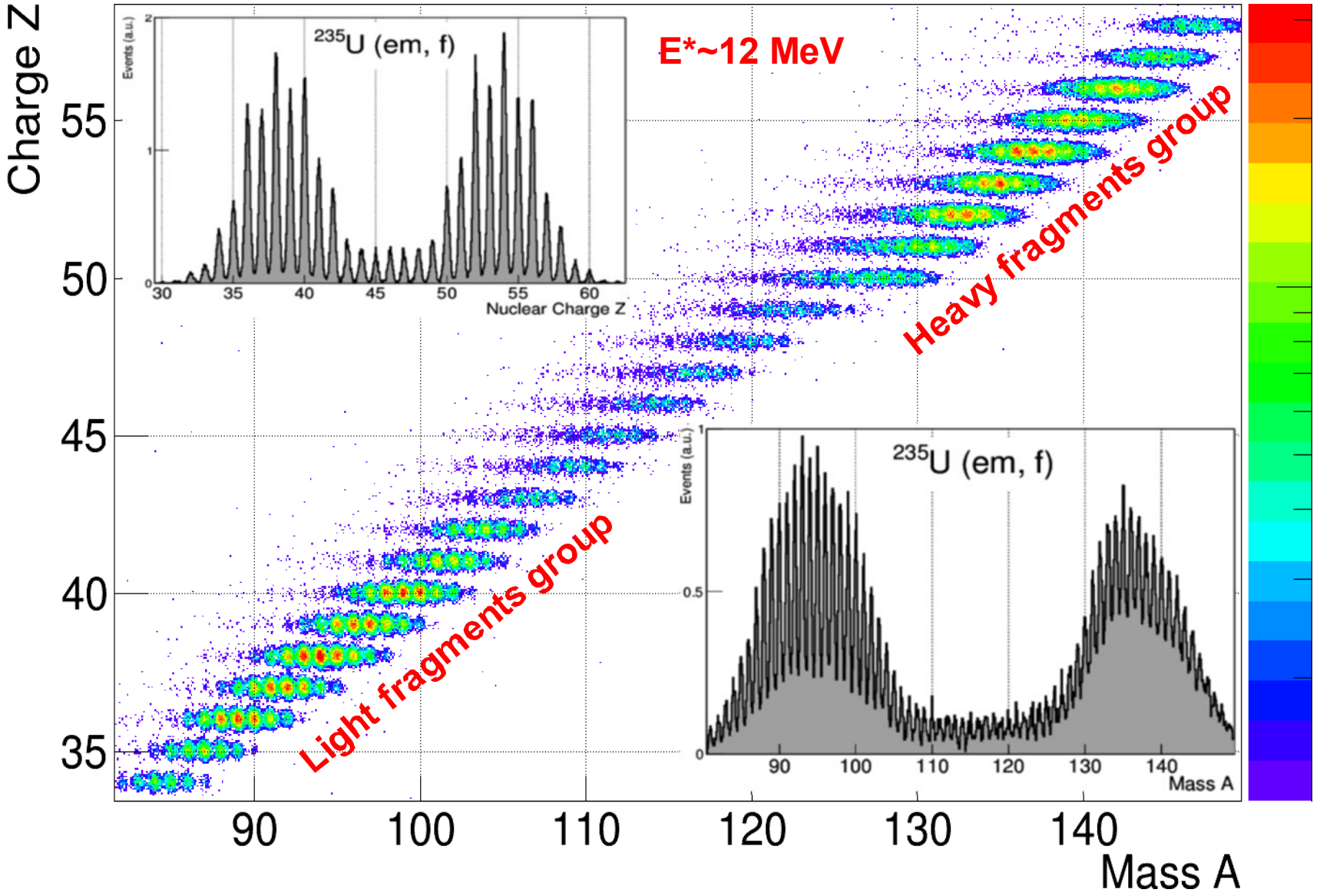

Detailed studies of EM-induced multi-modal fission in Ac-Th isotopic chains

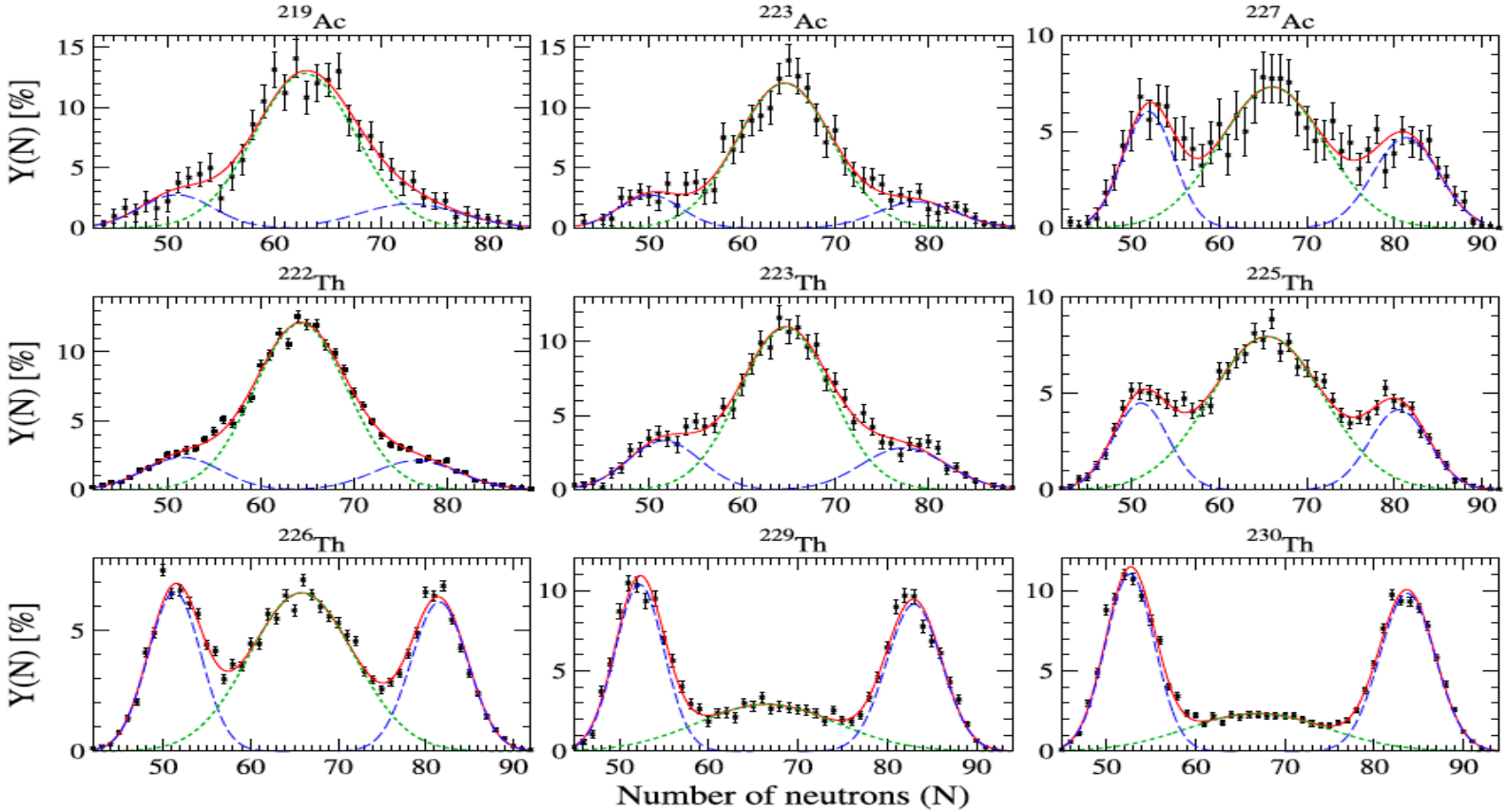

FIG. 1. Isotonic yields after prompt-neutron emission for each of the actinium and thorium isotopes fitted by a 3-Gaussian function. The data measured from the R3B/SOFIA experiments are in black. The error bars represent the statistical uncertainties. The total fit (full red lines) is decomposed into one symmetric (dotted green lines) and two asymmetric (dashed blue lines) components.

A. Chatillon et al. Phys. Rev. Lett. **124**, 202502 (2020)
A. Chatillon et al., PHYSICAL REVIEW C 106, 024618 (2022)

Dominance of Z=54 shell in fission of Ac-Pu

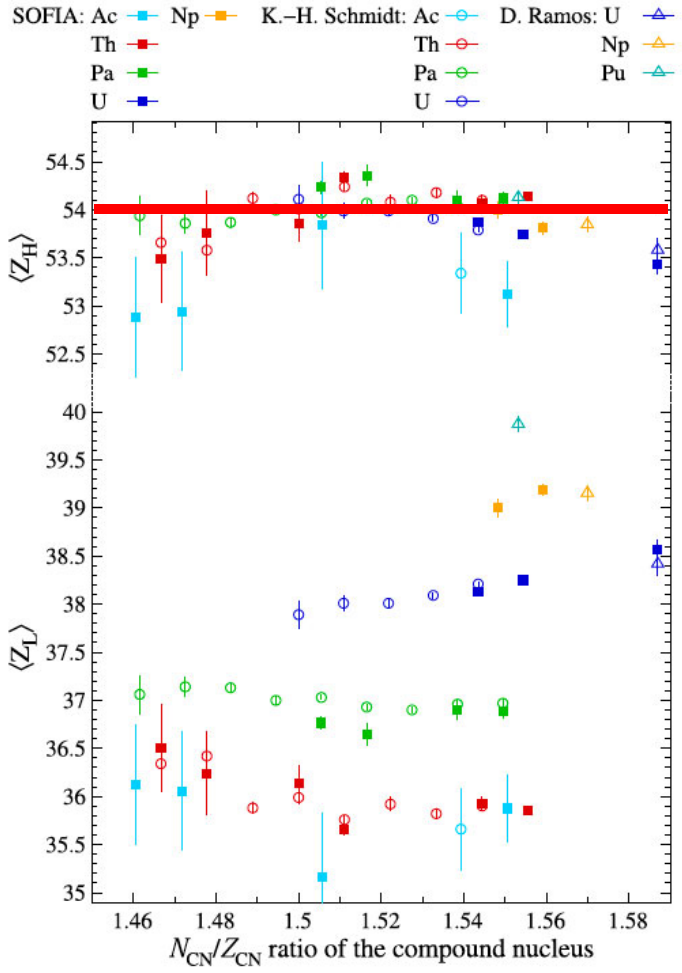

FIG. 4. The average value of the atomic number of the light and heavy fission fragments measured at R3B/SOFIA (full squares) are compared with data from Refs. [18,19] (open circles) and [24] (open triangles).

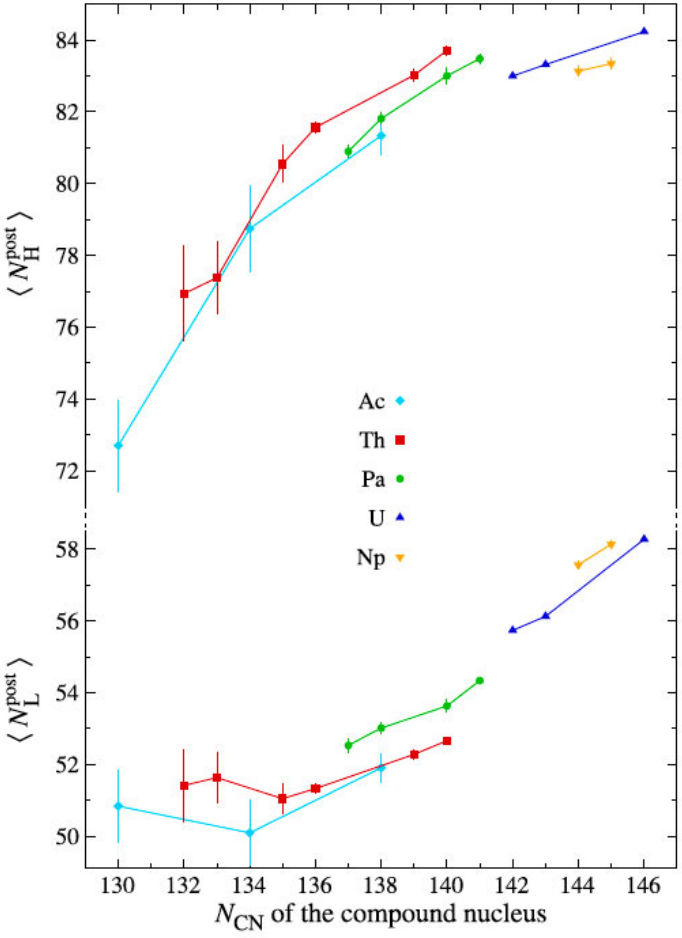

FIG. 5. Centroid positions of the light and heavy peaks of the isotonic yields measured after the prompt-neutron evaporation phase.

A. Chatillon et al., PHYSICAL REVIEW C 106, 024618 (2022)

SOFIA 2025: An asymmetric fission island driven by shell effects in light fragments

Article Nature, 641, 339 (2025)

An asymmetric fission island driven by shell effects in light fragments

https://doi.org/10.1038/s41586-025-08882-7
P. Morfouace[1,2✉], J. Taleb[1,2], A. Chatillon[1,2], L. Audouin[3], G. Blanchon[1,2], R. N. Bernard[4],

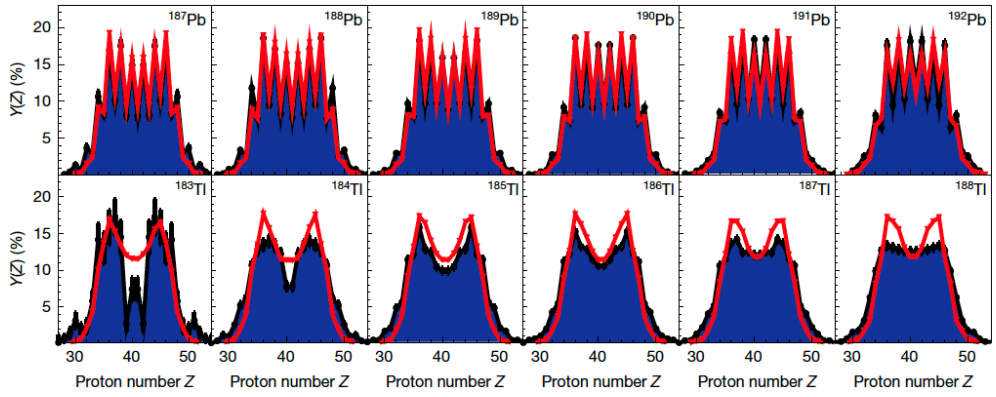

Fig. 3 | Charge yields of thallium and lead isotopes. Measured charge yields corresponding to statistical uncertainties are visible if not smaller than the

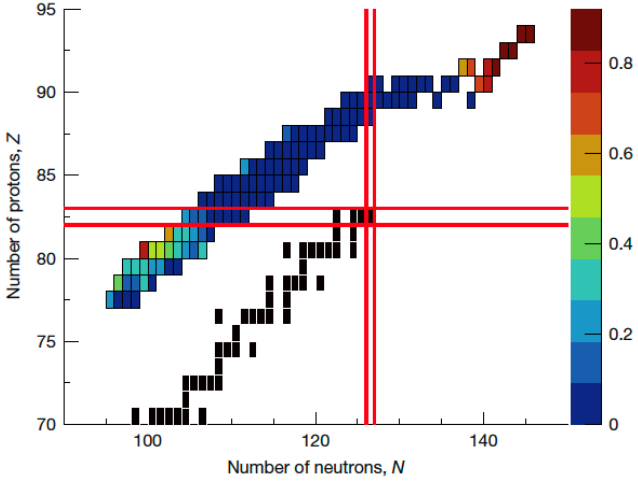

Fig. 2 | Map of the evolution of asymmetric fission. Experimental asymmetry

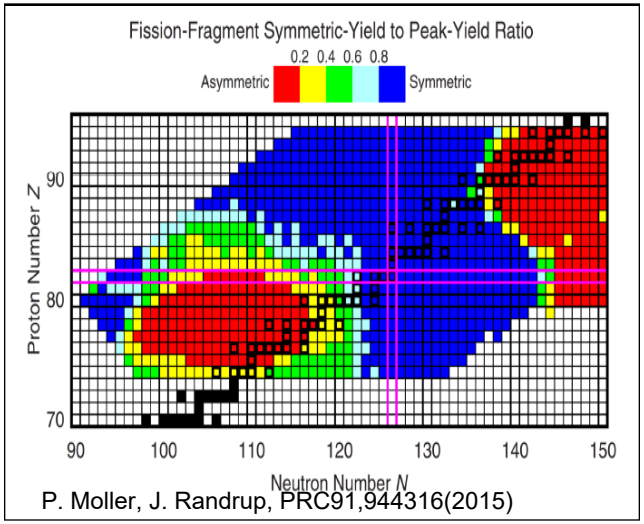

P. Moller, J. Randrup, PRC91,944316(2015)

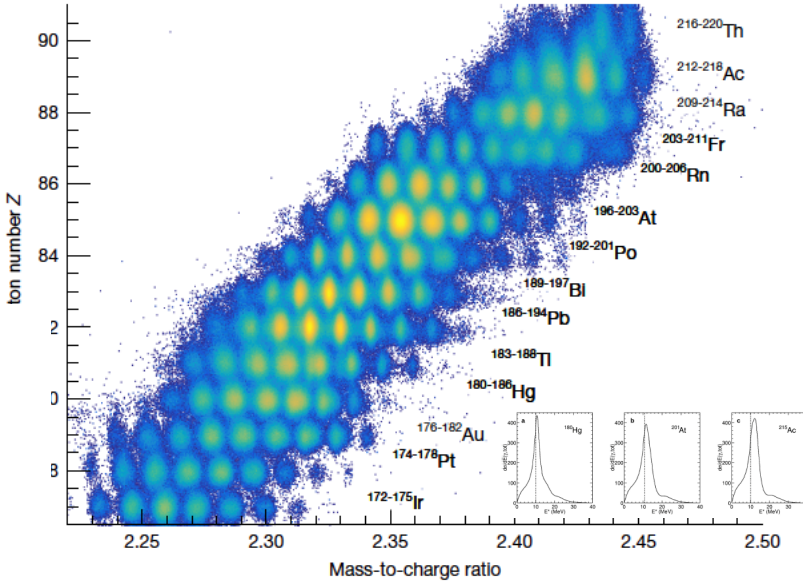

| Particle identification plot of the secondary beam. Particle

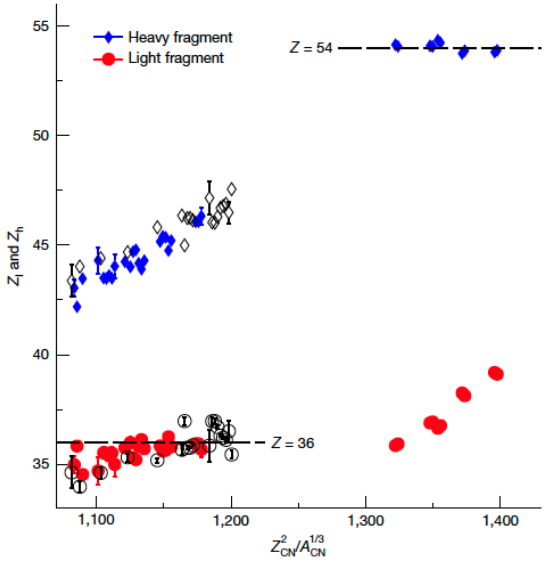

Fig. 4 | Evidence of Z = 36 stabilization of the light fragments. Light (red

ECDF: Q_{EC}-B_f systematics for heavy actinides

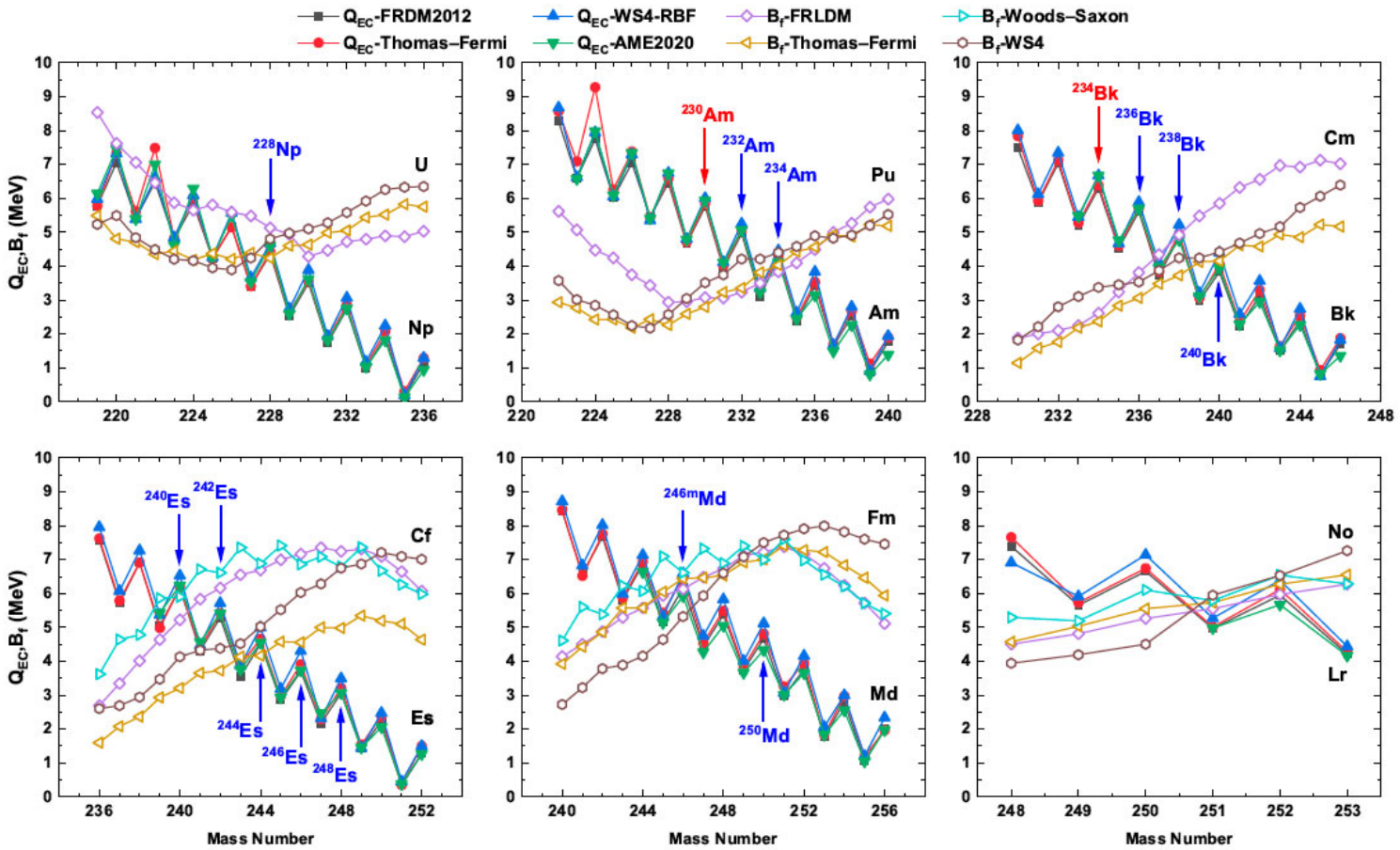

- Note the strong dependence on the fission barrier model for some isotopic chains!
- Very favorable conditions for the lightest Am and Bk chains with Q_{EC}-B_f >>0.
- $Q_{EC,exp}(^{234}Bk)$=6.5 MeV, $B_{f,calc}(^{234}Cm)$~2.5 MeV, with Q_{EC}-B_f =4 MeV
- Thus, we looked in the ECDF decay of ^{234}Bk and ^{230}Am at SHANS2

this work are shown in red.

Slide courtesy Z. C. Li, to be submitted to PRC soon

ECDF of ^{234}Bk at SHANS2(IMP-Lanzhou)

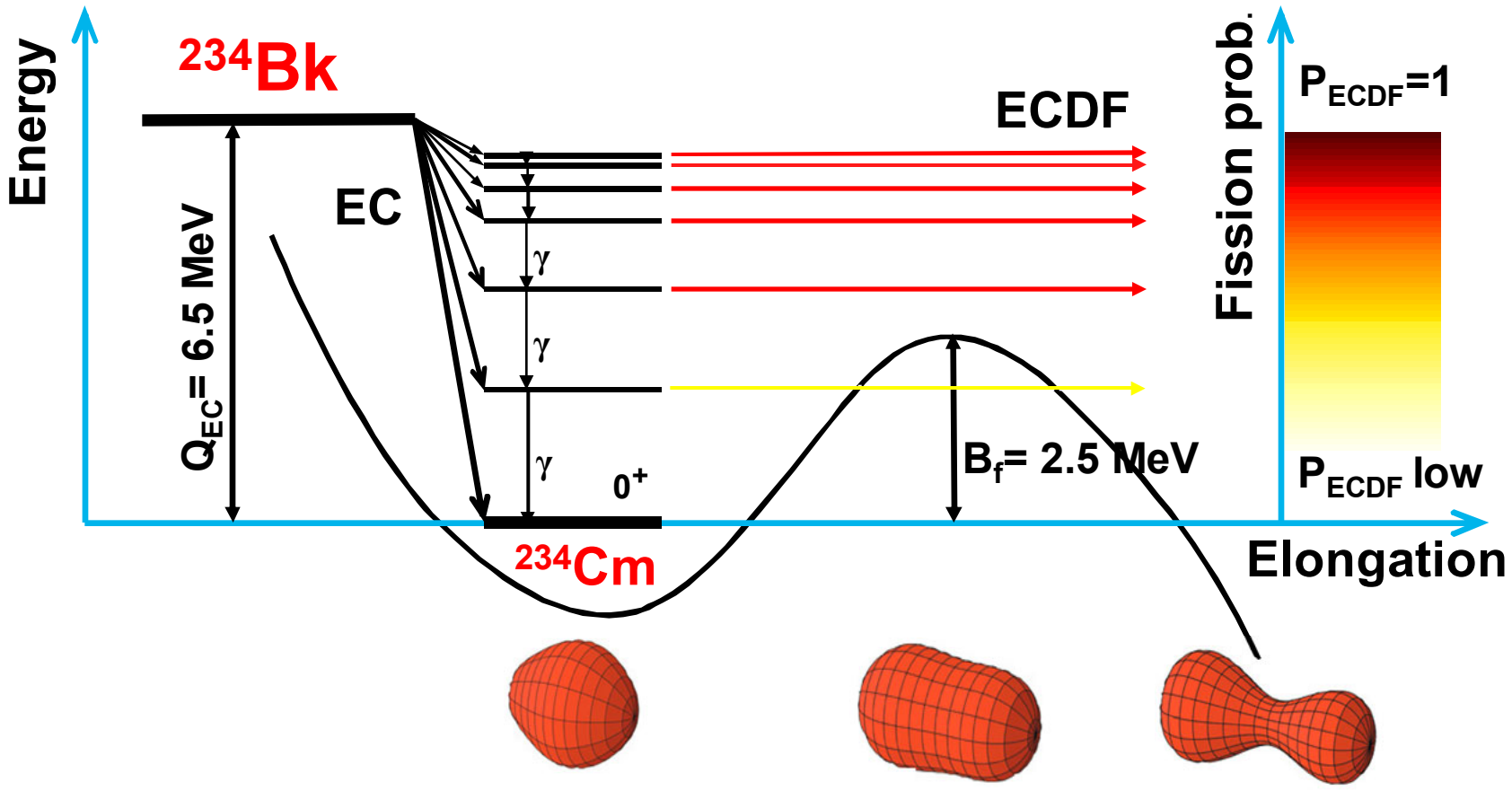

- Low-energy fission, E*<6.5 MeV, limited by Q_{EC}
- **$Q_{EC}(^{234}Bk)$-$B_f(^{234}Cm)$=4 MeV (FRDM/FRLDM values used)**

Gas-filled Recoil Separator SHANS2@IMP(Lanzhou, China)

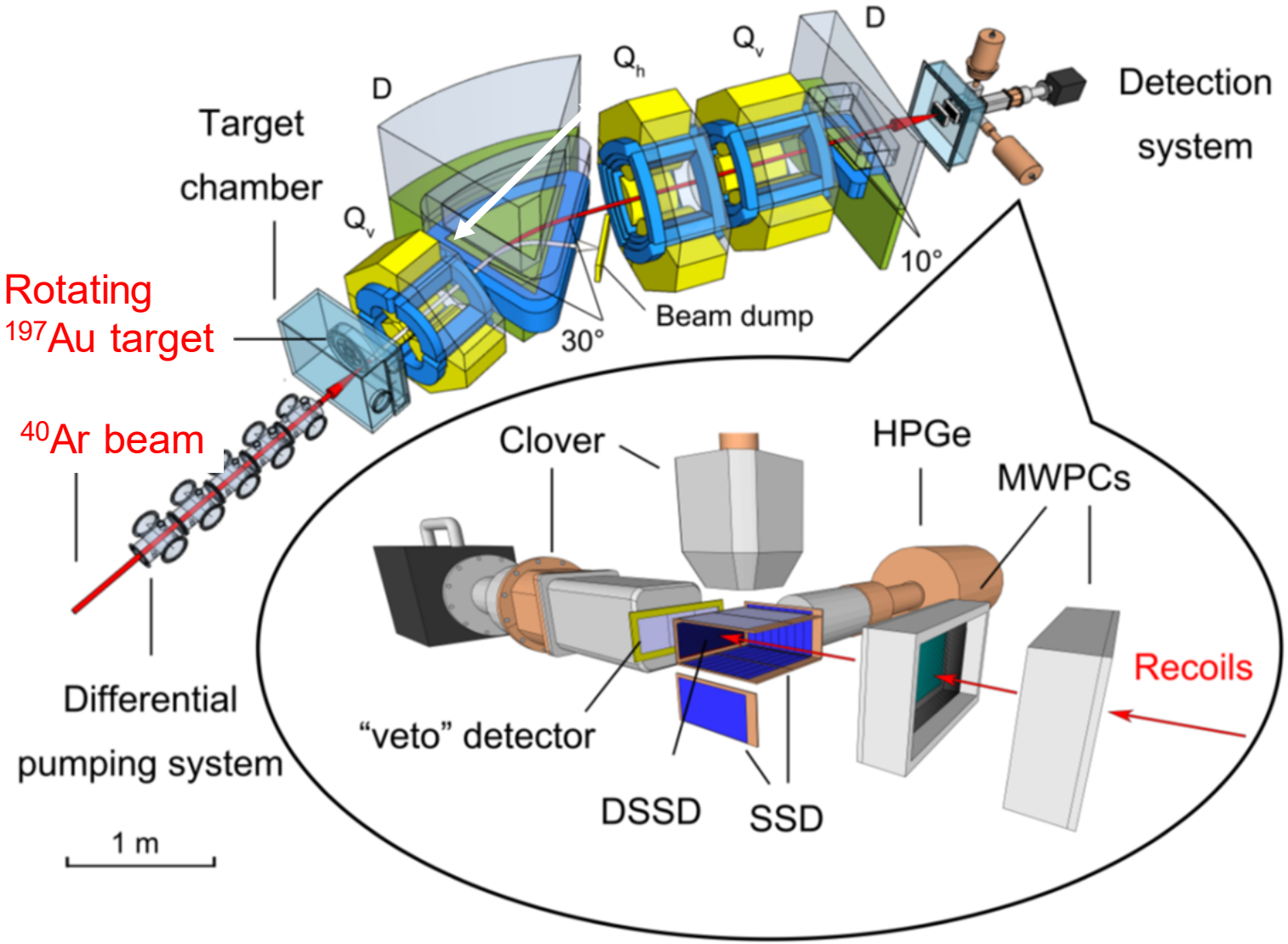

^{234}Bk decay scheme

(Z. Y. Zhang et al, submitted to PRL, March 2026)

Z. Y. Zhang (张志远),[1,2] Z. C. Li (李宗池),[1,2] J. G. Wang (王建国),[1,2,*] Z. G. Gan (甘再国),[1,2,3,†] A. N. Andreyev,[4,5,‡] M. H. Huang (黄明辉),[1,2,3] L. Ma (马龙),[1,3] H. B. Yang (杨华彬),[1,2] M. M. Zhang (张明明),[1,2] B. Andel,[6] S. Antalic,[6] F. P. Heßberger,[7,8] C. L. Yang (杨春莉),[1] Y. H. Qiang (强赟华),[1] X. Y. Huang (黄鑫源),[1,2] G. Xie (谢港),[1,2] L. Zhu (祝霖),[1,2] X. Zhang (张旭),[1,2] H. Zhou (周浩),[1,2] J. H. Zheng (郑佳卉),[1,2] L. C. Sun (孙路冲),[1,9] S. Y. Xu (徐苏扬),[1,2] Z. Zhao (赵圳),[1,2] F. Guan (管芳),[1,10] W. X. Huang (黄文学),[1,2,3] Y. L. Tian (田玉林),[1,2,3] Y. S. Wang (王永生),[1,3] J. Y. Wang (王均英),[1,3] X. L. Wu (吴晓蕾),[1,3] Z. H. Li (李泽浩),[1] Z. W. Lu (卢子伟),[1] Y. He (何源),[1,2] L. T. Sun (孙良亭),[1,2] Z. Z. Ren (任中洲),[11] S. G. Zhou (周善贵),[12,13] V. K. Utyonkov,[14] A. A. Voinov,[14] Yu. S. Tsyganov,[14] A. N. Polyakov,[14] D. I. Solovyev,[14] N. D. Kovrizhnykh,[14] M. V. Shumeiko,[14] and D. Ibadullayev[14,15]

The highest ever P_{ECDF} values so far!

Red values – new data from SHANS2

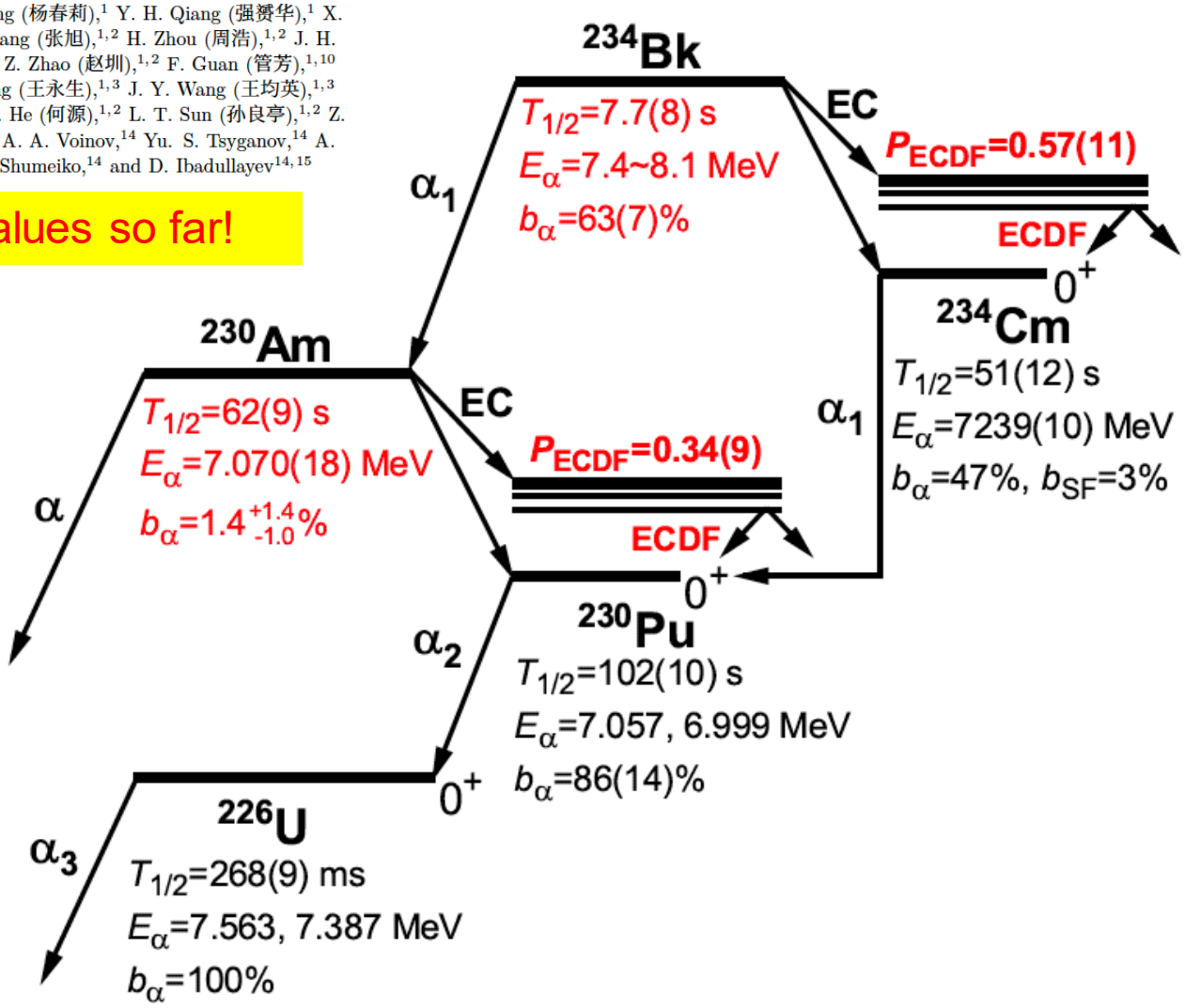

P_{ECDF} systematics: strong sensitivity to the fission barrier models!

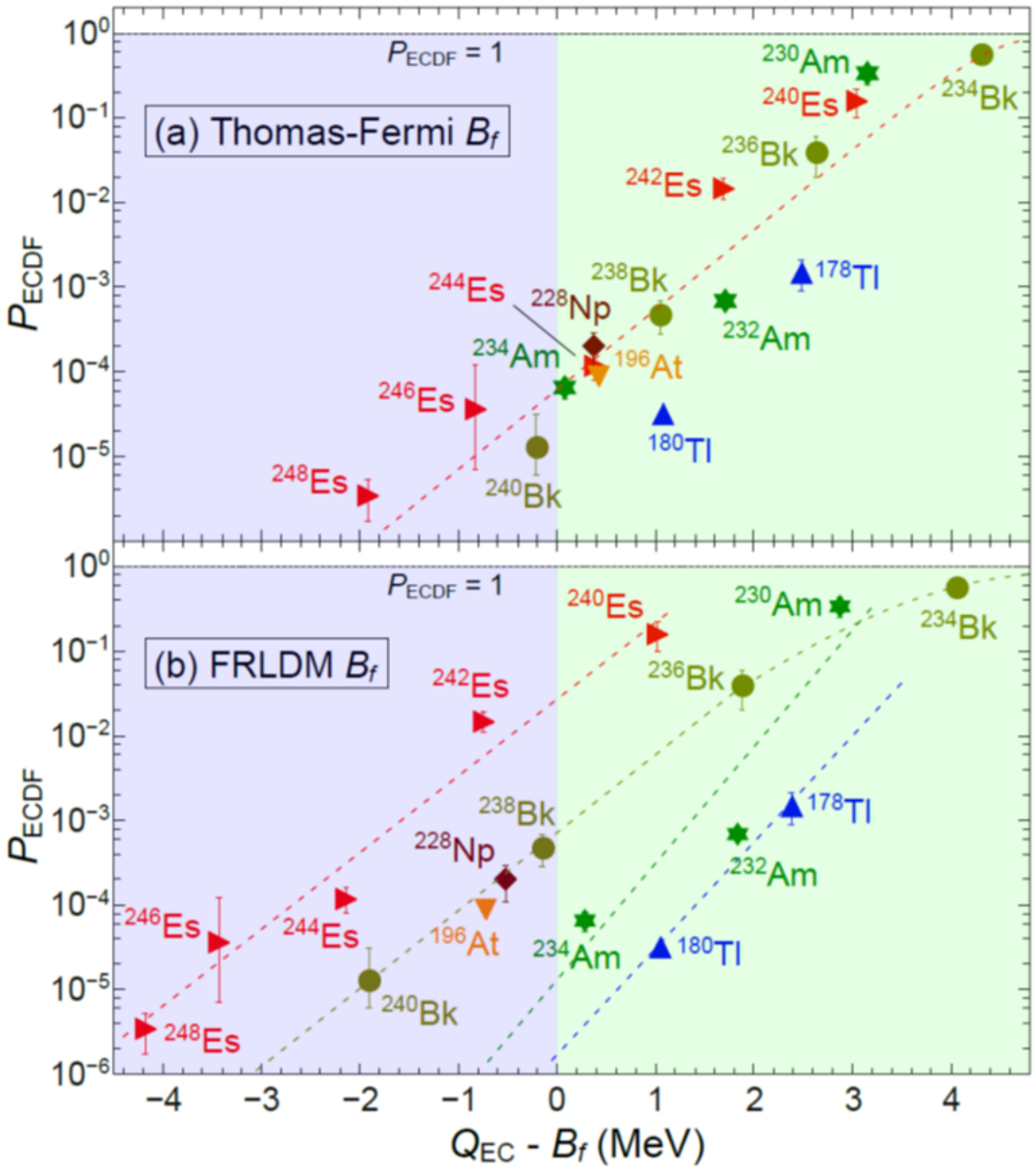

$$P_{\beta DF} = \frac{N_{\beta DF}}{N_\beta}$$

$N_{\beta DF}$ - number of beta-delayed fission events

N_β – number of beta decays

P_{ECDF} TF vs FRLDM differences

- TF: no Z-dependence for P_{ECDF}, but it is present in FRLDM
- TF barriers are, on average, lower, than FRLDM
- Due to this, most of cases are above barrier in TF, while a half of them are subbarrier in FRLDM

ECDF of ^{180}Tl vs ^{234}Bk

$Q_{EC}(^{180}Tl)-B_f(^{180}Hg)=0.5$ MeV
$P_{ECDF}(^{180}Tl)=3.6(7)\times10^{-5}$

$Q_{EC}(^{234}Bk)-B_f(^{234}Cm)=4$ MeV
$P_{ECDF}(^{234}Bk)=0.57(11)$

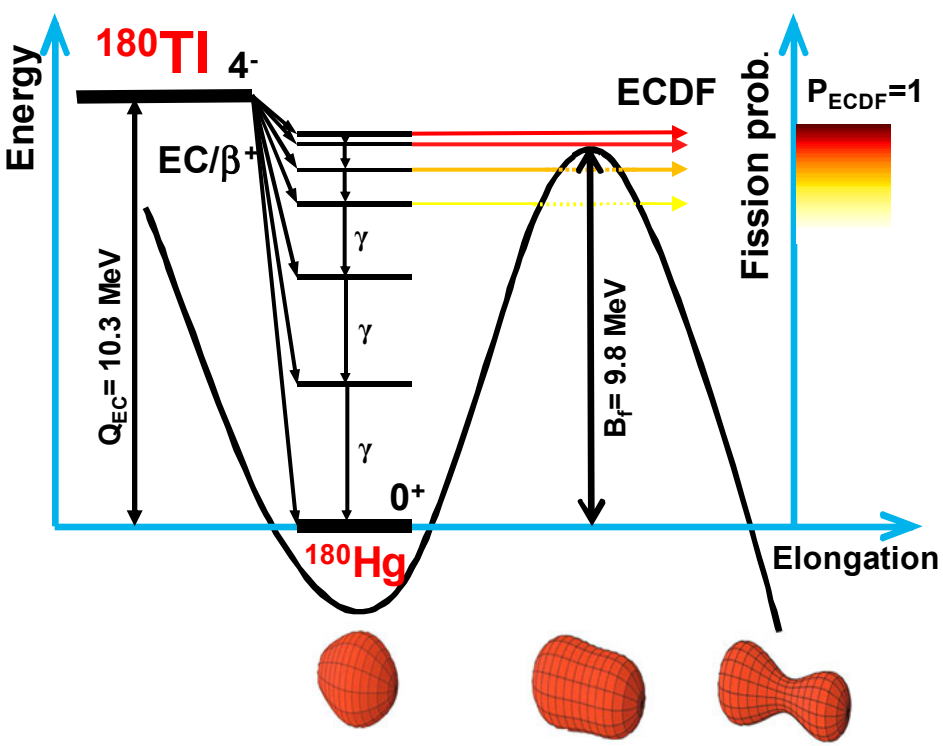

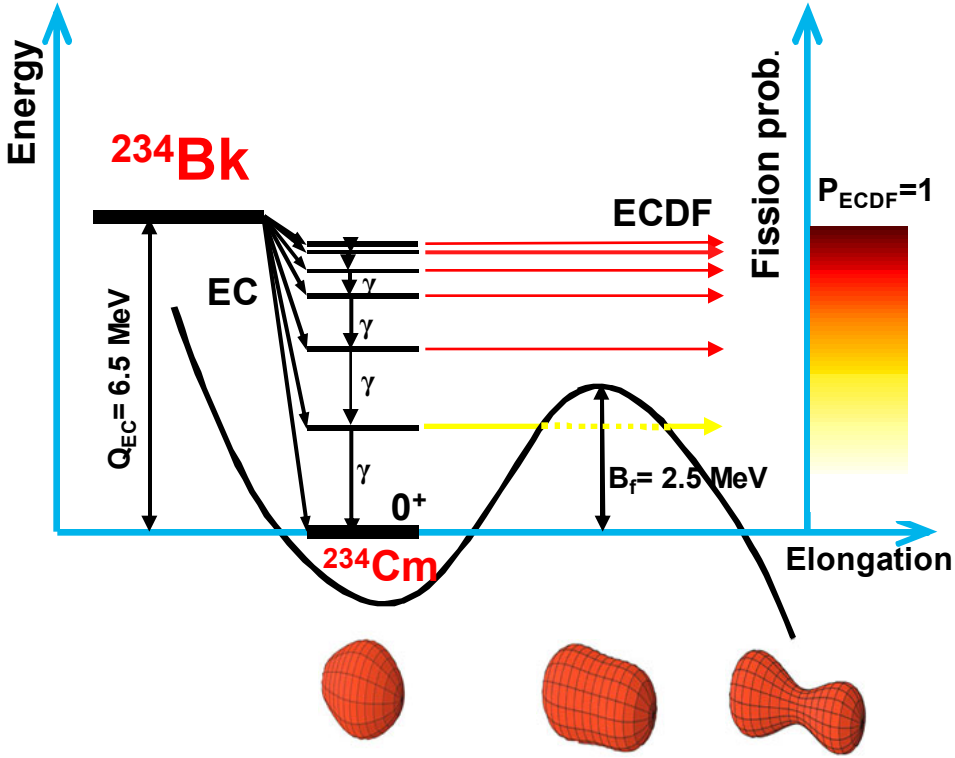

Fission is dominantly sub-barrier!
PES/B_f of ^{180}Hg will be more important, than the beta strength function, S_β

Fission is dominantly above-barrier?
Beta-decay strength function of ^{234}Bk will be more important? (**NEED THEORY!**)

^{180}Tl example: the use of P_{ECDF} to extract B_f
(or, vice versa)

PHYSICAL REVIEW C **86**, 024308 (2012)

Fission-barrier heights of neutron-deficient mercury nuclei

M. Veselský,[1,*] A. N. Andreyev,[2] S. Antalic,[3] M. Huyse,[4] P. Möller,[5] K. Nishio,[6] A. J. Sierk,[5] P. Van Duppen,[4] and M. Venhart[1,4]

$$P_{\beta DF} = \frac{N_{\beta DF}}{N_\beta} = \frac{\int_0^{Q_\beta} F(Q_\beta - E) S_\beta(E) \frac{\Gamma_f(E)}{\Gamma_f(E)+\Gamma_\gamma(E)} dE}{\int_0^{Q_\beta} F(Q_\beta - E) S_\beta(E) dE}$$

$$\Gamma_f(E^*) = \frac{1}{2\pi\rho_c(E^* - \Delta)} \times \int_0^{E^*-B_f-\Delta_{sp}} \rho_{sp}(E^* - B_f - \Delta_{sp} - E')dE'$$

Need to know:

- Q_β - 'easy', experimental values
- S_β – beta decay strength function
- Statistical model for decay widths
- B_f – model dependent

Only a small part of S_β goes in the [B_f:Q_{EC}] window!
This may explain the smallness of P_{ECDF}(^{180}Tl)
Also needed to scale the fission barrier by 15-20%

^{180}Tl beta-strength functions, S_β

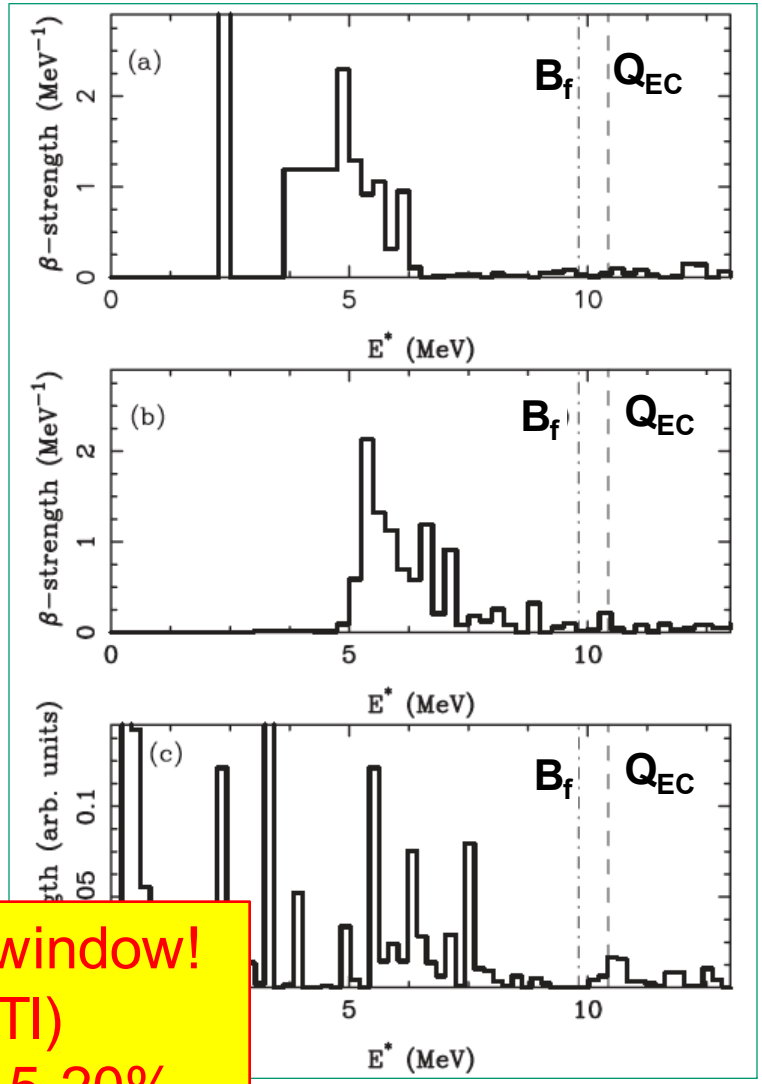

Recent fully microscopic theory efforts for P_{ECDF} calculations

PHYSICAL REVIEW C **111**, 065803 (2025)

New upper limits for β-delayed fission probabilities of ^{230,232}Fr and ^{230,232,234}Ac

ISOLDE βdf data
+ECDF ^{178,180}Tl

S. Bara,[1,*] A. Algora,[2] B. Andel,[3] A. N. Andreyev,[4] S. Antalic,[3] R. A. Bark,[5] M. J. G. Borge,[6] A. Camaiani,[7,8,1] T. E. Cocolios,[1] J. G. Cubiss,[4,9] H. De Witte,[1] C. M. Fajardo-Zambrano,[1,10] Z. Favier,[10] L. M. Fraile,[11] H. O. U. Fynbo,[12] S. Goriely,[13] R. Grzywacz,[14] M. Heines,[1] F. Ivandikov,[1] J. D. Johnson,[1] P. M. Jones,[5] D. S. Judson,[15] J. Klimo,[1] A. Korgul,[16] M. Labiche,[17] R. Lica,[18] M. Madurga,[14] N. Marginean,[18] C. Mihai,[18] J. Mišt,[3] E. Nácher,[2] C. Neacsu,[18] J. N. Orce,[19] C. A. A. Page,[4] R. D. Page,[15] J. Pakarinen,[20] P. Papadakis,[17] A. Perea,[6] M. Piersa-Siłkowska,[16] Zs. Podolyák,[21] R. Raabe,[1] W. Ryssens,[13] A. Sánchez-Fernández,[13] A. Sitarčík,[3] O. Tengblad,[6] J. M. Udías,[11] V. Van Den Bergh,[1] P. Van Duppen,[1] N. Warr,[22] A. Youssef,[1] and Z. Yue[4]

The process of β-delayed fission (βDF) of ^{230,232}Fr and ^{230,232,234}Ac was studied in an experiment performed at the ISOLDE facility at CERN. As no fission fragments were observed for any of the nuclei investigated, upper limits for their βDF probability ($P_{\beta DF}$) were determined. The experimental results were compared with theoretical calculations that were first benchmarked on ^{178,180}Tl $P_{\beta DF}$ experimental values. The $P_{\beta DF}$ values were calculated using the code TALYS to which β-strength functions obtained from the D1M Gogny parametrization and from the Skyrme functional SKO' were given as input together with fission paths obtained with BSkG3 and BSk14 models. Sensitivity studies of different β-strength functions, and fission paths scaling on the $P_{\beta DF}$ values were conducted, suggesting a stronger dependence of the $P_{\beta DF}$ on the fission paths rather than on the β-strength function used.

So far, no model is able to produce all the necessary inputs (i.e., β-strength functions, level densities, and fission paths) within one unique framework. Therefore, different models are used to calculate the various nuclear inputs. In this work all of the inputs were obtained from energy density functional based models. The β-strength functions were calculated within the QRPA framework either using the D1M Gogny parametrization [29], or using the Skyrme functional SKO' [30] (see

Benchmarking with different S_β and scaling of fission barriers

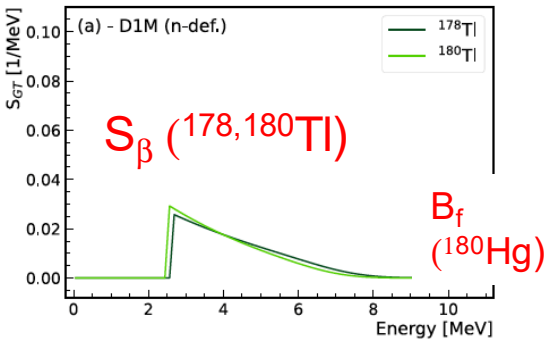

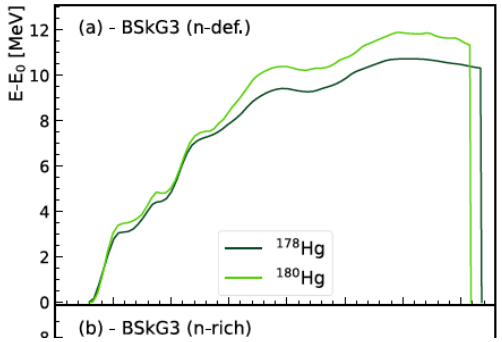

Different S_β

Need scaling of B_f

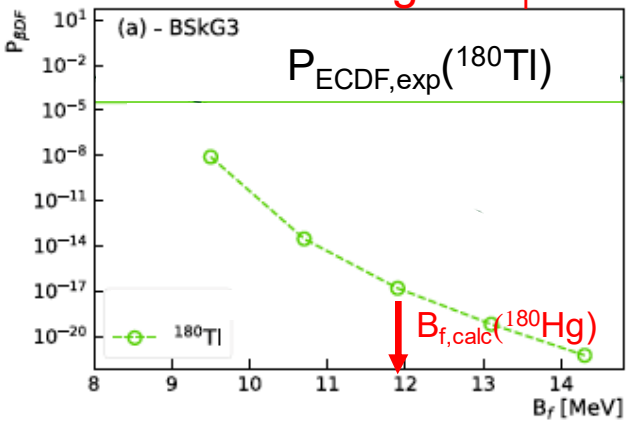

TABLE IV. Values of $P_{\beta DF}$ obtained using different β-strength functions: D1M, SKO' and a constant strength over the energy range of the daughter's excited states. The fission paths used were calculated with BSkG3. In the last column the experimental value of the $P_{\beta DF}$ or its upper limit found in this work (t.w.) is given for comparison.

	$P_{\beta DF}$ Theory			EXP $P^{exp}_{\beta DF}$	
Nuclide	D1M [29]	SKO' [30]	constant		
^{178}Tl	4.1×10^{-9}	/	1.2×10^{-4}	$1.5(6) \times 10^{-3}$	[27]
^{180}Tl	1.5×10^{-17}	/	8.7×10^{-14}	$3.2(2) \times 10^{-5}$	[28]
^{230}Fr	1.1×10^{-20}	4.6×10^{-18}	9.7×10^{-18}	$<3.3 \times 10^{-8}$	t.w.
^{232}Fr	9.1×10^{-20}	/	5.9×10^{-16}	$<1.3 \times 10^{-7}$	t.w.
^{230}Ac	7.4×10^{-13}	/	2.5×10^{-11}	$<4.3 \times 10^{-10}$	t.w.
^{232}Ac	3.7×10^{-20}	2.2×10^{-16}	2.7×10^{-16}	$<2.7 \times 10^{-9}$	t.w.
^{234}Ac	1.1×10^{-14}	/	7.5×10^{-11}	$<4.9 \times 10^{-6}$	t.w.

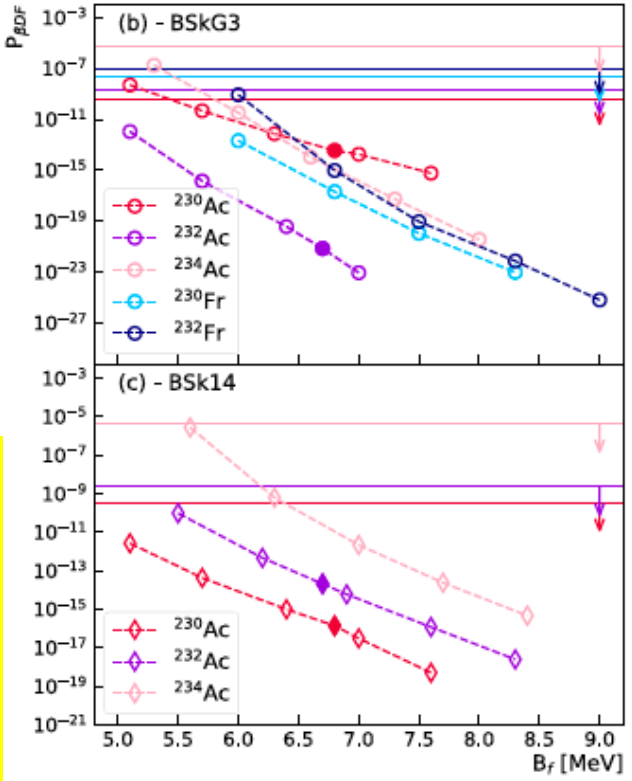

Failed to reproduce known $P_{ECDF}(^{178,180}Tl)$!
But, all those cases are strongly subbarrier!

That is why, SHANS2's ^{234}Bk/^{230}Am data, with high P_{ECDF}, may provide a totally new direction to such theory studies!

Fission in 21st Century: Some of the topics covered

- Beta Delayed Fission (βDF) at ISOLDE at 60 keV
- Transfer –induced fission with ACTAR/ISS at HIE-ISOLDE
- Coulex-induced fission with SOFIA@GSI at 1 AGeV
- Fusion-fission with heavy ions at Coulomb energies (Dubna, ANU, India..)
- Transfer-induced fission at Coulomb energies (VAMOS@GANIL, JAEA)
- n_ToF, n-induced fission experiments (ILL,n_ToF, LANSCE,J-PARC….)
- Future techniques: Photofission at ELI-NP with CBS-technique
- Future techniques: Fission in collision geometry with electrons (SCRIT@RIKEN)?

Thank You for your Attention!

- Bright future for fission studies with RIBs
- Access to both proton- and neutron- rich nuclei
- Un-precedented precision in Z,A determination!
- Control of excitation energy event-by-event!

- However, still the 'classical' methods work and allow to study both the isospin and excitation dependence of fission in the 'new' regions of Chart of Nuclides

$^{178}Hg^*$ fission in inverse kinematics at VAMOS

^{124}Xe(4.3 AMeV)+^{54}Fe->$^{178}Hg^*$, E*=34 MeV

PHYSICAL REVIEW LETTERS **126,** 132502 (2021)

Experimental Evidence for Common Driving Effects in Low-Energy Fission from Sublead to Actinides

C. Schmitt,[1,*] A. Lemasson,[2] K.-H. Schmidt,[3] A. Jhingan,[4] S. Biswas,[2] Y. H. Kim,[5] D. Ramos,[2] A. N. Andreyev,[6,7,8] D. Curien,[1] M. Ciemala,[9] E. Clément,[2] O. Dorvaux,[1] B. De Canditiis,[1] F. Didierjean,[1] G. Duchêne,[1] J. Dudouet,[10,11] J. Frankland,[2] B. Jacquot,[2] C. Raison,[6] D. Ralet,[2] B.-M. Retailleau,[2] L. Stuttgé,[1] and I. Tsekhanovich[12]

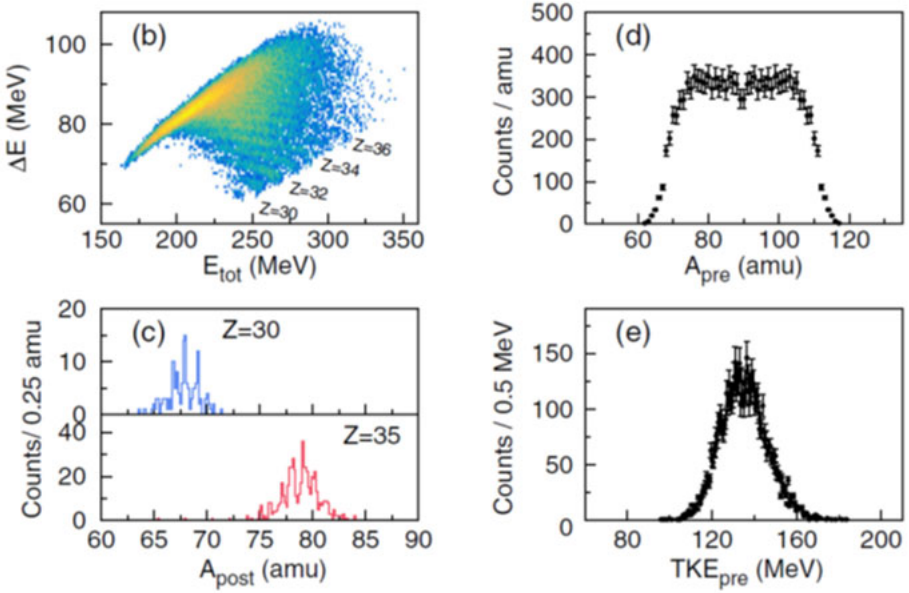

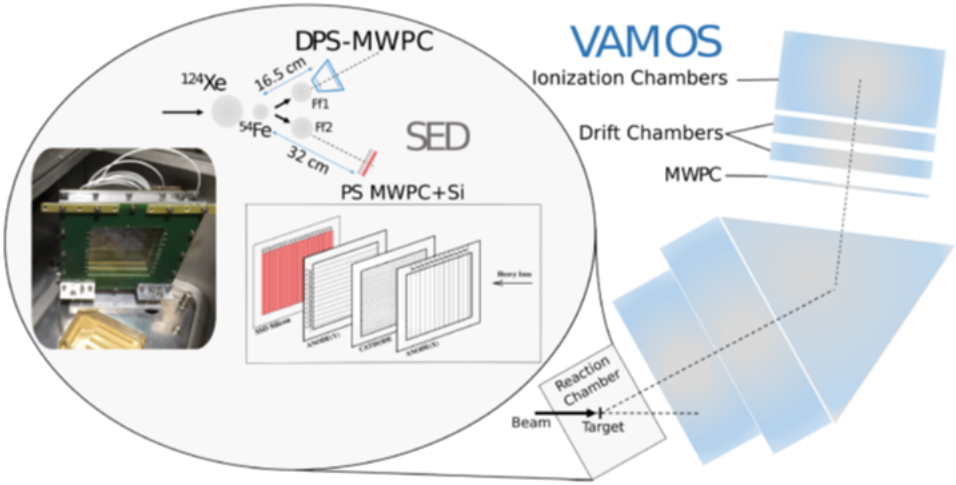

bdf of ^{178}Tl, ISOLDE, **E*~10 MeV**
V. Liberati et al, PRC88,044322 (2013)

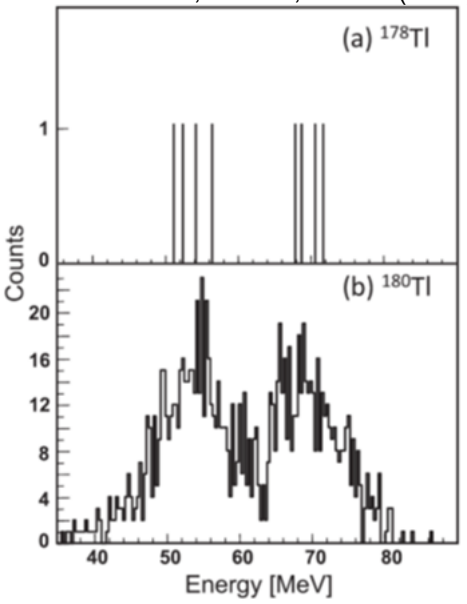

- **Coulomb barrier energies, inverse kinematics: high FF's energies,**
- **allows Z-identification.**
- **Confirmed asymmetric mass split of ^{178}Hg, even at a higher E***
- **First direct confirmation of importance of Z=36!**

Universality of shell effects in low-energy fission

Phys. Lett. B 865 (2025) 139459

Contents lists available at ScienceDirect

Physics Letters B

journal homepage: www.elsevier.com/locate/physletb

Letter

Universality of shell effects in fusion-fission mass distributions

J. Buete [a,*], B.M.A. Swinton-Bland [a,3], D.J. Hinde [a], K.J. Cook [a,b], M. Dasgupta [a], A.C. Berriman [a], D.Y. Jeung [a], K. Banerjee [a,1], L.T. Bezzina [a], I.P. Carter [a], C. Sengupta [a,2], C. Simenel [a,c], E.C. Simpson [a]

[a] Department of Nuclear Physics and Accelerator Applications, Research School of Physics, Australian National University, Canberra, ACT 2601, Australia
[b] Facility for Rare Isotope Beams, Michigan State University, MI 48824, USA
[c] Department of Fundamental and Theoretical Physics, Research School of Physics, Australian National University, Canberra, ACT 2601, Australia

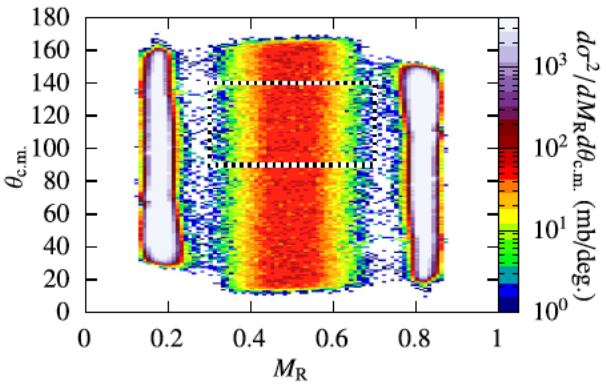

Fig. 1. The mass-angle distribution for ^{176}Os. The vertical high intensity bands

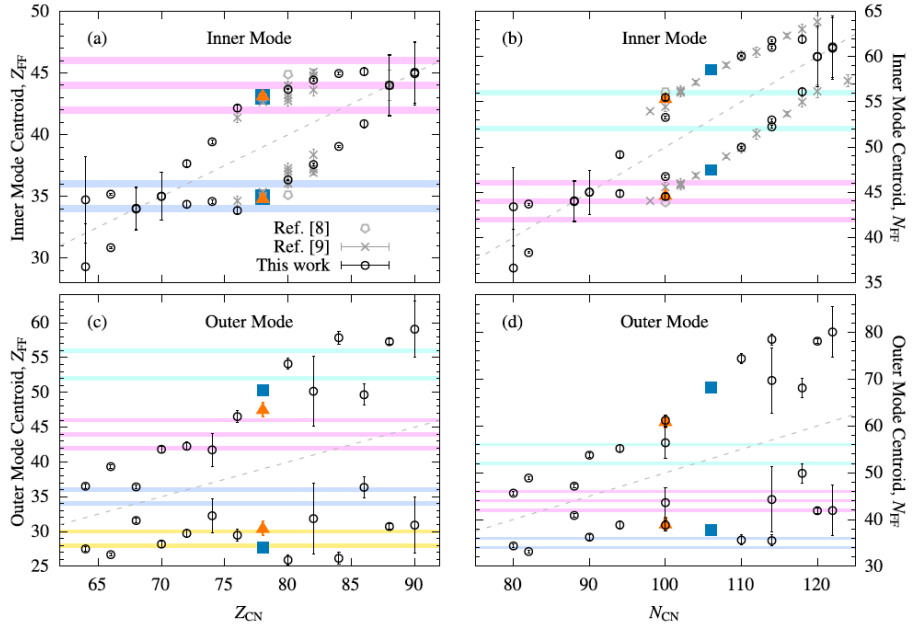

Fig. 4. The proton Z (left) and neutron N (right) numbers for the shell-driven fission modes determined via a two-dimensional fit to the mass-RTKE distribution

Reaction	CN	Z_{CN}	$E_{c.m.}$ (MeV)	E^*_{gs} (MeV)	E^*_{sp} (MeV)
^{32}S + ^{112}Cd	^{144}Gd	64	114.6	69.8	38.0
^{32}S + ^{116}Sn	^{148}Dy	66	115.3	65.6	36.7
^{32}S + ^{124}Te	^{156}Er	68	117.4	65.1	37.1
^{16}O + ^{144}Sm	^{160}Yb	70	89.84	61.4	36.3
^{32}S + ^{134}Ba	^{166}Hf	72	119.4	58.3	35.3
^{32}S + ^{142}Ce	^{174}W	74	120.3	60.0	39.0
^{32}S + ^{144}Nd	^{176}Os	76	117.6	49.9	32.5
^{34}S + ^{144}Sm	^{178}Pt	78	117.6	37.7	23.8
^{32}S + ^{152}Sm	^{184}Pt	78	118.9	55.4	39.5
^{32}S + ^{158}Gd	^{190}Hg	80	119.4	54.1	40.4
^{32}S + ^{164}Dy	^{196}Pb	82	120.5	53.8	42.0
^{32}S + ^{166}Er	^{198}Po	84	120.6	45.1	35.7
^{32}S + ^{172}Yb	^{204}Rn	86	120.2	42.9	34.9
^{32}S + ^{176}Hf	^{208}Ra	88	125.1	42.8	36.4
^{32}S + ^{180}W	^{212}Th	90	128.9	41.1	36.1

Future(?): Fission via Electron scattering from unstable nuclei

e.g. electron scattering from unstable nuclei (colliding accelerated electrons and low-energy radioactive ions!)

SCRIT at RIKEN (Japan) and ELISe at GSI (Darmstadt, Germany)

SCRIT@RIKEN

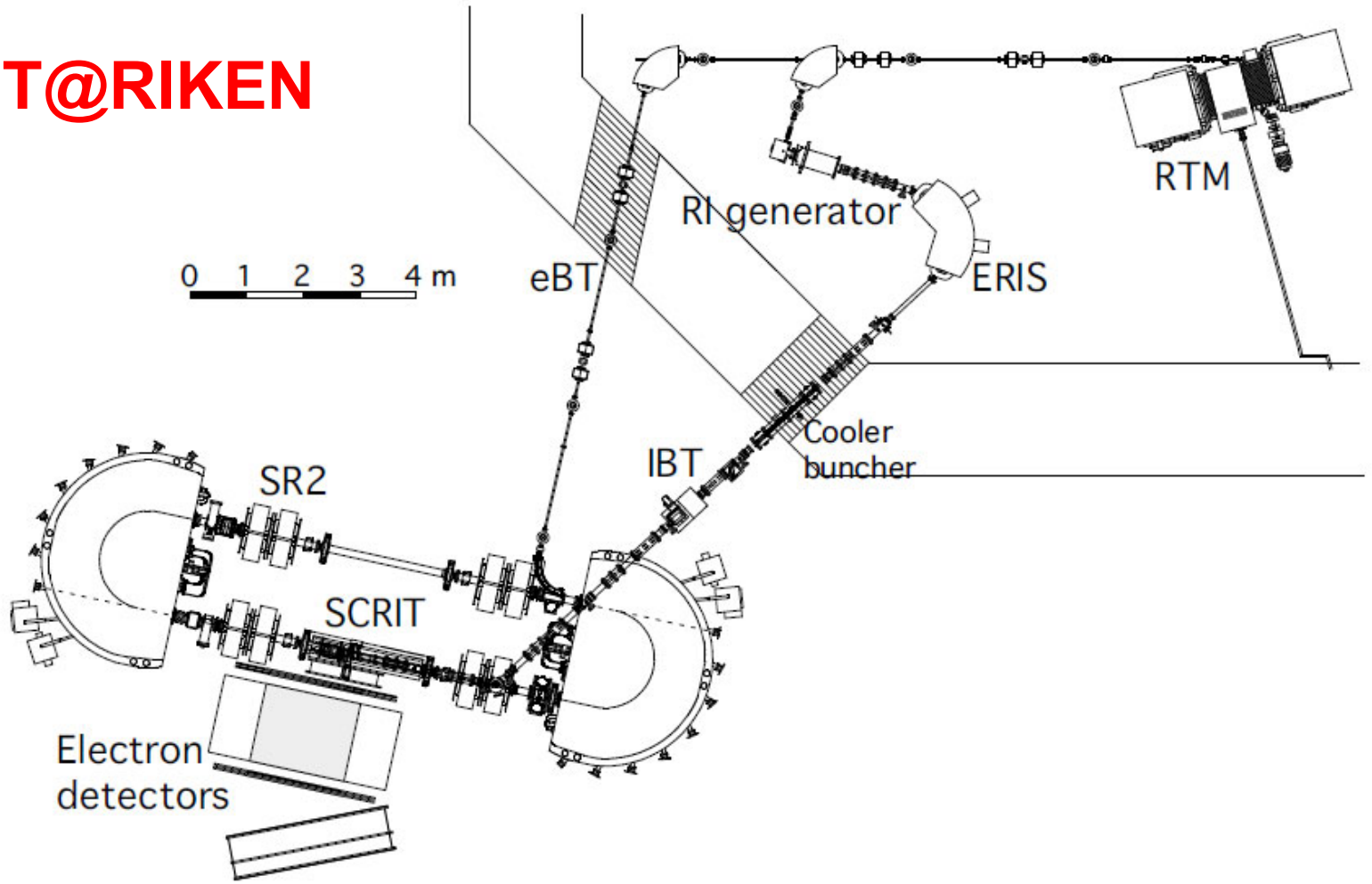

Fission studies with CBS brilliant gamma beams at ELI-NP

✓ The potential energy landscape

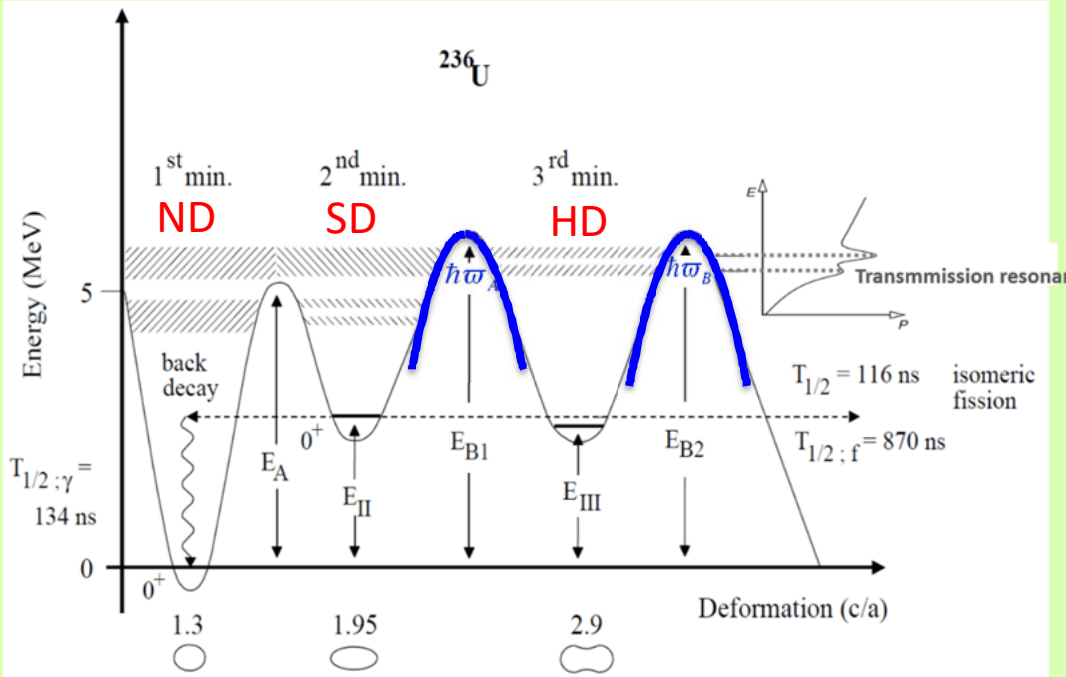

✓ Fission cross-section

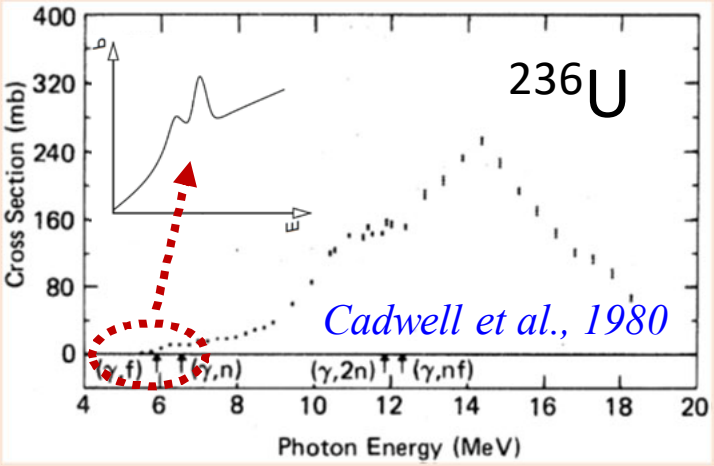

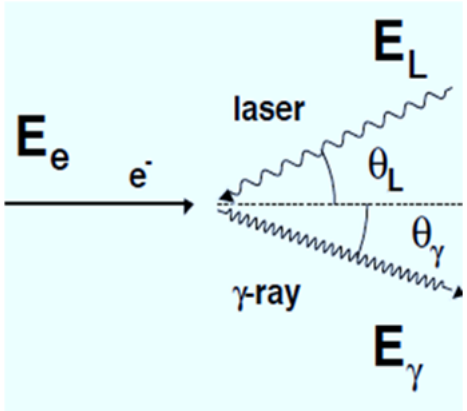

Compton Backscattering

Fission-Fragment Detectors for ISS@ISOLDE

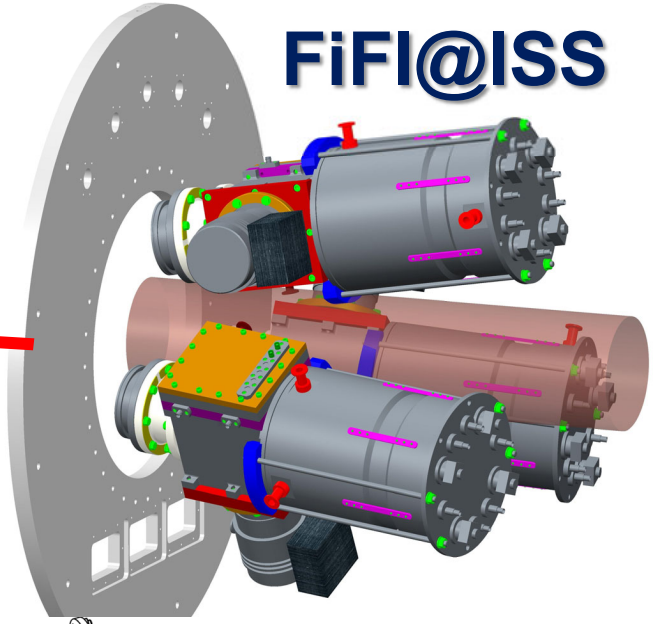

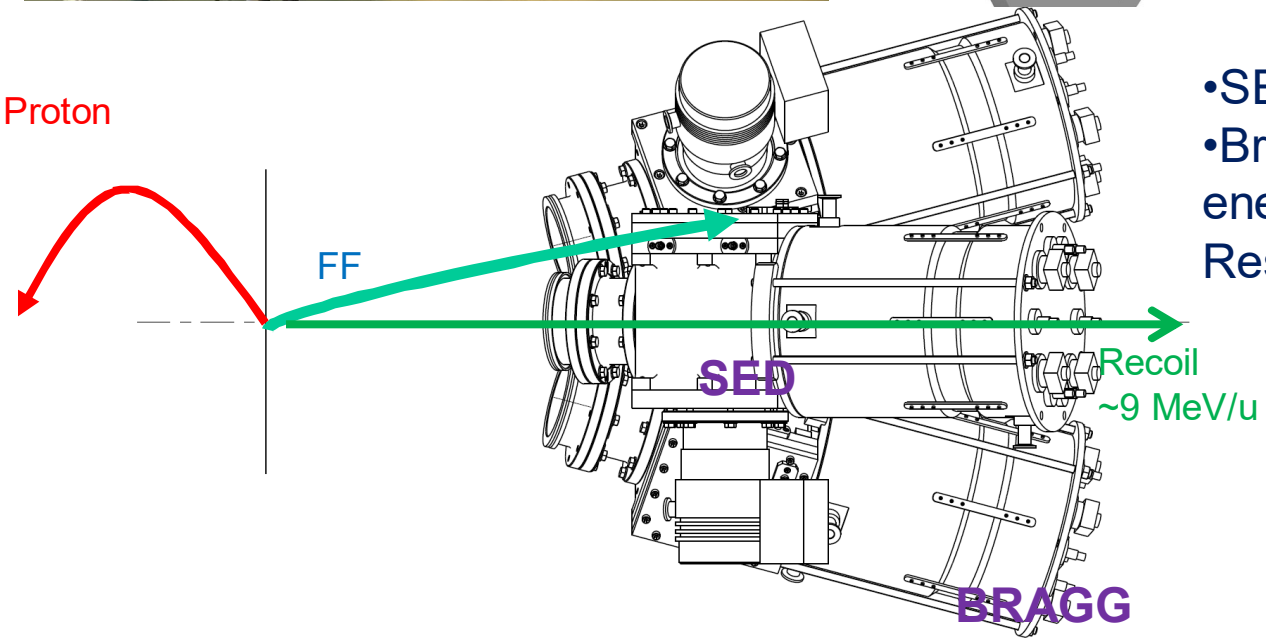

- SED MCP for ns FF timing
- Bragg ion chamber for FF energy measurement (~1MeV Resolution)

Example 2: d,pf transfer-induced fission of post-accelerated RIBs in inverse kinematics with ISOLDE Solenoidal Spectrometer (ISS-ISOLDE)